UNIVERSIDAD DE GRANADA

Programa de doctorado en Bioquímica

y Biología Molecular (B16.56.1)

PhD dissertation

BCL7A implications in acute myeloid leukemia

PhD candidate:

Juan Rodrigo Patiño Mercau

PhD supervisors:

Pedro Pablo Medina Vico, PhD.

Juan Carlos Álvarez Pérez, PhD.

Genyo

CENTRO PFIZER-UNIVERSIDAD DE GRANADA-JUNTA DE ANDALUCÍA
DE **GENÓMICA** E **INVESTIGACIÓN ONCOLÓGICA**

Gene Expression Regulation and Cancer Group (CTS-993)

Editor: Universidad de Granada. Tesis Doctorales
Autor: Juan Rodrigo Patiño Mercau
ISBN: 978-84-1195-249-1
URI: https://hdl.handle.net/10481/90810

A mis padres

El doctorando / The doctoral candidate [**Juan Rodrigo Patiño Mercau**] y los directores de la tesis / and the thesis supervisor/s: [**Pedro Pablo Medina Vico** y **Juan Carlos Álvarez Pérez**]

Garantizamos, al firmar esta tesis doctoral, que el trabajo ha sido realizado por el doctorando bajo la dirección de los directores de la tesis y hasta donde nuestro conocimiento alcanza, en la realización del trabajo, se han respetado los derechos de otros autores a ser citados, cuando se han utilizado sus resultados o publicaciones.

/

Guarantee, by signing this doctoral thesis, that the work has been done by the doctoral candidate under the direction of the thesis supervisor/s and, as far as our knowledge reaches, in the performance of the work, the rights of other authors to be cited (when their results or publications have been used) have been respected.

Lugar y fecha / Place and date: **En Granada a 8 de marzo 2024**

Director/es de la Tesis / Thesis supervisor/s:	Doctorando / Doctoral candidate:
Firma / Signed	Firma / Signed

Table of Contents

Figure index

Main Figures

Supplementary Figures

Table index

Main Tables

Supplementary Tables

List of abbreviations

5'UTR	5' Untranslated Region
ALL	Acute lymphocytic leukemia
AMKL	Acute megakaryoblastic leukemia
AML	Acute myeloid lukemia
APL	Acute promyelocytic leukemia
ARID1A	AT-rich interaction domain 1A
ASXL1	Additional sex combs like transcriptional regulator 1
ATP	Adenosine triphosphate
BCL2	B-Cell CLL/Lymphoma 2
BCL7A	B-Cell CLL/lymphoma 7 protein family member A
Bcl7a$^{fl/fl}$	Homozygous floxed *Bcl7a*
BD	Becton, Dickinson and Company manufacturer
BM	Bone marrow
bp	Base pairs
Cas	CRISPR-associated nuclease
cDNA	Complementary DNA
CEBPA	CCAAT enhancer binding protein alpha
CHD	Chromodomain-helicase-DNA binding
ChIP-seq	Chromatin immunoprecipitation followed by NGS
CLL	Chronic lymphocytic leukemia
CML	Chronic myeloid leukemia
C-MYC	MYC Proto-Oncogene, BHLH Transcription Factor
CpG	Cytosine-guanine dinucleotides
CRISPR	Clustered regularly interspaced short palindromic repeats
CTCL	Cutaneous T-cell lymphoma
Decitabine / DAC	5-aza-2'-deoxycytidine
DepMap Portal	Dependency Map Portal database
DiR	DNMT1-interacting RNA
DLBCL	Diffuse large B-Cell lymphoma
DMEM	Dulbecco's modified Eagle cell culture medium
DNA	Deoxyribonucleic acid
DNMT1	DNA methyltransferase 1
DNMT3A	DNA methyltransferase 3 alpha

E. coli	Escherichia coli
EDTA	Ethylenediaminetetraacetic acid
ERT2	Human estrogen receptor ligand binding domain
EV	Empty vector
EZH2	Enhancer of zeste 2 polycomb repressive complex 2 subunit
FAB classification	French-American-British acute myeloid leukemias
FBS	Fetal bovine serum
FDR	False discovery rate
FLT3	Fms-like tyrosine kinase 3
GAPDH	Glyceraldehyde 3-phosphate dehydrogenase
GC	Germinal center
gDNA Meth	Commercial human genomic DNA totally methylated
gDNA Unmeth	Commercial human genomic DNA totally unmethylated
GO	Gene ontology
HMA	Hypomethylating agent
HRP	Horseradish peroxidase
HSC	Hematopoietic stem cells
IDH1	Isocitrate dehydrogenase (NADP(+)) 1
IDH2	Isocitrate dehydrogenase (NADP(+)) 2
IgG	Immunoglobulin G
INO80	Inositol requiring 80
ISWI	Imitation switch
IU	Infective units / mL
KO	Knock-out
LB	Luria–Bertani medium
LC–MS/MS	Liquid chromatography with tandem mass spectrometry
LFQ	Label-free quantification
MDS	Myelodysplastic syndrome
MOI	Multiplicity of infection
mRNA	Messenger RNA
MSP	Methylation-Specific PCR
mSWI/SNF	Mammalian SWI/SNF
ncRNA	Non-coding RNA
NGS	Next-generation sequencing
NPM1	Nucleophosmin 1

NRAS	Neuroblastoma rat sarcoma viral oncogene homolog
NSG	NOD.scid Il2rgtm1Wjl/SzJ mouse strain
N-terminal	Amino terminal domain
o/n	Overnight
PBS	Phosphate-buffered saline buffer
PCR	Polymerase Chain Reaction
PML	Promyelocytic leukemia gene
qRTPCR	Quantitative real-time PCR assays
RARA	Retinoic acid receptor alpha
RBC	Red blood cells
rcf	Relative centrifugal force
RNA	Ribonucleic acid
rpm	Revolutions per minute
RPMI	Roswell Park Memorial Institute 1640 cell culture medium
rRNA	Ribosomal RNA
RUNX1	Runt-related transcription factor 1
SDS	Sodium dodecyl sulfate
sgDiRs	Single guide RNA including a DiR
sgRNA	Single guide RNA
SMARCA2	SWI/SNF related, matrix associated, actin dependent regulator of chromatin, subfamily A, member 2
SMARCA4	SWI/SNF related, matrix associated, actin dependent regulator of chromatin, subfamily A, member 4
SWI/SNF	Switch/sucrose-non-fermenting
TAE	Tris-Acetate-Ethylenediaminetetraacetic acid
TARGET	Therapeutically Applicable Research to Generate Effective Treatments
TCGA-LAML	The Cancer Genome Atlas Program - Acute Myeloid Leukemia Project
TET2	Tet methylcytosine dioxygenase 2
TP53	Tumor protein P53
TSS	Transcription start site
UBC	Ubiquitin C
WB	Western blot
WBC	White blood cells
WT	Wild-type

WT1 WT1 transcription factor

Δ27-BCL7A Mutant BCL7A variant lacking its first 27 amino acids from its N-terminal domain

Abstract / Resumen

Abstract

Cancer is a critical global health issue of our time. It encompasses a wide variety of diseases characterized by uncontrolled cell growth, often resulting from genetic mutations and epigenetic alterations. In recent decades, cancer research has led to the discovery of new biomarkers that improve both diagnosis and patient prognosis, and has paved the way for innovative targeted therapies. Despite these promising results, cancer remains as one of the leading causes of death worldwide. Therefore, further research into the molecular basis of cancer initiation and progression is still of paramount importance.

Hematologic malignancies are among the most common forms of cancer. Within hematologic malignancies, acute myeloid leukemia (AML) is the second most common form of leukemia. Although cytogenetic aberrations and genetic mutations are involved in the development and progression of AML, this disease is also conditioned by aberrations in epigenetic mechanisms.

Chromatin remodeling is one of the major epigenetic mechanisms. The mammalian switch/sucrose-non-fermenting (mSWI/SNF) complex family is one of the major chromatin remodeling families whose alterations have been found to be highly associated with cancer. B-Cell CLL/lymphoma 7 protein family member A (BCL7A) is a mSWI/SNF subunit which has been observed to be clearly related to hematologic disorders. In fact, in a previous research project carried out in our laboratory, *BCL7A*

was found to be recurrently mutated in diffuse large B-Cell lymphoma (DLBCL) patients' samples and cell lines. The experimental approaches performed along this project showed that *BCL7A* plays a tumor suppressor role in DLBCL models.

AML has been observed to be related to epigenetic disorders (including chromatin modifiers), and *BCL7A* has been strongly associated with hematologic disorders in previous studies. Therefore, we hypothesized that *BCL7A* may even play a role in this type of leukemia. Indeed, in a preliminary analysis of data from AML patients, we found that the *BCL7A* methylation level was inversely correlated with the *BCL7A* expression level. This downregulation by DNA methylation is a common tumor suppressor inactivation mechanism that is naturally selected by tumor cells. Furthermore, we performed phenotypic assays using AML cell models in which *BCL7A* was silenced by genomic DNA methylation. These assays suggest that *BCL7A* plays a tumor suppressor role in AML models both *in vitro* and *in vivo*.

We also generated a *Bcl7a* conditional knock-out (KO) mouse model to study the putative effects of *Bcl7a* in hematologic cells and tissues *in vivo*. Nevertheles, *Bcl7a* ablation did not result in any phenotypic changes.

On the other hand, using a clustered regularly interspaced short palindromic repeats (CRISPR) based molecular tool, we performed a targeted demethylation of the *BCL7A* locus in one of our human cell models to evaluate its phenotype after the

expected restoration of *BCL7A* expression. The slight *BCL7A* expression restoration yielded at messenger ribonucleic acid (mRNA) and protein levels might be the explanation for the absence of any phenotypic change in cell growth capability.

The results obtained in this PhD thesis suggest that *BCL7A* plays a tumor suppressor role in AML. However, further research is necessary to provide more information to determine whether or not *BCL7A* is an AML useful biomarker in the diagnosis, classification and prognosis of AML patients. Ultimately, this research might yield valuable knowledge for the development of novel therapies to provide more promising outcomes for AML patients.

Resumen

El cáncer es un grave problema de salud a nivel global en nuestra época. Engloba una amplia variedad de enfermedades caracterizadas por el crecimiento celular descontrolado, a menudo resultado de mutaciones genéticas y alteraciones epigenéticas. En las últimas décadas, la investigación en cáncer ha conducido al descubrimiento de nuevos biomarcadores que mejoran tanto el diagnóstico como el pronóstico del paciente, y ha abierto camino para terapias dirigidas innovadoras. A pesar de estos resultados prometedores, el cáncer sigue siendo una de las principales causas de muerte en todo el mundo. Entonces, la investigación acerca de las bases moleculares de la iniciación y progresión del cáncer sigue siendo de suma importancia.

Las neoplasias hematológicas se encuentran entre las formas más comunes de cáncer. Dentro de estas, la leucemia mieloide aguda (AML, por sus siglas en inglés) es la segunda forma más común de leucemia. Aunque las aberraciones citogenéticas y las mutaciones genéticas están involucradas en el desarrollo y progresión de la AML, esta enfermedad también está condicionada por alteraciones en mecanismos epigenéticos.

La remodelación de la cromatina es uno de los principales mecanismos epigenéticos. La familia de complejos mSWI/SNF (mammalian switch/sucrose-non-fermenting) es una de las familias principales de remodeladores de la cromatina cuyas alteraciones se han encontrado muy frecuentemente asociadas

con el cáncer. La proteína B-Cell CLL/lymphoma 7 (BCL7A) es una subunidad de mSWI/SNF que se ha observado está claramente relacionada con neoplasias hematológicas. De hecho, en un proyecto de investigación previo realizado en nuestro laboratorio, se descubrió que *BCL7A* estaba recurrentemente mutado en muestras de pacientes y líneas celulares de linfoma difuso de células B grandes (DLBCL, por sus siglas en inglés). Los experimentos llevados a cabo en este proyecto demostraron que *BCL7A* desempeña un papel de supresor tumoral en modelos de DLBCL.

Se ha observado que la LMA está relacionada con trastornos epigenéticos (incluyendo modificadores de la cromatina), y *BCL7A* se ha encontrado muy asociado con neoplasias hematológicas en estudios previos. Por tanto, hipotetizamos que *BCL7A* también puede desempeñar un papel en este tipo de leucemia. De hecho, en un análisis preliminar de datos de pacientes con AML, encontramos que el nivel de metilación de *BCL7A* estaba inversamente correlacionado con el nivel de expresión de *BCL7A*. Esta regulación a la baja por metilación del ADN es un mecanismo común de inactivación de genes supresores tumorales seleccionado naturalmente por las células tumorales. Además, realizamos ensayos fenotípicos utilizando modelos de células AML en los que *BCL7A* estaba silenciado por metilación del ADN genómico. Estos ensayos sugieren que *BCL7A* desempeña un papel de supresor tumoral en modelos de AML tanto *in vitro* como *in vivo*.

También generamos un modelo de ratón Knock-out (KO) inducible de *Bcl7a* para estudiar los posibles efectos de *Bcl7a* en células y tejidos hematológicos *in vivo*. Sin embargo, la deleción de *Bcl7a* no dio lugar a cambios fenotípicos.

Por otro lado, utilizando una herramienta molecular basada en CRISPR (repeticiones palindrómicas cortas agrupadas y regularmente interespaciadas), llevamos a cabo una desmetilación dirigida del locus de *BCL7A* en una de nuestras líneas celulares de origen humano para evaluar su fenotipo después de la esperada restauración de la expresión de *BCL7A*. La ligera restauración de la expresión de *BCL7A* a nivel de ARN mensajero (ARNm) y proteína podría ser la explicación de la ausencia de cambios fenotípicos en la capacidad de crecimiento celular.

Los resultados obtenidos en esta tesis doctoral sugieren que *BCL7A* desempeña un papel de supresor tumoral en AML. Sin embargo, se necesitan más proyectos de investigación para obtener más información y determinar si *BCL7A* es o no un biomarcador útil para el diagnóstico, clasificación y pronóstico de pacientes de AML. En última instancia, esta investigación podría brindar conocimientos valiosos para el desarrollo de nuevas terapias y ofrecer resultados más prometedores para los pacientes con AML.

Objectives / Objetivos

Objectives

1. Study the B-Cell CLL/Lymphoma 7 Protein Family Member A (*BCL7A*) mutational and methylation status in external cohorts of acute myeloid leukemia (AML) patients.

2. Use appropriate AML cell models to perform *in vitro* and in *vivo* phenotypic assays to assess the potential tumor suppressor role of *BCL7A* in AML.

3. Evaluate the interactions of BCL7A protein with the rest of the mammalian switch/sucrose-non-fermenting (mSWI/SNF) complexes subunits in the context of AML.

4. Generate a conditional *Bcl7a* knock-out mouse model to study the putative implications of *Bcl7a* on hematological tissues and cells *in vivo*.

5. Perform an *in vitro* restoration of BCL7A expression in a cell model through targeted demethylation and assess whether there are phenotypic alterations.

Objetivos

1. Estudiar el estado mutacional y de metilación de *BCL7A* en cohortes externas de pacientes con AML.

2. Utilizar modelos celulares de AML apropiados para realizar ensayos fenotípicos *in vitro* e *in vivo* con el fin de evaluar el posible papel supresor tumoral de *BCL7A* en la AML.

3. Evaluar las interacciones de la proteína BCL7A con el resto de subunidades de los complejos mSWI/SNF en el contexto de la AML.

4. Generar un modelo de ratón knock-out condicional de *Bcl7a* para estudiar las posibles implicaciones de *Bcl7a* en tejidos y células hematológicas *in vivo*.

5. Realizar una restauración *in vitro* de la expresión de *BCL7A* en un modelo celular mediante desmetilación dirigida y evaluar si existen alteraciones fenotípicas.

Chapter 1.

Introduction

Chapter 1. Introduction

The main aim of this opening chapter is to provide a broad overview of the subjects to be studied within this doctoral thesis dissertation. The results chapters (Chapters 3 to 5) also include a brief background section that intends to introduce the reader to the data shown there.

This section begins with a description of cancer, the hematologic malignancy and the acute myeloid leukemia (AML) from a molecular biology perspective. Then, it ends giving details about the main character of this PhD research project: the *BCL7A* gene.

1.1 Cancer

Cancer is a term that encompasses a group of diseases characterized by uncontrolled cell growth which can originate in almost any tissue. Carcinogenesis is a complex, multistage process mainly involving genetic mutations which also may harbor epigenetic changes that result in the transformation of a healthy cell into a cancerous one (epigenetics is explained in greater depth in section "1.5 Epigenetic mechanisms"). These variations enable the cancer cell to acquire specific characteristics that allow it to surpass the proliferative rate of a healthy cell, leading to the formation of a tumor or neoplasm. In addition to uncontrolled growth, cancer cells can even invade

other organs in a process known as metastasis, which is the leading cause of death in cancer patients (Massagué & Obenauf, 2016).

Variations in exposure to risk factors and life expectancy contribute to the global diversity in the most prevalent cancer types. However, cancers do not occur randomly throughout the body, and this distinction is particularly obvious when comparing pediatric and adult malignancies (see Figure 1). Pediatric cancers are relatively uncommon (affecting 1 in 440 children). They exhibit a relatively low genetic mutational burden and typically originate during embryonic development. In contrast, one out of every two adults develop cancer, characterized by a higher mutational burden, and predominantly arises within epithelial tissues after the age of sixty. These patterns strongly indicate that cancer is not a stochastic process but is instead influenced by consistent factors in the development and aging of tissues (Jassim et al., 2023).

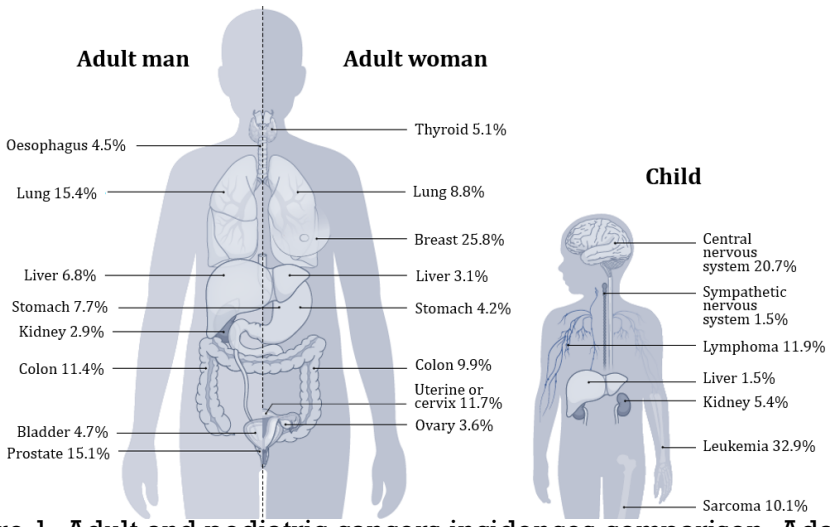

Figure 1. Adult and pediatric cancers incidences comparison. Adapted from (Jassim et al., 2023).

Worldwide, it's estimated that there were around 19.3 million new cancer cases and nearly 10.0 million cancer-related deaths in the year 2020. In addition, the global cancer burden is on the rise, driven by factors such as population growth, aging, and shifting patterns of risk factors associated with socioeconomic development. There is a connection between cancer's incidence on premature mortality and a nation's social and economic development level (Sung et al., 2021).

Cancer cells accumulate numerous genetic alterations over time, but only a selected few, known as driver mutations, are directly responsible for cancer progression and / or development. These driver mutations can differ between cancer types and individuals, sometimes remaining inactive for extended periods before becoming active at specific stages of cancer development. In some cases, they may only promote cancer when combined with other mutations. Identifying driver mutations is particularly difficult due to the significant heterogeneity in mutations, biochemical changes, and histological variations among tumors. Besides, the different types of cancer may present a different average number of driver mutations. For instance, in sarcomas, thyroid, and testicular cancers, typically one driver mutation per patient is identified, while bladder, endometrial, and colorectal cancers show an average of about four driver mutations per patient. The vast majority of driver mutations involve single-nucleotide substitutions or point mutations (Ostroverkhoa et al., 2023).

Also, the classical model that included "driver" and "passenger" mutations in cancer suggested that only the first mutations significantly impact tumor progression, while the last have no effect. However, recent research suggests that some putative passengers might have a subtle impact on tumor cell fitness by either promoting or inhibiting tumor growth. In other words, it has been observed that passenger mutations (which account for the largest number of mutations in cancer, around the 99%) collectively contribute to tumorigenesis beyond the influence of typical driver mutations (Kumar et al., 2020). Thus, this means that there are several degrees of impact among driver mutations as well as among passenger ones.

Among the cancer-associated genes identified through high-throughput sequencing and conventional methods, two key categories have garnered significant interest: tumor suppressor genes and oncogenes. In fact, tumor development can be driven by the activation of proto-oncogenes and / or by the loss of function of tumor suppressor genes. This interplay regulates the cell cycle mechanisms that promote tumor initiation and progression (Zhu et al., 2015).

a) Oncogenes:

In their wild-type (WT) condition, they are called proto-oncogenes. In this condition, they naturally participate in the control of cell proliferation and differentiation since they may function as growth factors, transducers of cellular signals, and

nuclear transcription factors (Kontomanolis et al., 2020; Torry & Cooper, 1991). However, they may be activated (and become oncogenes) by mutation, structural rearrangement or gene copy number gains, and potentially trigger the initiation of the tumor development (Soh et al., 2009). Some examples of well-known proto-oncogenes are: Ki-ras2 Kirsten rat sarcoma viral oncogene homolog (*KRAS*) and neuroblastoma rat sarcoma viral oncogene homolog (*NRAS*), which code for GTP-binding proteins; and MYC Proto-Oncogene, BHLH Transcription Factor (*C-MYC)* or MYCN Proto-Oncogene, BHLH Transcription Factor (*N-MYC)*, which are nuclear proteins (transcription factors) (Haschek et al., 2010).

b) Tumor suppressor genes:

The identification of genetically dominant, "activated" oncogenes contributed to the notion that a separate category of "antioncogenes" might restrain their actions and inhibit tumor formation. In fact, prior experiments had indicated the presence of genes capable of suppressing tumorigenicity which now are known as tumor suppressor genes. These genes play certain roles in regulating cell cycle checkpoints, signaling pathways related to cell growth, protein degradation, deoxyribonucleic acid (DNA) repair, responses to DNA damage, responses to low oxygen levels (hypoxia), and several stress responses. These metabolic pathways highlight the wide range of cell-autonomous processes that can be disrupted in cancer cells. Many well-known tumor suppressor genes have been discovered, such as tumor protein TP53 (*TP53*, nuclear transcription factor), phosphatase and tensin

homolog (*PTEN*) (modulates cell proliferation and apoptosis) and breast cancer type 1 susceptibility protein (*BRCA1*) (modulates cell cycle) among others. Usually, these genes need only one functional copy to exert their "cancer-preventive effects" (J. Sherr, 2004).

Maintaining a proper balance between proto-oncogenes and tumor suppressor genes is critical for normal cell function. External stimuli can promote or suppress the production and function of these proteins. Mutations that increase oncoprotein activity or inhibit tumor suppressor protein function can transform differentiated cells into cancer cells (Figure 2). This shift leads to uncontrolled growth and proliferation, which is a "metabolic switch" (Ghashghaeinia et al., 2019).

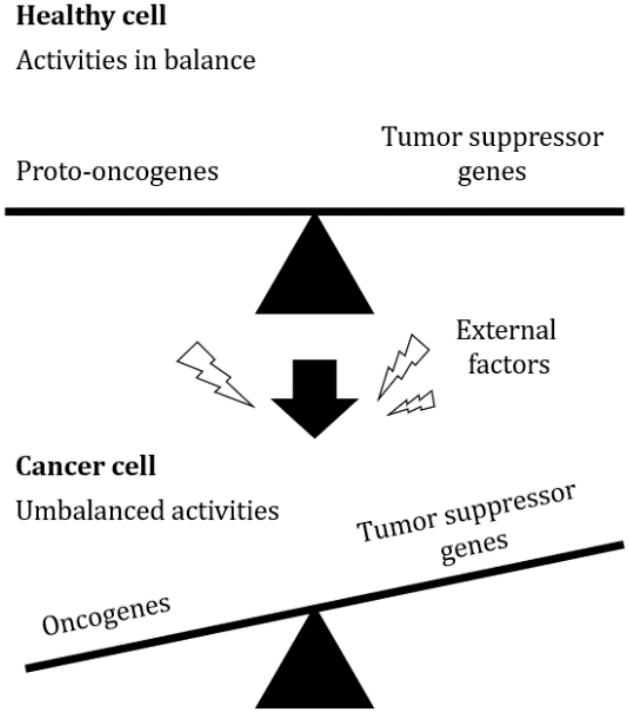

Figure 2. Schematic representation of the transformation of a healthy cell into a tumor cell due to an imbalance in the activity of proto-oncogenes and tumor suppressor genes. Adapted from (Ghashghaeinia et al., 2019).

These two gene categories in oncogenesis may seem antithetical. Paradoxically, some genes can exhibit both oncogenic and tumor-suppressor functions depending on the context. For instance, Notch receptors, crucial components of the evolutionarily conserved Notch signaling pathway, can be categorized as both oncogenes and tumor-suppressor genes. They play an oncogenic role in T-lineage acute lymphoblastic leukemia while performing a tumor-suppressor function in squamous epithelial cells (Aster et al., 2017; Shen et al., 2018).

Besides, in contrast to oncogenes, tumor suppressor genes typically adhere to the two-hit hypothesis. According to this theory, both alleles responsible for encoding a specific protein must be altered to give rise to an effect. If only one allele of the gene is damaged, the unaffected allele can still produce sufficient quantities of the correct protein to maintain its proper function. In simpler terms, mutant tumor suppressor alleles are generally recessive, while mutant oncogene alleles are usually dominant (Knudson, 1971). However, exceptions to the two-hit hypothesis for tumor suppressors exist, like specific mutations in the *TP53* gene. In such cases, mutated TP53 protein can act as a dominant negative, blocking the function of the natural protein produced by the non-mutated allele (Baker et al., 1990).

Another type of cancer related genes are the DNA damage response related genes. Eukaryotic cells use various enzymatic activities, like nucleases, helicases, polymerases, and more, for DNA repair. The precise regulation of these tools is crucial as their

misuse or inappropriate access to DNA can damage its integrity. Cells have developed strategies (through evolution) to accurately recruit and activate these factors at the right time and location. In fact, their deregulation can increase the chances for the development of several diseases such as cancer, neurological or immunological disorders (Ciccia & Elledge, 2010).

In an effort to try to provide a detailed definition of "what is cancer?", the Hallmarks of Cancer were introduced as a group of functional abilities that human cells acquire during their transition from a normal condition to a neoplastic growth state. In fact, these functional abilities, are vital for their ability to develop malignant tumors. The purpose in defining these Hallmarks of Cancer was to establish a conceptual framework that can enable the rationalization of the intricate characteristics of diverse human tumor types and variations by relating them to a shared set of fundamental cellular factors (Hanahan & Weinberg, 2000, 2011).

The first six defined Hallmarks of Cancer were: "resisting cell death", "sustaining proliferative signaling", "evading growth suppressors", "enabling replicative immortality", "activating invasion and metastasis" and "inducing angiogenesis" (Figure 3) (Hanahan & Weinberg, 2000).

Eleven years later, these authors even included two emerging hallmarks: "deregulating cellular energetics" and "avoiding immune destruction" (Hanahan & Weinberg, 2011). Besides, at that time they also defined two "enabling

characteristics": "genome instability and mutation" and "tumor-promoting inflammation". Since these last two "hallmark traits" on their own do not encompass the complexities of cancer pathogenesis, which involve the specific molecular and cellular mechanisms enabling preneoplastic cells to undergo the process of tumor development and acquire these abnormal phenotypic characteristics during malignant progression, they were named as "enabling characteristics" (Figure 3) (Hanahan & Weinberg, 2011).

The two emerging hallmarks mentioned above ("deregulating cellular energetics" and "avoiding immune destruction") have undergone enough validation, so they have been recently included within the fundamental set as Hallmarks of Cancer too (Figure 3) (Hanahan, 2022).

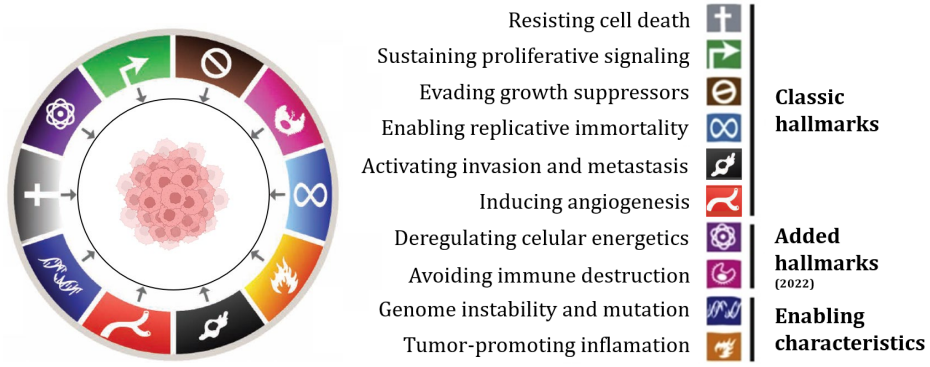

Figure 3. The Hallmarks of Cancer. Here are shown the currently accepted eight hallmarks of cancer and two enabling characteristics. Adapted from (Hanahan, 2022), and made using BioRender.com.

The progression of cancer follows an evolutionary path. As cancer cells evolve, they face several barriers within the body, including the primary tumor, the bloodstream, and different metastatic sites. To prevent or restrain the progression of cancer, it's necessary to understand the molecular evolutionary processes involved (Somarelli et al., 2020).

1.2 Hematologic malignancies

Hematopoiesis is the process that generates all of the blood cellular components. The hematopoietic stem cells (HSCs), primarily located in the bone marrow (BM), give rise to all blood cell types. The blood is a highly regenerative and adaptable tissue that constantly replaces millions of "aged" blood cells with new ones every second throughout an individual's life (Rieger & Schroeder, 2012).

The HSCs are able to carry out asymmetric and symmetric cellular divisions to achieve both self-renewal and the generation of differentiated blood cells. The equilibrium between these two modes of cell division is regulated by developmental and environmental signals, ensuring the generation of the required numbers of both stem cells and differentiated blood cells (Morrison & Kimble, 2006).

Hematologic malignancies are a spectrum of disorders that result from the disruption of normal hematopoiesis, giving rise to

a cancer cell. Depending on the lineage of this cell of origin, the hematologic malignancies include lymphocytic and myeloid leukemias (see Supplementary Figure 1), and depending on the speed of development they can be classified in chronic (slower) and acute (faster). Therefore, leukemias in general can be classified in four major groups as follows: chronic lymphocytic leukemia (CLL), chronic myeloid leukemia (CML), acute lymphocytic leukemia (ALL) and acute myeloid leukemia (AML) (Figure 4) (Karagianni et al., 2021).

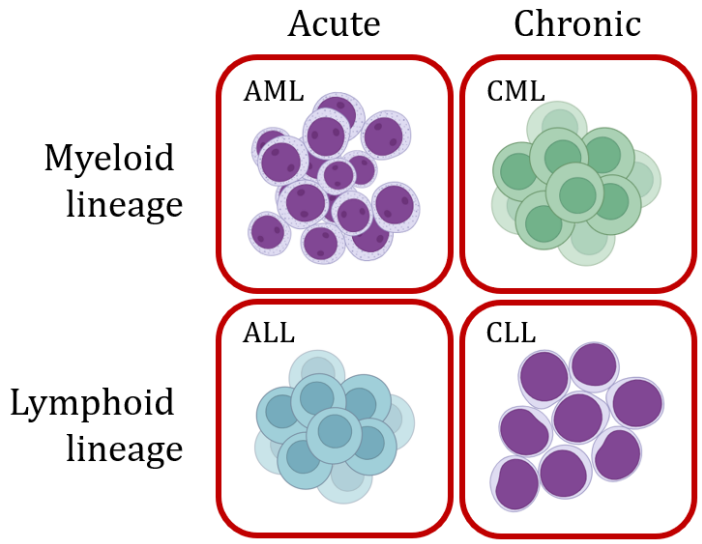

Figure 4. Types of leukemias depending on lineage and progression rate: acute myeloid leukemia (AML), chronic myeloid leukemia (CML), acute lymphocytic leukemia (ALL) and chronic lymphocytic leukemia (CLL). Figure made using BioRender.com.

Leukemia generally initiates within the BM and disseminates via the bloodstream (also considered as "liquid tumors"), whereas lymphoma typically begins in lymph nodes or the spleen (therefore, these are more similar to solid tumors) and disseminates through the lymphatic system.

While leukemia rates are decreasing worldwide, they are increasing in developed areas such as several European countries (for instance: France, Spain and Slovenia). Understanding the occurrence and mortality rates of hematologic malignancies is critical. This knowledge is vital for directing efforts towards prevention, enhancing clinical practices, and allocating research resources effectively (N. Zhang et al., 2023). Therefore, research projects focused on deciphering the molecular characteristics of hematologic disorders can lead to improvements in patient outcomes.

1.3 Acute myeloid leukemia

AML encompasses various hematopoietic malignancies originating from myeloid precursors and is associated with unfavorable outcomes. Although AML is not very frequently diagnosed, it represents approximately 1.1% of cancer patients and it stands as the second most prevalent leukemia form, contributing to about 1.9% of cancer-related deaths (considering the U.S. population) (Stubbins et al., 2022). Typically, to diagnose AML, the patient should present at least 20% blasts in the BM or peripheral blood (Döhner et al., 2010).

Non-random cytogenetic abnormalities are the primary determinant of AML prognosis. In fact, the diagnostic karyotype allows the identification of the different AML subtypes and therefore the determination of their relative prognosis. These

cytogenetic alterations together with common AML genetic mutations are taken into account to decide the best risk-adapted treatment (Grimwade et al., 2010; Mrózek et al., 2007).

Besides, AML exhibits a relatively low mutational burden compared to other cancer types, indicating a significant reliance on epigenetic mechanisms like abnormal methylation and chromatin remodeling alterations (explanations in greater depth about DNA methylation and chromatin remodeling are included in sections "1.5 Epigenetic mechanisms" and "1.6 Chromatin remodeling" respectively) (M. S. Lawrence et al., 2013; The Cancer Genome Atlas Research Network, 2013). These epigenetic dysregulations occur because the epigenetic regulators are often altered in AML by chromosomal translocations, somatic mutations, or genomic amplifications. In fact, many of these alterations directly influence the development of AML. Mutations in these regulators are frequently found in the initial clone and persist after therapy, suggesting their potential role in creating a premalignant state that is susceptible to acquiring further mutations and becoming fully malignant (Y. Sun et al., 2018). Therefore, despite the low mutational burden in AML, the genes involved in epigenetic modulation are usually dysregulated in this cancer type, promoting AML development and / or progression.

With the technological advancements and the knowledge provided by the omic sciences, the classification of the different subtypes of AML has been undergoing several modifications and updates since the 1970s. However, before this, in the 1970s, a

consortium of leukemia experts from France, the United States, and the United Kingdom (FAB) classified AML into 9 distinct subtypes based on the cell of origin and the level of cellular maturity, relying on the visual appearance of leukemia cells under routine staining with a microscope (Table 1).

FAB subtype	Name
M0	Undifferentiated acute myeloblastic leukemia
M1	Acute myeloblastic leukemia with minimal maturation
M2	Acute myeloblastic leukemia with maturation
M3	Acute promyelocytic leukemia (APL)
M4	Acute myelomonocytic leukemia
M4 eos	Acute myelomonocytic leukemia with eosinophilia
M5	Acute monocytic leukemia
M6	Acute erythroid leukemia
M7	Acute megakaryoblastic leukemia

Table 1. The French-American-British (FAB) classification of AML. Adapted from www.cancer.org .

Due to the important advances in biomedical research technology (next-generation sequencing [NGS] and flow cytometry, among other technologies) in the last decades, it has become evident that the genetic characteristics of each case of AML must also be taken into consideration in order to establish its most accurate prognosis and to decide the most promising specific treatment. In fact, a group of authors with extensive expertise in the clinical, pathological, and genetic aspects of these conditions, recently formulated the International Consensus Classification (ICC) of myeloid neoplasms and acute leukemias

(Daniel A. Arber et al., 2022). The ICC aims to streamline the diagnosis and prognosis of these neoplasms, improve the treatment of affected patients, and enable the development of innovative clinical trials.

Simultaneously, the World Health Organization (WHO) recently published the 5th edition of the WHO Classification of Haematolymphoid Tumours. This classification method is based on the integration of morphological (cytology and histology), immunophenotypic, molecular, and cytogenetic data (Alaggio et al., 2022; Khoury et al., 2022). The authors here state that the disease types are still defined and diagnosed using various clinicopathologic parameters, but the focus is now on refining diagnostic criteria and identifying actionable biomarkers for treatment and prognosis (Khoury et al., 2022).

In short, each of these two cutting-edge classifications include by far more than 9 subtypes of AML, since they have been developed considering molecular and clinical data. However, there is a small proportion of AML cases that still do not have a clear or accurate subtype assignment with the consequences that this implies when deciding the treatment.

Besides, it is important to define here the myelodysplastic syndrome (MDS) due to its close relationship to AML. MDS is a hematological malignancy which is among the most prevalent ones. According to the definition, patients with MDS typically have a myeloblast count below 20%. However, around 30% of MDS

patients eventually develop AML (commonly termed "secondary AML to MDS"), which is diagnosed when the blast count increases to 20% or more of total nucleated cells in the BM (Menssen & Walter, 2020).

MDS has been observed clearly associated to advanced age individuals and to prior exposure to chemotherapy and radiation. It is characterized by cytopenias (a decrease in the amount of mature blood cells) and morphological dysplasia. Furthermore, AML originated from pre-existing MDS can be distinguished from de novo AML by the presence of distinct mutations, such as those affecting splicing factors and specific epigenetic regulators (Sperling et al., 2017).

Despite the usual low mutation burden of AML compared to other cancer types (M. S. Lawrence et al., 2013), NGS has revealed numerous frequently occurring somatic mutations in AML patients. The recurrently mutated genes in AML are fms-like tyrosine kinase 3 (*FLT3*), nucleophosmin 1 (*NPM1*), DNA methyltransferase 3 alpha (*DNMT3A*), isocitrate dehydrogenase (NADP(+)) 1 (*IDH1*), isocitrate dehydrogenase (NADP(+)) 2 (*IDH2*), tet methylcytosine dioxygenase 2 (*TET2*), Runt-related transcription factor 1 (*RUNX1*), *TP53*, *NRAS*, CCAAT enhancer binding protein alpha (*CEBPA*) and WT1 transcription factor (*WT1*). Mutations of many of them are currently considered relevant molecular risk factors in AML (Kantarjian et al., 2021; Metzeler et al., 2016).

The *FLT3* gene encodes a receptor tyrosine kinase which is mainly found in hematopoietic progenitor cells. This receptor mediates the proliferation and differentiation of these cells, and it is one of the most mutated gene in AML. Approximately 25% of adult AML patients will exhibit *FLT3* internal tandem duplication, and 10% will have *FLT3* tyrosine kinase domain point mutations or deletions (Sandhöfer et al., 2016; J. C. Zhao et al., 2022).

Regarding the *NPM1* gene, it encodes a ubiquitous multifunctional protein that is mainly present within the nucleolus. Notably, *NPM1* mutations are prevalent in adult AML, affecting around to 30% of cases. In normal conditions, the NPM1 protein is involved in ribosome synthesis, genomic stability, DNA repair, cellular proliferation and stress response. A hallmark characteristic of *NPM1* mutants is their aberrant presence in the cytoplasm. This fact allowed the researchers to detect this mutation through immunohistochemistry before the NGS era. The presence of *NPM1* mutations in a population of cells showing clonal hematopoiesis seems to be enough for the development of AML (Falini et al., 2020; Hindley et al., 2021; Zarka et al., 2020).

Furthermore, a better understanding of key molecular characteristics, such as genes with tumor suppressor properties in AML, can refine the classification of AML patients and, consequently, treatment approaches for this devastating disease (Wallwitz et al., 2021).

Genes related to DNA methylation (an epigenetic mechanism), such as *DNMT3A*, *IDH1*, *IDH2*, and *TET2*, exhibited frequent mutations, particularly in cytogenetically normal karyotype AML cases. DNA methylation, that yields the silencing of tumor-suppressor genes, has been related not only to the development of leukemia but also to the clonal progression from MDS to AML. Around 20% of the AML cases present mutations in *DNMT3A*, *IDH1* or *IDH2*, while *TET2* is mutated in approximately the 10%. *IDH1* and *IDH2* are metabolic enzymes whose mutations affect alpha-ketoglutarate dependent enzymes such as the TET family enzymes and lysine demethylases, resulting in a characteristic hypermethylated phenotype (Ferrone et al., 2020; Issa & DiNardo, 2021; Park et al., 2020).

The transcription factor *RUNX1* is critical for normal hematopoiesis development. This gene is generally regarded as a tumor suppressor in myeloid neoplasms. Inactivating mutations in *RUNX1* are frequently identified in individuals diagnosed with MDS and cytogenetically normal AML (Goyama et al., 2013). In addition, *TP53* activity is related to cell cycle control and DNA damage response. *TP53* mutations are present in around 10% of AML cases, constituting an independent subtype associated with an unfavorable prognosis (Grob et al., 2022).

Among the above-mentioned genes, some have been shown to act as tumor suppressor genes specifically in AML, such as *WT1*, *TET2* and the promyelocytic leukemia (*PML*) gene. The *WT1* transcription factor plays a critical role in cell growth and

development, with varying levels of expression at different stages of cell development. In normal human BM, *WT1* has low expression in HSC and acts as a tumor suppressor gene (Kavianpour et al., 2016; Ogawa et al., 2002).

Regarding *PML*, it functions as a tumor suppressor gene in normal cells, forming nuclear structures known as *PML* nuclear bodies. These bodies play various intracellular roles, including cell cycle regulation, inhibition of cell growth, promotion of apoptosis, and modulation of transcription, among others. In acute promyelocytic leukemia (APL, M3 in the FAB classification), the *PML* gene fuses with the retinoic acid receptor alpha (*RARA*) gene to form the t(15;17) fusion protein found in 97% of APL patients. This PML-RARA fusion protein inhibits the differentiation of myeloid hematopoietic cells. Currently, the presence of this fusion protein generally indicates a favorable prognosis. Detection of the *PML-RARA* fusion gene is critical for the diagnosis of APL and the identification of minimal residual disease, allowing the prediction of relapse even in the absence of t(15;17) by methods such as karyotyping and fluorescent in situ hybridization (Kavianpour et al., 2016; Salomoni & Pandolfi, 2002).

Mutations in *TET2*, often seen as deletion or uniparental disomy, increase the self-renewal capacity of leukemic stem cells. These mutations result in impaired hematopoiesis, monocytosis, and the occurrence of hematopoiesis outside the BM. They are associated with older patient populations, higher white blood cell and blast cell counts, decreased platelet counts, normal

chromosomal structure, intermediate risk cytogenetics, and concurrent mutations in *NPM1* and in additional sex combs like transcriptional regulator 1 (*ASXL1*). Notably, *TET2* mutations are usually found in association with *IDH* genes mutations, as *TET2* mutations are sometimes caused by neomorphic *IDH* mutations (Kavianpour et al., 2016; Moran-Crusio et al., 2011).

Some other genes that have been observed to play a tumor suppressor role in AML are *DNMT3A*, *ASXL1*, *TP53*, *NPM1*, *CEBPA,* enhancer of zeste 2 polycomb repressive complex 2 subunit (*EZH2*) and GATA binding protein 2 (*GATA2*) (Panuzzo et al., 2020).

Besides, *ASXL1* is a chromatin-binding protein that belongs to the polycomb group and may play a role in epigenetic regulation. This gene is frequently mutated in various myeloid malignancies such as AML, MDS, myeloproliferative neoplasms and chronic myelomonocytic leukemia. These mutations are often associated with aggressive disease behavior and poor clinical prognosis (Fan et al., 2021).

The Cancer Genome Atlas Research Network in 2013, as well as Grimwade and colleagues, outlined nine categories of genes commonly mutated in AML patients that affect basic cellular functions. On average, each patient had mutations in 13 genes, with the most common mutations occurring in genes involved in signaling activation pathways (Figure 5) (Grimwade et al., 2016; The Cancer Genome Atlas Research Network, 2013).

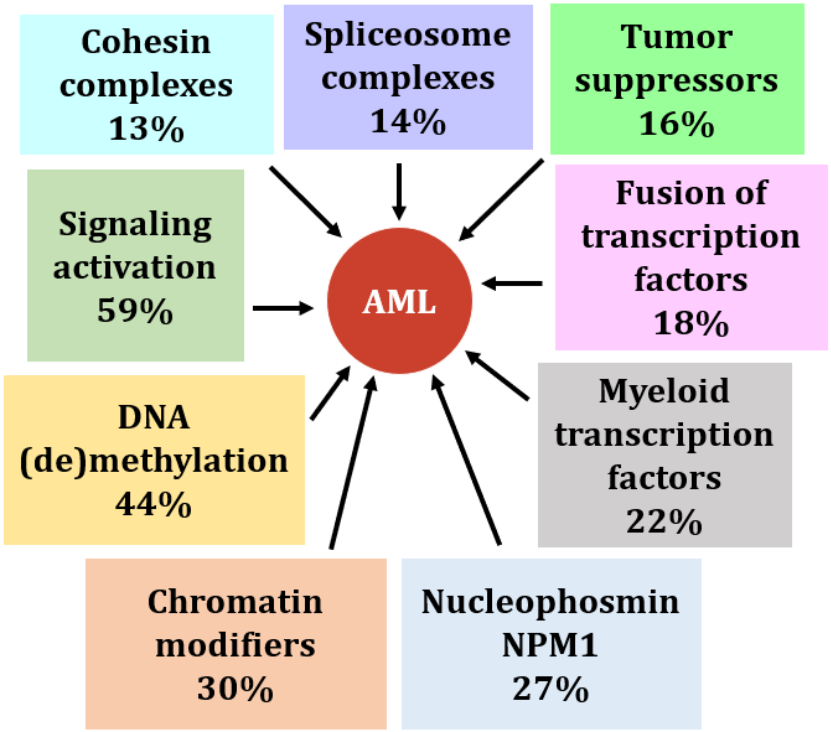

Figure 5. Classification of frequently mutated genes and their frequencies among AML patients. Since most AML cases involve mutations in at least two genes, the percentages indicate the prevalence of occurrence. Adapted from (Wallwitz et al., 2021).

In regard to the AML treatments, the progress in comprehending the pathophysiology and advancing AML therapy has accelerated in the last decades. For instance, the introduction of cytarabine and anthracyclines in the 1970s, combined into the "7+3 regimen" was a longstanding standard of care, yielding long-term cures for 30-40% of younger AML patients. The following figure displays AML outcomes at MD Anderson for patients over the period from 1970 to 2017 (Figure 6) (Kantarjian et al., 2021).

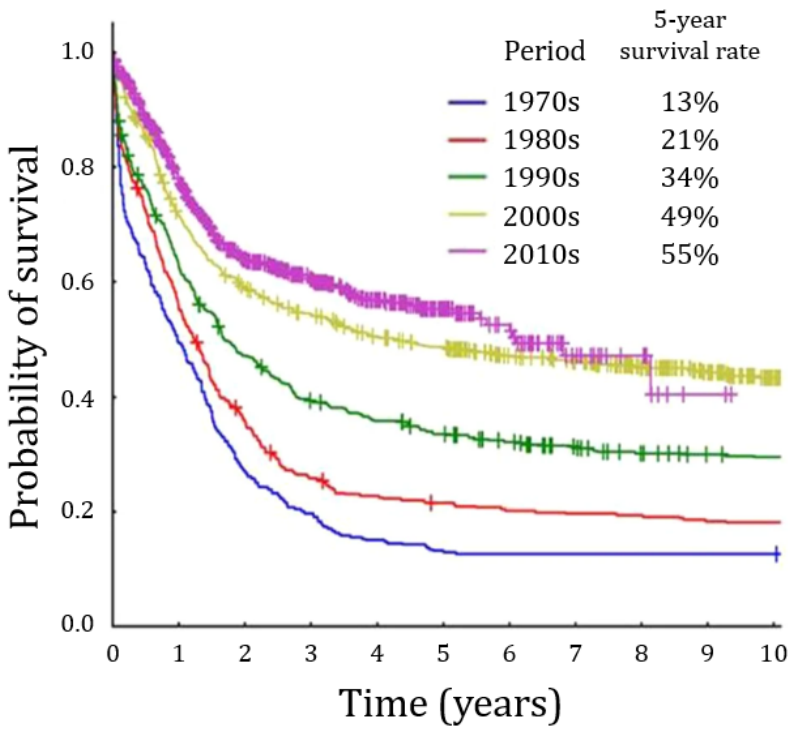

Figure 6. Survival rates improvement of de novo acute myeloid leukemia (AML) at MD Anderson from 1970 until 2017 in AML patients under 60 years old. Adapted from (Kantarjian et al., 2021).

This improvement in the survival of AML patients over the last few decades demonstrates the relevance of the results of biomedical research in this field.

Currently, ongoing research and recently approved treatments for AML patients encompass:

- Combining epigenetic therapy with hypomethylating agents (HMAs) like azacitidine and decitabine (DAC), along with venetoclax, a B-Cell CLL/Lymphoma 2 (*BCL2*) inhibitor *BCL2* being an apoptosis regulator, for older or less fit patients. For younger and healthier patients,

combinations of intensive chemotherapy and venetoclax are being explored.

- Researching on the use of *FLT3* inhibitors, such as gilteritinib, midostaurin, sorafenib, quizartinib, crenolanib, and others, in conjunction with intensive chemotherapy or low-intensity therapy for *FLT3*-mutated AML.
- Studying the addition of IDH inhibitors (ivosidenib for *IDH1* and enasidenib for *IDH2*) and / or venetoclax for AML with *IDH1/2* mutations.
- Exploring the roles of the anti-cancer agent APR-246, a *TP53* modulator, and magrolimab, an anti-CD47 monoclonal antibody that enhances macrophage-mediated phagocytosis, in *TP53*-mutated AML.
- Assessing menin inhibitors for mixed-lineage leukemia (MLL1)-rearranged acute leukemia.
- Evaluating the combination of small-molecule targeted therapies, with or without standard intensive chemotherapy or HMAs, to extend survival and potentially improve cure rates in previously incurable AML subsets.
- Establishing maintenance therapy as a crucial strategy in AML, similar to ALL.
- Developing oral anti-AML treatments like oral decitabine and oral azacitidine to replace and enhance the effects of injectable therapies.
- Enhancing T-cell immune responses to AML through approaches such as Bi-specific T-cell engagers (BiTEs),

checkpoint inhibitors, and chimeric antigen receptor (CAR)-T-cell therapies (Kantarjian et al., 2021).

Remarkably, 30% of the AML cases have mutations in chromatin modifiers, and 44% of them have an aberrant DNA methylation (see Figure 5). Therefore, studying these molecular features to better understand the complexity of AML basis may lead to an improvement in the clinic for the diagnosis and classification of AML patients.

In addition, recent advancements in single-molecule resolution technologies reveal that fluctuations in transcription dynamics (gene expression) and resulting transcript numbers contribute to cell-to-cell variability, perhaps affecting tissue homeostasis and diseases, including cancer and AML (Wheat & Steidl, 2021).

1.4 Chromatin and gene expression regulation

In usual circumstances, all the diverse cell types in the human body share identical genetic material. The DNA serves as an adaptable resource for responding to various environmental and developmental cues through different gene expression patterns. To manage this, eukaryotic cells present a highly dynamic DNA storage system known as chromatin, where DNA is organized into nucleosomes by wrapping it around histone proteins (Gibson et al., 2023).

A nucleosome core is formed when two sets of each histone protein (H2A, H2B, H3, and H4) come together to create an octamer. This core structure consists of approximately 145-147 base pairs (bp) of DNA wrapped around it. This nucleoprotein complex is highly conserved and appears approximately every 200 ± 40 bp within all eukaryotic genomes (Luger et al., 1997).

The technological advances in genomics and high-throughput techniques have revealed that the nucleosome-free regions are a distinctive feature of actively transcribed genes, particularly when their regulatory elements (promoters and enhancers) are exposed and accessible (Lai & Pugh, 2017). Therefore, the arrangement of nucleosomes plays a crucial role in regulating access to genetic information, affecting various cellular processes that require DNA unwinding, such as replication, DNA repair, and transcription (Luger et al., 2012).

Gene expression is the conversion of genetic information into function. This takes place through the transcription of ribonucleic acid (RNA), which can code for proteins or serve other roles as functional non-coding RNA (ncRNA) such as ribosomal RNA (rRNA), transfer RNA (tRNA) and small RNAs among others (Doug Chung & Le Roch, 2013).

Gene expression regulation is a pivotal phenomenon in many fundamental biological processes, from the development of organisms and cellular differentiation to maintenance of tissue homeostasis, immunity processes and responses to cellular stress.

Besides, gene expression can be subject to regulation and modulation at various stages, including transcription initiation, splicing and alternative splicing, messenger RNA (mRNA) stability, post-transcriptional regulation, and, ultimately, through translational and post-translational mechanisms (Doug Chung & Le Roch, 2013).

Over the past two decades, substantial progress has been achieved in the knowledge of the molecular basis of transcription, the significance of chromatin and its modifications, and the roles of enhancers and non-coding RNAs (Pope & Medzhitov, 2018). In fact, emerging technologies such as single-cell approaches (single cell Assay for Transposase-Accessible Chromatin using sequencing [scATAC-seq] and single cell RNA sequencing [scRNA-seq], among others) have provided deeper insights into genome functionality and the mechanisms underlying gene expression patterns spanning diverse cell types and tissues (Heumos et al., 2023). However, these innovative approaches gave rise to new inquiries regarding the same subject (Pope & Medzhitov, 2018).

Various diseases and syndromes, such as cancer, autoimmune disorders, neurological diseases, diabetes, cardiovascular issues, and obesity, can result from mutations in regulatory regions. These mutations may affect the transcription factors, co-factors, chromatin regulators, and ncRNAs that interact with these genomic elements, showing the huge relevance of the

gene expression regulation molecular mechanisms over disease development (Lee & Young, 2013).

1.5 Epigenetic mechanisms

In 1942, Waddington introduced the term 'epigenetics,' defining it as alterations in phenotype that occur independently of genotype changes. This concept aimed to elucidate developmental aspects that lacked detailed mechanistic explanations (Waddington, 1942). Currently, we understand that epigenetic processes facilitate the transmission of gene expression patterns without modifying the DNA sequence. Instead, they modify chromatin, the dynamic structure of our genetic information. In healthy cells, the epigenetic mechanisms complement the DNA code, ensuring the stability of gene expression profiles and the determination of cell identities. Although the significance of epigenetic regulation has been acknowledged for some time, the precise enzymatic characterization of distinct chromatin states that activate or suppress gene functions was previously absent (Allis & Jenuwein, 2016).

In fact, technological advancements, including techniques like chromatin immunoprecipitation followed by NGS (ChIP–seq) and its variants, have facilitated the precise analysis of the epigenome down to the base-pair level. This has enabled comprehensive 'epigenomic profiling' in both healthy and

diseased cells and tissues. Essentially, many of the known chromatin epigenetic modifications are reversible, offering significant potential for therapeutic interventions that harness the dynamic nature of epigenetic control (Allis & Jenuwein, 2016).

It is known that epigenetics encompasses a range of covalent modifications affecting nucleic acids and histone proteins that modulate gene function, expression, and chromatin structure. This epigenetic control happens on multiple levels, comprising DNA methylation, histone modifications, chromatin remodeling, and the modulation of ncRNAs (Figure 7) (Y. L. Wu et al., 2023).

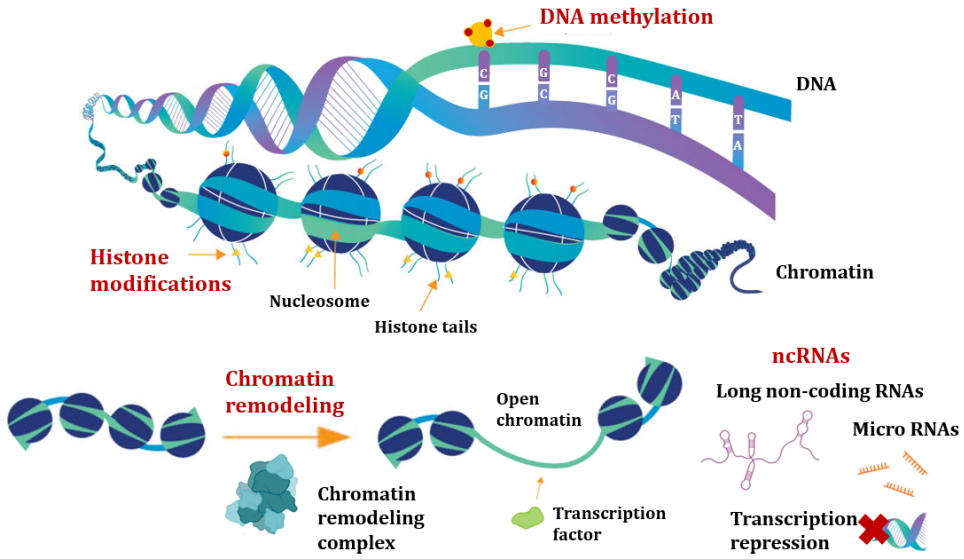

Figure 7. Schematic representation of the main epigenetics mechanisms: DNA methylation, histone modifications, chromatin remodeling and ncRNAs' regulation. Adapted from www.whatisepigenetics.com and www.foghorntx.com .

Regarding DNA methylation, the methylation of the fifth carbon of cytosines (5-methylcytosine) is an ancient modification

found in bacteria and early eukaryotes, mainly in the context of cytosine-guanine (CpG) dinucleotides. In mammals, this modification plays a role in transcriptional repression, genomic imprinting, and X-chromosome inactivation. CpG methylation is widespread, and its dysregulation is linked to various diseases, especially cancer. DNA methylation also serves to repress transposons, control germline-specific genes, and is enriched in certain repetitive sequences and gene bodies, although its exact functions in these contexts remain unclear. During embryogenesis, the mammalian genome undergoes two waves of CpG methylation reprogramming, post-fertilization and after germline cell specification. Recent advancements in genetics and epigenomics research have shed light on the dynamics of DNA methylation during development, and precise epigenome editing tools are increasingly being used to study its locus-specific functions (Greenberg & Bourc'his, 2019).

Besides, a CpG island is a DNA region spanning at least 200 base pairs, exhibiting a GC content exceeding 50%, and having a CpG ratio (observed versus expected) equal to or greater than 0.6 (Gardiner-Garden & Frommer, 1987). While CpG sites included in CpG islands are typically not methylated in mammalian genomes, CpG sites in other genomic regions are predominantly methylated and are less abundant due to the high mutation rate at 5-methylcytosine (Antequera & Bird, 1999). Remarkably, tumor suppressors' promoter CpG islands hypermethylation is a prevalent feature observed across all types of human cancers, impacting diverse cellular pathways with a distinct profile for

each tumor type. In addition to classical tumor-suppressor and DNA repair genes, this hypermethylation affects genes associated with premature aging and microRNAs that possess growth-inhibitory functions (Esteller, 2007; Lopez-Serra & Esteller, 2012; Nishiyama & Nakanishi, 2021). Moreover, methylation within gene promoters has received considerable attention because it is typically associated with downregulation or silencing of gene expression. Recently, however, it has also been observed that methylation within the first intron is often negatively correlated with gene expression (Anastasiadi et al., 2018).

Concerning histone modifications, the nucleosome core is formed by histones' globular regions, while their amino terminal domain (N-terminal) tails protrude and are rich in posttranslational modifications. These modifications can occur on the nucleosome core's lateral surface which is in contact with the DNA, impacting chromatin structure by changing histones' charge, interactions between nucleosomes, and recruiting specific proteins. Histone modifications are modulated by enzymes and may be produced in response to internal and / or external cues. These modifications may affect chromatin compaction, nucleosome dynamics, and gene transcription. Dysregulation of these processes are commonly detected in human cancers, since they can disrupt the balance of gene expression through gene gain or loss of function, increased expression, suppression through promoter hypermethylation, chromosomal translocations, or mutations affecting histone-modifying enzymes or even the modification site of the histone.

Additionally, mutations in chromatin-bound proteins are frequently found in cancer, and some may drive cancer progression. Overall, this dysregulation can lead to uncontrolled cell growth, invasion, metastasis, and resistance to treatment (M. Lawrence et al., 2016; Z. Zhao & Shilatifard, 2019).

On the other hand, most of the human transcriptome consists of ncRNAs originating from intergenic, antisense, or overlapping regions with protein-coding genes. ncRNAs make up the vast majority of the human genome (around the 98%). For a long time, these ncRNAs were considered as "transcriptional noise". However, advances in RNA sequencing and bioinformatics have unveiled their substantial roles in gene expression regulation. In fact, recent comprehensive transcriptomic analyses of ncRNAs in tissues and circulating fluids of cancer patients have revealed these RNAs as promising biomarkers. Thus, ncRNAs hold potential for enhancing cancer diagnosis and prognosis (Le et al., 2021).

In addition, epigenetic dysregulation, triggered by recurrent translocations or mutations in transcription factors and chromatin regulators, is a hallmark of AML. Hence continued research and advancement in epigenetic therapies could significantly enhance outcomes for AML patients (Fennell et al., 2019).

Last but not least, chromatin remodeling consists of modifications in the nucleosomes leading to changes in the

chromatin compaction degree, hence affecting DNA transcription, enabling or preventing the binding of transcription factors and other DNA-interacting proteins that regulate gene expression (Tang et al., 2010). In the following section, we describe chromatin remodeling in greater depth since it is one of the main topics related to this doctoral thesis.

1.6 Chromatin remodeling

Chromatin allows DNA compaction, but it also plays a crucial role in regulating DNA transcription, as described earlier. Specifically, in eukaryotic organisms, the expression of certain genes is restricted until they become accessible to the RNA polymerase and transcription factors. Hence, to enable gene expression, chromatin must undergo a process referred to as "chromatin remodeling" to open up and allow access to RNA polymerase and transcription factors (Jiang et al., 2023).

Chromatin remodeling complexes, also known as chromatin remodelers, are large multi-protein assemblies. Typically, these complexes consist of multiple subunits and use energy from adenosine triphosphate (ATP) hydrolysis to alter nucleosome structure and / or relocate nucleosomes yielding DNA accessibility during processes such as transcription, DNA replication and DNA repair (Centore et al., 2020; Clapier et al., 2016; Jiang et al., 2023; Tang et al., 2010). In general, their function is to enable the transcription machinery to access DNA. However,

certain chromatin remodelers are associated with transcriptional repression, hence these hinder DNA accessibility such as the mammalian Polycomb repressive complexes (Piunti & Shilatifard, 2021).

Nowadays, the ATP-dependent chromatin remodelers are classified into four distinct families based on the similarities and differences between their ATPase subunits and other subunits: switch/sucrose-non-fermenting (SWI/SNF), imitation switch (ISWI), chromodomain-helicase-DNA binding (CHD) and inositol requiring 80 (INO80) (Figure 8). Each subfamily specializes in achieving specific chromatin outcomes: assembly, access, or editing (Clapier et al., 2017; Reyes et al., 2021; Tyagi et al., 2016).

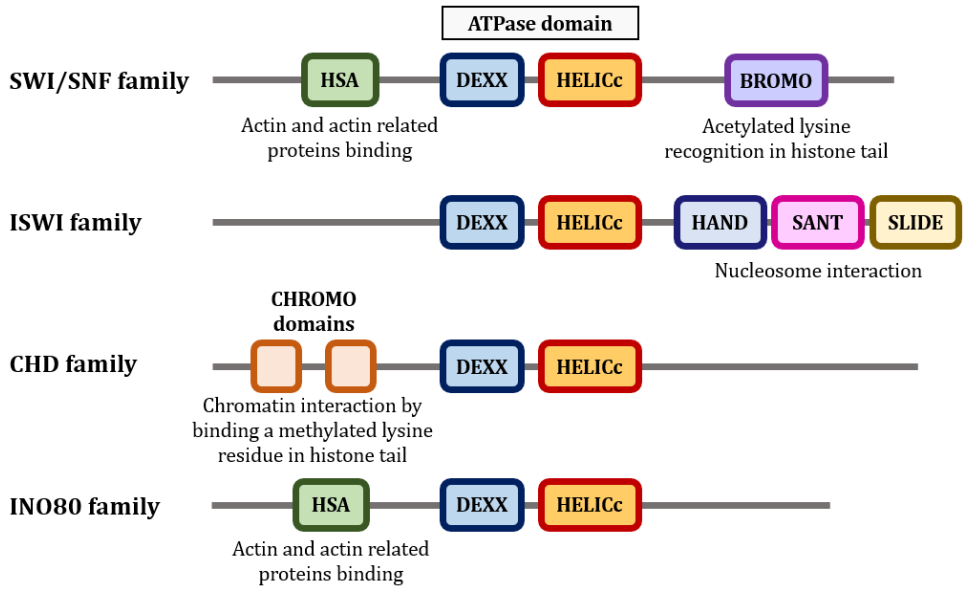

Figure 8. Diagram showing the major domains present in the different families of chromatin remodelers. All families contain DEXX and HELICc domains (helicase activity) within their ATPase modules. Adapted from (Tyagi et al., 2016).

Several chromatin remodelers functions have been unveiled so far: moving nucleosomes along the DNA, rearranging DNA around the histone octamer, removing part of the histone octamer (especially the H2A/H2B dimers), exchanging histone variants within the nucleosomes and removing the whole nucleosome from a DNA sequence (Figure 9) (Bracken et al., 2019).

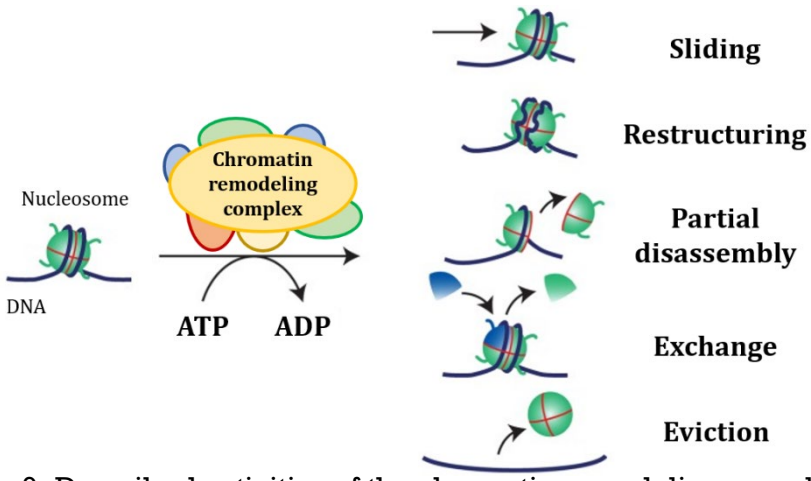

Figure 9. Described activities of the chromatin remodeling complexes. Adapted from (Bracken et al., 2019).

It is essential to point out that, extensive research over the past two decades has demonstrated that the aberrant activity of chromatin remodelers contributes significantly to genome reprogramming, that can lead to cancer development or even to resistance to cancer therapies (Y. Li et al., 2021; F. L. Zhang & Li, 2022).

Furthermore, in the context of AML, several studies have demonstrated the involvement of chromatin remodelers. For instance, the Chromodomain Helicase DNA Binding Protein 4

(CHD4) was found to be essential for cell growth of myeloid leukemic cells (Heshmati et al., 2018), and the Bromodomain PHD Finger Transcription Factor (BPTF) subunit of the Nucleosome Remodeling Factor (NURF) complex (part of the ISWI family), was observed to play a crucial role in regulating the survival of AML cells (Radzisheuskaya et al., 2023). Therefore, the knowledge at the molecular level of chromatin remodelers in myeloid disorders may guide the development or use of targeted enzyme inhibitors to address maturation defects that drive myeloid malignancies (Kongkiatkamon Sunisa et al., 2021).

1.7 The SWI/SNF complex

The SWI/SNF family of chromatin remodeling complexes was first identified in yeast (*Saccharomyces cerevisiae*) through independent screenings searching for mutations affecting the mating-type switching (SWI) and sucrose fermentation (Sucrose Non Fermenting [SNF]) pathways (Sudarsanam Priya & Winston Fred, 2000; Workman & Kingston, 1998). Also, a genetic screening looking for suppressive mutations of SWI/SNF phenotypes revealed that various histones and chromatin components were affected, indicating the potential involvement of these complexes in histone binding and chromatin organization (Winston Fred & Carlson Marian, 1992).

Notably, it has been observed that the SWI/SNF chromatin remodeling complexes represent a highly conserved group of

proteins found across various eukaryotic organisms (Hernández-García et al., 2022). Mammalian SWI/SNF (mSWI/SNF) complexes are large, weighing around 1 to 1.5 megadaltons. The latest studies have demonstrated that these complexes are composed of proteins encoded in 29 genes, some of which have multiple paralogs, resulting in a wide range of possible compositions (Mashtalir et al., 2018). In fact, up to 15 of these subunits can form part of a single mSWI/SNF complex (Kadoch et al., 2017). Therefore, this high combinatorial potential gives rise to tissue-specific and context-dependent mSWI/SNF complexes (Lessard et al., 2007; Ryme et al., 2009).

As of today, 3 subtypes of mSWI/SNF complexes have been discovered, taking into account which of the 29 subunits are specifically constituting one complex: canonical BRG1/BRM-associated factor (BAF), polybromo-associated BAF (PBAF) and non-canonical BAFs (ncBAF). Besides, the assembly order of these 3 subtypes of complexes has been described (Figure 10). Each mSWI/SNF complex always includes one ATPase subunit, specifically either SWI/SNF related, matrix associated, actin dependent regulator of chromatin, subfamily A, member 4 (SMARCA4, also known as BRG1) or SWI/SNF related, matrix associated, actin dependent regulator of chromatin, subfamily A, member 2 (SMARCA2, also called BRM) (Mashtalir et al., 2018).

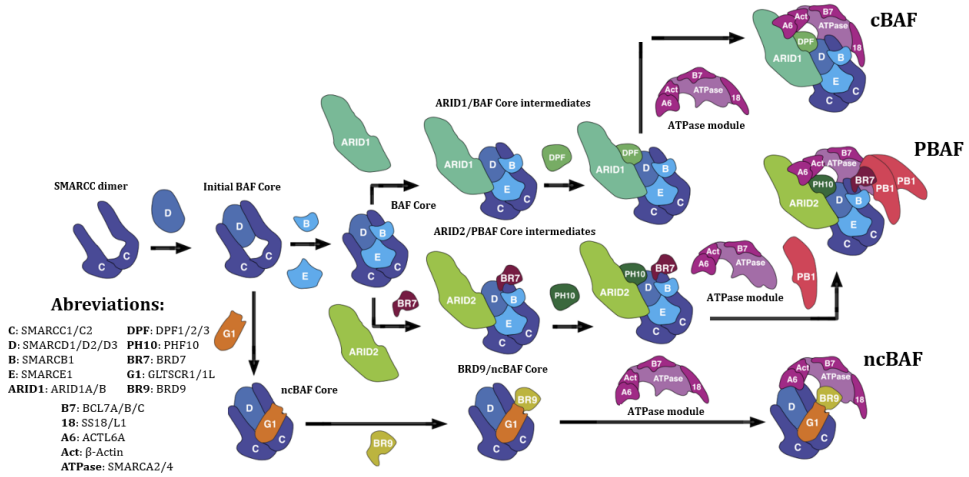

Figure 10. Assembly order (shown with black arrows from left to right) of the 3 mSWI/SNF complexes subtypes: canonical BRG1/BRM-associated factor (cBAF), polybromo-associated BAF (PBAF) and non-canonical BAFs (ncBAF). Adapted from (Mashtalir et al., 2018).

On the other hand, regarding the nomenclature of the mSWI/SNF subunits, it remains controversial and exhibits variability in its use within the literature. However, the SWI/SNF-related, matrix- associated, actin- dependent regulator of chromatin (SMARC) nomenclature was established and adopted by the Human Genome Organization (HUGO), and this nomenclature now is widely used around the bibliography (see Supplementary Table 1) (Mittal & Roberts, 2020).

In addition, mSWI/SNF complexes have called significant attention due to the notably high mutation rates in the genes encoding their subunits, spanning various human diseases, including cancer and neurological disorders. In fact, previous exome sequencing studies unveiled that more than 20% of human cancers carry mutations in genes encoding mSWI/SNF subunits (Kadoch et al., 2013). However, more recent deep sequencing

studies have shown that the mSWI/SNF complexes are among the most recurrently mutated functional elements across all tumor types in human, reaching an overall mutation rate of 25% (Mittal & Roberts, 2020). Along with this data, there is even increasing evidence suggesting that the mSWI/SNF complex plays a broad tumor suppressor role in cancer (Lu & Roberts, 2013; Tolstorukov et al., 2013).

Besides, several mSWI/SNF subunits have been more widely studied and better characterized than others. For instance, two well characterized subunits are the ATPase subunit SMARCA4 and AT-rich interaction domain 1A (ARID1A). SMARCA4 has been found to be mutated in approximately 5% to 7% of human cancers, and it is known that this gene acts as a tumor suppressor in several cancer types, such as lung, colon, bladder, and breast cancers among others (Mardinian et al., 2021; Medina et al., 2008). Regarding ARID1A, it stands out as the most commonly mutated SWI/SNF subunit in cancer (Mittal & Roberts, 2020; M. Zhou et al., 2021). Interestingly, despite the fact that *ARID1A* has been already observed acting as a tumor suppressor gene in many different cancer types (J. N. Wu & Roberts, 2013), it has been also found playing a dual role in liver related cancers acting as a tumor suppressor or as an oncogene depending on the context (Otto & Kadoch, 2017; X. Sun et al., 2017; S. Zhao et al., 2021). These findings supported the novel idea of a putative dual role (oncogenic and tumor suppressor) of already known cancer-related genes, depending on the context.

Along with the previous details, recent research has identified recurrent mutations in the mSWI/SNF subunits ARID1A, AT-Rich Interaction Domain 1B (ARID1B), SMARCA2, and AT-Rich Interaction Domain 2 (ARID2) in myeloid neoplasms (MDS and AML) (Madan et al., 2016; Yao et al., 2022). Moreover, despite the well-known widespread tumor suppressor role of mSWI/SNF complexes in cancer, several studies have found that these chromatin remodelers are also associated with the maintenance of AML (Buscarlet et al., 2014; Shi et al., 2013). Taking into account all the above information present in the literature, there is a straightforward relationship between mSWI/SNF complexes and AML.

Therefore, further studies for the understanding in depth of the roles of mSWI/SNF complexes in the development of myeloid neoplasias harbor a huge relevance. In fact, these research projects can provide useful data for the improvement of diagnostic and prognostic tools, based on patients' molecular details. In addition, these may even lead to the development of myeloid neoplasia targeted molecular therapies targeting mSWI/SNF subunits.

1.8 The mSWI/SNF subunit BCL7A

The mSWI/SNF subunit B-Cell CLL/Lymphoma 7 Protein Family Member A (BCL7A), the subject of study in this PhD thesis, is found among the not very well characterized subunits. In fact,

the specific molecular function of BCL7A protein remains unknown.

In 1996, the *BCL7A* gene was described (and named) for the first time when a research group cloned a complex molecular translocation present in the Wien 133 cell line (a Burkitt lymphoma cell model) and sequenced it to identify the unknown involved genes in the mentioned translocation (Zani et al., 1996).

Later in 1998, two other human genes of the BCL7 gene family, whose encoded proteins share 90% identity with the first 51 amino acids of human BCL7A, were first described: *BCL7B* and *BCL7C* (Jadayel et al., 1998) (see Supplementary Figure 2). They are paralogous genes of *BCL7A*, that are also known members of mSWI/SNF complexes (Kadoch et al., 2013). BCL7A, BCL7B and BCL7C are shared subunits of the 3 mSWI/SNF complexes subtypes (Supplementary Table 1), meaning that every mSWI/SNF complex harbor one subunit that belongs to the BCL7 gene family (Figure 10) (Mashtalir et al., 2018; Mittal & Roberts, 2020). Regarding this gene family, in several human tissues, like lung, liver, skeletal muscle, brain, and kidney, the expression of *BCL7A*, *BCL7B*, and *BCL7C* mRNA remains consistently low (Jadayel et al., 1998).

So far, two isoforms of the human BCL7A protein have been described. They are produced due to an alternative splicing in exon 5 (Figure 11).

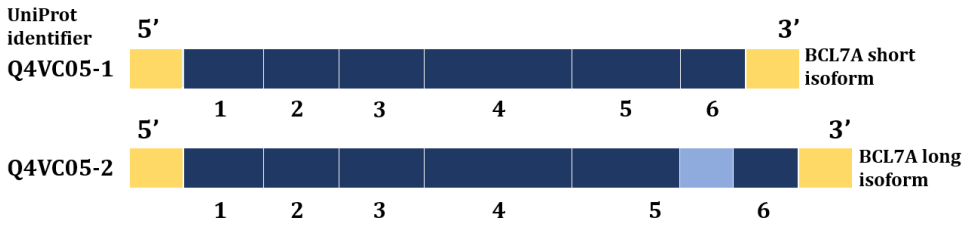

Figure 11. Diagram shownig human *BCL7A* gene genomic organization. Untranslated regions are colored in yellow and exons are colored in dark blue. The differential region within exon 5, distinguishing between short and long isoforms, is highlighted in light blue. Adapted from (Baliñas-Gavira et al., 2020).

After the *BCL7A* gene discovery, it has been reported in several occasions in the literature that the alterations of *BCL7A* are related to hematological disorders. In fact, a previous study that analyzed 44 published genome and / or exome sequencing studies to compare the mutation frequencies of the mSWI/SNF subunit genes found that *BCL7A* presented mutations in 19.7% of non-Hodgkin lymphomas and 21.7% of multiple myelomas (Kadoch et al., 2013).

Besides, it has been observed that, in the B-cell lineage, *BCL7A* is notably expressed in the germinal center (GC) reaction (Gao, 2007), a specific micro-environment found in secondary lymphoid tissues during T-cell-dependent antibody responses (Maclennan, 1994). However, it's absent in naive or memory B-cells. In contrast, *BCL7B* and *BCL7C* present uniform low-level expression across naive, GC, and memory B-cells (Klein et al., 2003).

In a previous research project developed by our research group, *BCL7A* was found to be clearly implicated in the

pathogenesis of Diffuse Large B-Cell Lymphoma (DLBCL), as BCL7A was experimentally shown to play a tumor suppressor role in *in vitro* and *in vivo* approaches. Furthermore, in a large cohort of DLBCL patients (N = 1575), our group found that there was a recurrent mutation in the first splice donor site of *BCL7A* (a previously overlooked non-coding mutation). This mutation results in a truncated protein (termed Δ27-BCL7A) that lacks its first 27 amino acids from its N-terminal domain and is unable to bind the rest of the mSWI/SNF complex. Notably, it must be pointed out that this Δ27-BCL7A variant does not play the tumor suppressor role shown by the WT BCL7A protein variant (Baliñas-Gavira et al., 2020; Carlos Baliñas-Gavira, 2020).

Furthermore, the results of the project described above highlighted the relevance of non-coding mutations. Hence, it prompted an additional study performed in our laboratory which showed that several key DLBCL genes frequently undergo splice site mutations. These mutations yield a predicted resulting aberrant mRNA in several cases (Andrades et al., 2022), giving a higher relevance to the usually overlooked mutations that are not within the gene coding sequences.

Along with our studies described above, the results from multiple previous research lines have also suggested that *BCL7A* may have significant roles in B-cell related malignancies (Blenk et al., 2007; Chapman et al., 2011; Kadoch et al., 2013; Ramos-Medina et al., 2013). In addition, there are several studies that have found alterations of *BCL7A* (such as gene deletion or gene silencing due

to genomic DNA methylation) related to cutaneous T-cell lymphoma (CTCL), and also related to the most frequent CTCL subtype: mycosis fungoides. Therefore, the authors of some of these studies suggest the putative tumor suppressor role of *BCL7A* in this cancer type (Carbone et al., 2008; Litvinov et al., 2013; Martinez-Delgado et al., 2004; Tracey et al., 2003; Van Doorn et al., 2005).

Overall, the literature has shown that there is a clear relationship between *BCL7A* expression and alterations in healthy and malignant lymphoid tissues (Baliñas-Gavira et al., 2020; Litvinov et al., 2013; Ramos-Medina et al., 2013). Nevertheless, regarding the relationship between *BCL7A* and the myeloid hematologic lineage, only one previous study suggested that *BCL7A* loss may be involved in CML progression and drug resistance based on the evidences observed in one CML patient (Yu et al., 2017).

Therefore, the *BCL7A* tumor suppressor role in hematologic malignancies has been previously well characterized in our research group (DLBCL) and in other research groups (CTCL) where *BCL7A* was found to be silenced by promoter methylation (Baliñas-Gavira et al., 2020; Van Doorn et al., 2005). Moreover, it is noteworthy that the gene silencing through DNA methylation is a common feature of tumor suppressors (Lopez-Serra & Esteller, 2012; Nishiyama & Nakanishi, 2021). Considering that the epigenetic mechanisms, chromatin modifiers and tumor suppressor genes are frequently altered in AML development, we

hypothesized that the BCL7A subunit of the mSWI/SNF complex may also play a relevant role in AML.

Then, novel research projects to study the *BCL7A* activity in the myeloid hematologic context were necessary to address several scientific questions, including functional approaches to complement the sequencing data. Eventually, these projects might provide relevant and useful knowledge for the development of innovative diagnostic and prognostic methods and / or new molecular therapies for patients with myeloid malignancies.

Chapter 2.

Materials

and Methods

Chapter 2. Materials and Methods

In this section we included a detailed description of the materials and methods that have been used to perform all of the scientific experiments and analyses that yielded the results of this PhD thesis project.

Regarding the Chapter 5, as the Clustered regularly interspaced short palindromic repeats (CRISPR)- DNMT1-interacting RNA (CRISPR-DiR) platform methods are part of the authors' and Harvard University's intellectual property, we cannot provide a detailed description here. However, the methods may be extrapolated from (Y. V Liu et al., 2020).

2.1 In silico analysis of *BCL7A* in AML patients and cell lines

To assess the frequency of mutation of the *BCL7A* gene in the external AML datasets, data from the Dependency Map (DepMap) Portal (https://depmap.org/portal/; data version 22Q2; disease subtype "AML", N = 53), the Cancer Genome Atlas Program (TCGA) Acute Myeloid Leukemia Project (TCGA-LAML: N = 160), and Therapeutically Applicable Research to Generate Effective Treatments (TARGET) (TARGET-AML: N = 17) were used. TCGA and TARGET data were obtained through the Genomic Data Commons (GDC) Data Portal (Data Release 31.0). Taking into

account these three cohorts together, a total of 230 patients (N = 230) were collected.

The *BCL7A* mRNA expression (RNA Seq V2 RSEM) and methylation (Illumina HM450 Bead-Chip) data of 160 AML patients from the TCGA-LAML were obtained through the cBioPortal database (https://www.cbioportal.org). Likewise, the gene expression and methylation data were downloaded from the TARGET-AML cohort using the R package 'TCGAbiolinks', as well as from Glass et al. cohort (Glass et al., 2017) from Gene Expression Omnibus (GEO; accession IDs: GSE6891 for gene expression, GSE98350 for methylation). In each case, the methylation values were obtained as the beta value of the probe or genomic position whose expression was most anticorrelated with the *BCL7A* expression, previously restricting the analysis to the *BCL7A* locus ± 400 bp.

Gene expression and reduced-representation bisulfite sequencing (RRBS-Seq) data of 32 AML cell lines were obtained from the DepMap Portal database. Negative correlations between expression and beta values of individual CpGs were evaluated using the Pearson correlation coefficient and p-values were false discovery rate (FDR) corrected for multiple comparisons.

2.2 Statistical analyses

Unless specified otherwise, all of the statistical analyses were performed using R (version 3.6.1). Normality of continuous data was evaluated using Q-Q plots and Shapiro–Wilk tests and the subsequent statistical tests were chosen in accordance with the previous tests.

2.3 Cell culture

The NB4 (FAB M3: APL) and M07e (FAB M7: acute megakaryoblastic leukemia, [AMKL]) cell lines were obtained from the German Collection of Microorganisms and Cell Cultures (Cat# ACC 207 and ACC 104 respectively, Deutsche Sammlung von Mikroorganismen und Zellkulturen, DSMZ, https://www.dsmz.de/).

These cell lines were grown in a cell culture incubator at 37 °C within a 5% (v/v) CO_2 atmosphere. They were cultured in Roswell Park Memorial Institute (RPMI) 1640 cell culture medium (Cat# L0498-500, Biowest, Riverside, MO, USA) always supplemented with 10% (v/v) of Fetal Bovine Serum (FBS) (Cat# 10,270–106, Gibco™ Thermo Fisher Scientific, Waltham, MA, USA), 1% (v/v) of L(+)-Glutamine (Cat# X0550-100, VWR, Radnor, PA, USA), 100 U/mL of penicillin and streptomycin using a ready-to-use solution (Cat# P0781-100ML, Sigma Aldrich / Merck KGaA, Darmstadt, Germany) and with 1% (v/v) of amphotericin B (Cat#

L0009-100, VWR, Radnor, PA, USA). From now on this culture medium will be called supplemented RPMI.

The NB4 and M07e cell lines underwent mycoplasma contamination analysis using Venor GeM-qEP (Minerva Biolabs, Berlin, Germany) yielding negative results.

All of the procedures including live cell lines were carried out inside a cell culture hood to ensure a sterile environment and prevent culture contaminations.

2.4 Bacterial transformation for plasmid amplification

When it was necessary to amplify a DNA plasmid, a bacterial transformation protocol was performed.

Here, the DH5α strain chemically competent *Escherichia coli* (E. coli.) that are cryopreserved in 200 µL aliquotes at -80°C in 1.5mL tubes (Cat# MCT-150-C, Axygen) was first thawed on ice. Then, at least 10 µL of a 0.1 ng/µL aqueous solution was prepared diluting the plasmid to be amplified using ultrapure distilled water (Water Purification system - Milli Q®, Merck Life Sciences, Darmstadt, Germany)

Once the bacteria were totally thawed, 10uL of the previously described plasmid dilution was added over the

bacteria and gently mixed by finger flicking the tubes (avoiding mixing by pipetting, since it can impair the bacteria). Then we incubated the mixture 30 min on ice.

The following step was the thermal shock at 42°C for 40-45s, using a waterbath without shaking the tubes to allow the artificial bacterial transformation (exogenous plasmidic DNA uptake). This step was followed by a 2 min incubation on ice to allow the bacteria to recover after the heat shock.

Afterwards, 100 µL of Luria–Bertani (LB) medium without antibiotics is added, followed by incubation of the samples for 30-45 min at 37°C, shaking at 600 revolutions per minute (rpm).

Next,100 µL of the previous bacterial culture is plated in a LB agar plate including 100 µg/mL of ampicillin, since all of the plasmids used for this project featured the Ampicillin Resistance cassette (sequence encoding for a β-Lactamase) (Cumming et al., 2022). The liquid bacteria culture was spread on the plate using a disposable spreader L-shaped (Cat# 612-1561, VWR, Radnor, PA, USA), followed by overnight (o/n) incubation at 37°C placing the plate upside down in the bacteria incubator shelf.

The following day, the plate with the bacteria colonies may be sealed using Parafilm® M (Cat# 291-1212, VWR, Radnor, PA, USA) and stored at 4 °C.

The LB mediums and the LB agar plates with ampicillin were prepared by the General Services Unit of our research center

(Pfizer-University of Granada-Junta de Andalucía Center for Genomics and Oncology Research, GENYO).

2.5 Plasmid amplification by miniprep or maxiprep

Upon having the plate with the transformed clones of bacteria, the proceedings were continued through single colony picking using one 100 µL micropipette tip per colony, and placing each within a disposable culture tube (Cat# 211-0085, VWR, Radnor, PA, USA) with 3-5 mL of liquid LB medium including ampicillin 100 µg/mL. Then, incubate at 37 °C o/n shacking at 260 rpm.

Depending on the amount of plasmid DNA needed miniprep (Cat# 21.222-4212, Biotools B & M Labs Ltd., Madrid, Spain) was performed for little amounts, or maxiprep (Cat# NA0310-1KT, Merck Life Sciences, Darmstadt, Germany) for larger amounts to amplify it, following their corresponding protocols.

From this 3-5 mL culture, miniprep can be directly performed, but to do a maxiprep, a 300 mL bacteria culture has to be produced. Therefore, to generate this larger bacteria culture, it is needed to pour the previous 3-5mL preculture in 300 mL of liquid LB medium including ampicillin 100 µg/mL contained in a

1L Erlenmeyer flask and incubate it at 37 °C o/n shacking at 260 rpm.

In general, the yield of a miniprep is around 100-600 ng/ µL in a total of 30 µL of ultrapure distilled water, and the common yield of a maxiprep is around 700-1300 ng/ µL in a total of 1-2 mL ultrapure distilled water. The different yields depend on each plasmid.

The concentration and purity of the amplified plasmids are always determined using a NanoDrop™ 2000 spectrophotometer (Cat# ND-2000, Thermo Fisher Scientific, Waltham, MA, USA).

2.6 Genomic DNA bisulfite conversion

To perform the genomic DNA bisulfite conversion, the EZ DNA Methylation-Gold™ Kit (Cat# D5005, Zymo Research, Irvine, CA, USA) was used. In addition, two commercial human genomic DNAs that were totally methylated (gDNA Meth) and unmethylated (gDNA Unmeth) (Cat# 59,695, QIAGEN, Hilden, Germany) were purchased to be used as controls.

2.7 Methylation-Specific PCR (MSP)

The Methylation-Specific Polymerase Chain Reaction PCR (MSP) is a molecular method able to rapidly assess the

methylation status of virtually any group of CpG sites within a CpG island (Herman et al., 1996).

Here, the MSP was performed using bisulfite converted genomic DNA as template. The two commercial genomic DNAs previously described (gDNA Meth and gDNA Unmeth) were included as controls. The kit KAPA HiFi Hotstart ReadyMix 1,25 mL (Cat# KK2601, 07958927001, Roche) was used.

The sequences of the MSP primers were obtained from Okada et al. (Okada et al., 2013). The couple of primers (forward and reverse: FW and RV respectively) to amplify the methylated sequence (M) was:

- MSP FW (M): 5'-GGTAGGCGACGTTTTAGTTC-3'
- MSP RV (M): 5'-GAATTAAAAACACCGATTCG-3'

And those to amplify the unmethylated sequence (U) were:

- MSP FW (U): 5'-TGGGGTAGGTGATGTTTTAGTTT-3'
- MSP RV (U): 5'-CCAAATTAAAAACACCAATTCAA-3'

The theoretical PCR (or MSP) product sizes were 110 bp for the (M) pair and 115 bp for the (U) pair due to primer length differences. Considering the (U) couple of primers, the exact genomic location of the amplicon is: chr12:122,459,288–122,459,402, within the GRCh37/hg19 genome assembly. The same amplicon location relative to the *BCL7A* start codon is 688 bp

upstream for the 3' end nucleotide of the FW primers, and 598 bp upstream for the first G closest to the 5' end of the RV primers.

These primers allow the evaluation of the methylation status of a total of 6 CpG sites, 3 CpG sites within the FW primer annealing sequence, and 3 CpG sites included within the RV primer annealing region.

It was followed the next PCR program:

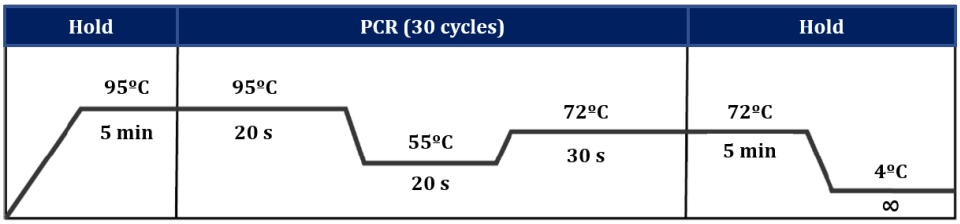

The Orange DNA Loading Dye (6x) (Cat# R0631, Thermo Fisher Scientific, Waltham, MA, USA) was added to the PCR products to be able to run them on 2% (m/v) agarose (Cat# H350004, LONZA) in Tris-Acetate-Ethylenediaminetetraacetic acid (TAE) buffer gels. Afterwards, the DNA amplicons were stained using the DNA intercalating agent ethidium bromide and visualized under an ultraviolet (UV) illumination device (LIAS Slite140, Avegene Life Sciences, Taipei, Taiwan), allowing the capture of the images too.

2.8 Bisulfite sequencing

Having the bisulfite converted DNA, we performed TA-cloning(Holton & Graham, 1991; Marchuk et al., 1991; Mead et al., 1991; M.-Y. Zhou & Gomez-Sanchez, 2000) was performed. The TA-cloning method was carried out to get quantitative bisulfite sequencing results. After bisulfite conversion, the DNA was amplified through PCR using the kit KAPA HiFi Hotstart ReadyMix 1,25 mL (Cat# KK2601, 07958927001, Roche).

A 579 bp long fragment was analyzed, whose exact genomic location is Chr12:122,459,192—122,459,770 considering the GRCh37/hg19 genome assembly (from 806 to 227 bp upstream from the *BCL7A* translation start codon). The primers were:

- BiSeq FW: 5'-TAGAAAATTTTTTAGTATTTAAGGT-3'
- BiSeq RV: 5'-TACACAAAACAAAAAAAACC-3'

This amplicon includes 61 CpG sites whose methylation status was evaluated.

After PCR amplification, an agarose (Cat# H350004, LONZA) in TAE buffer gel purification of the PCR product was performed using GenElute™ Gel Extraction Kit (Cat# NA1111-1KT, Merck Life Sciences, Darmstadt, Germany) followed by 3' overhanging Adenine tailing (A-tailing) by incubating at 70 °C for 35 min with the Taq DNA Polymerase (Cat# D4545, Merck Life

Sciences, Darmstadt, Germany), which naturally adds an A-overhang to the insert (PCR product) in both 3' ends.

Then, a ligation protocol (TA-cloning ligation) was performed to include the insert into a T-overhanging vector using pGEM®-T Easy Vector Systems (Cat# A1360, Promega, Madison, WI, USA) followed by transforming DH5α strain chemically competent E. coli. and colony picking for plasmid extraction by Miniprep (Cat# 21.222–4212, Biotools B & M Labs Ltd., Madrid, Spain) (as described in methods section 2.5).

Once the plasmid was amplified, Sanger sequencing (STAB VIDA Lda., Caparica, Portugal) was carried out to reveal the exact location of the methylated CpG sites by sequence alignment of the bisulfite treated DNA (insert sequence) and the genomic DNA sequence applying the pairwiseAlignment() function from the Biostrings R package (v2.52). CpG sites status with their sequencing errors or undetermined bases were marked as unresolved and these were excluded from the analysis. The methylation fraction of a given CpG site was calculated considering the number of methylated reads divided by the total sequencing coverage (9 inserts were sequenced, N = 9, Supplementary Figure 3).

2.9 Total protein extraction

The total protein from the cell models was extracted using the radioimmunoprecipitation assay (RIPA) lysis buffer (150 mM NaCl, 1% (v/v) NP-40, 0.5% (m/v) sodium deoxycholate, 0.1% (m/v) sodium dodecyl sulfate (SDS) and 50 mM Tris–HCl pH 7.5) supplemented with protease and phosphatase inhibitors: 0.2 mM phenylmethylsulfonyl fluoride (PMSF), 7 mM orthovanadate (VO_4) and one complete Mini ethylenediaminetetraacetic acid (EDTA)-free Protease Inhibitor Cocktail Tablet (Cat# A32955, Thermo Fisher Scientific, Waltham, MA, USA).

The cells were washed twice with phosphate-buffered saline (PBS) and pelleted in 1.5 mL tubes centrifuging for 5 min 1200 rpm 4 °C. Then, the pellet was resuspended and lysed by pipetting with the corresponding volume of the previously described lysis buffer (the proportion applied is 70 μL of lysis buffer for each 3 million of cells), and incubated for 15 min on ice mixing it by vortex every 5 min. After the incubation, the samples were centrifuged for 15 min 13,300 rpm 4 °C. The supernatant (including the proteins) was moved into a new 1.5 mL tube and stored at -20 °C.

The protein concentration in each lysate was estimated following the Bradford protocol described elsewhere (Bradford, 1976).

2.10 Western blot

To detect specific proteins, the Western blot (WB) technique was performed.

To prepare each sample, 30-50 μg from the total protein lysate plus the corresponding amount of the WB loading buffer 4x (Tris-HCl: 0.2 M, Dithiothreitol [DTT]: 0.4 M, SDS: 277 mM, 8.0% (m/v), Bromophenol blue: 6 mM and Glycerol: 4.3 M) were mixed by pipetting in 1.5 mL tubes, heated for 5 min at 95°C and then incubated on ice for 2 min to ensure protein denaturation.

The prepared protein samples were loaded into a SDS protein acrylamide gel electrophoresis (SDS-PAGE) to separate the proteins depending on their molecular weight once an electric field was applied (usually constant 120 V for 90-120 min). 10x WB running buffer composition:

Compound	For 1L
Tris base	30.2 g
Glycine	144 g
10% (m/v) SDS solution	100 mL
Distilled water	up to 1L

Table 2. Recipe for 1L of 10x WB running buffer.

It needs to be diluted to 1x (1/10 dilution) with ultrapure distilled water before use.

Afterwards, the separated proteins were transferred to a polyvinylidene difluoride (PVDF) membrane applying again an electric field (usually constant 400 mA for 90 min). 10x WB transfer buffer composition:

Compound	For 1L
Tris base	30.2 g
Glycine	144 g
Distilled water	up to 1L

Table 3. Recipe for 1L of 10x WB transfer buffer.

Here, to prepare 1L of 1x WB transfer buffer it is necessary to add 100 mL of the previous 10x WB transfer buffer + 200 mL of methanol + 700 mL of distilled water.

After the transference, the membrane including the proteins was blocked for 1 h using 5% (m/v) powder non-fat milk and 0.1% (v/v) Tween-20 both dissolved in PBS.

Then, the blocked membrane was incubated with the corresponding antibodies to reveal the proteins that were required to be studied. The primary antibodies used were:

- Anti-BLC7A rabbit polyclonal antibody (Cat# HPA019762, Sigma Aldrich / Merck KGaA, Darmstadt, Germany).
- Anti-β-actin mouse monoclonal antibody (Cat# A5441, Sigma Aldrich / Merck KGaA, Darmstadt, Germany), which was used as a WB loading control.

- Anti-α-tubulin mouse monoclonal antibody (Cat# sc-23948, Santa Cruz Biotechnology, Santa Cruz, CA, USA)

The secondary antibodies used were:

- Anti-Rabbit goat polyclonal immunoglobulins conjugated with horseradish peroxidase (HRP) (Cat# P0448, Dako Agilent Technologies, Santa Clara, CA, USA).
- Anti-Mouse goat polyclonal immunoglobulins conjugated with HRP (Cat# P0447, Dako Agilent Technologies, Santa Clara, CA, USA).

The membranes were first incubated in darkness for 5 min with a commercial solution of the HRP substrate. The Clarity™ Western ECL Substrate kit (Cat# 1705060, Bio-Rad Laboratories, Hercules, CA, USA) was used to reveal large amounts of protein, and for reduced amounts of protein, the SuperSignal™ West Femto Maximum Sensitivity Substrate kit (Cat# 34095, Thermo Fisher Scientific, Waltham, MA, USA) was used.

Then, to get the WB chemiluminescence images, the ImageQuant™ LAS 4000 device (General Electric Healthcare, Chicago, IL, USA) was used. The WB protein bands were quantified by ImageJ v1.52a software. The quantification data was normalized versus β-actin values.

2.11 Total RNA extraction

To extract the total RNA from the cell models, 0.5-1 mL (depending on the cells pellet size) of TRI Reagent® (Cat# T9424-200ML, Sigma Aldrich / Merck KGaA, Darmstadt, Germany) was added. Subsequently, the cell pellet was resuspended by pipetting until it had a homogeneous appearance and the samples were incubated for 5 min at room temperature.

Then, 100-200 μL of chloroform was added (in proportion to the TRI Reagent® previously added), vigorously mixed by vortex for 15 s and incubated 3 min at room temperature. Then, a centrifugation was performed for 15 min 12,000 relative centrifugal force (rcf), 4 °C, the upper phase was taken and moved into a new 1.5 mL tube, 250-500 μL of isopropanol were added (again in proportion to the TRI Reagent® previously added) and the samples were incubated for 30 min at -20°C (or o/n for smaller amounts of RNA).

Later, the samples were centrifuged for 10 min 12,000 rcf 4°C and removed the supernatant. Now, the pellet was washed with 1 mL of 75% ethanol, briefly mixed it by vortex and centrifuged for 5 min 7,500 rcf 4°C.

Finally, the supernatant was completely removed and gently resuspended by pipetting the RNA pellet in 15-30 μL of ultrapure distilled water.

2.12 Quantitative real-time PCR

To quantify the mRNA levels of the genes under analysis, quantitative real-time PCR assays (qRTPCR) were performed in a QuantStudio™ 3 Real-Time PCR System, 96-well device (Cat# A28136, Thermo Fisher Scientific, Waltham, MA, USA) using the KAPA SYBR® FAST kit (Cat# KK4618, Sigma Aldrich / Merck KGaA, Darmstadt, Germany).

The template molecule for the qRTPCR was complementary DNA (cDNA) obtained from the total RNA from the cell models. 1 μg of total RNA was used for reverse transcription with the RevertAid RT Kit (Cat# K1691, Thermo Fisher Scientific, Waltham, MA, USA) using random primers (provided in the kit) and following the manufacturer's instructions to generate the mentioned cDNA.

To specifically amplify the *BCL7A* mRNA by qRTPCR, the following primers were designed:

- *BCL7A*-Fw: 5´-GTGACACATCCCTACGAATCTAC-3´
- *BCL7A*-Rv: 5´-CACTTCTCGTCCTTGCCTTT-3´.

Each qRTPCR reaction contained 30 ng of total cDNA, 5 μL SYBR Green (2x) and 0.2 μL of each primer at 10 μM. The qRTPCR conditions were 2 min at 50 °C, 10 min at 95 °C and 40 cycles of 15 s at 95 °C and 1 min at 60 °C. The samples were always measured in three technical replicates.

For each experimental sample, the amount of *BCL7A* mRNA and the endogenous reference gene glyceraldehyde 3-phosphate dehydrogenase (GAPDH) mRNA were determined.

To specifically amplify the *GAPDH* mRNA by qRTPCR, the primers detailed below were used:

- GAPDHq-Fw: 5´-GAAGGTGAAGGTCGGAGTC-3´
- GAPDHq -Rv: 5´-GAAGATGGTGATGGGATTTC-3´.

The relative expression levels of *BCL7A* were obtained applying the 2ˆ(–delta delta CT) method (Rao et al., 2013).

2.13 Decitabine treatment

1.2×10^6 of cells (NB4 or M07e) per condition were used. They were cultured into T-25 flasks (Cat# 734-2311P, VWR, Radnor, PA, USA) in a final volume of 6.2 mL of supplemented RPMI 1640 cell culture medium. The NB4 cells were treated with a final concentration of 2 μM 5-aza-2'-deoxycytidine (also known as decitabine, DAC), and the M07e cells were treated with final concentrations of 2 μM and 4 μM (two independent conditions) DAC (Cat# A10292-10, Quimigen, Madrid, Spain) resuspended in dimethyl sulfoxide (DMSO) (Cat# VWRC23486.297, VWR, Radnor, PA, USA) during 96 h. The culture medium with DAC or only DMSO (added on the control condition) were renewed every 24 h.

After the 96 h treatment, cell pellets were collected for total RNA and / or total protein extraction to assess *BCL7A* expression levels.

2.14 Plasmids

The plasmids Human Immunodeficiency Virus (HIV) packaging (psPAX2) and VSV-G envelope (pMD2.G) were obtained from Addgene repository (#12,260 and #12,259 respectively, Addgene, Watertown, MA, USA) and they are described elsewhere (Naldini et al., 1996). The pMD2.G plasmid encodes the vesicular stomatitis virus (VSV) G glycoprotein and the plasmid psPAX2 encodes gag, pol, tat, and rev genes.

The lentiviral vector (LV) pLVX-IRES-ZsGreen1 (Cat# 632,187, Clontech, Shiga, Japan) used contains a human cytomegalovirus immediate early promoter (PCMVIE), which drives a bicistronic transcript including our insert and the fluorophore ZsGreen1 as reporter protein. The pLVXIRES-ZsGreen1 vector also features the Woodchuck Posttranscriptional Regulatory Element (WPRE) and the central Polypurine Tract (cPPT).

The plasmid pUltra-Chili-Luc was acquired from Addgene repository (Cat# 48,688, Addgene, Watertown, MA, USA) and was used to yield the stable expression of Luciferase in the NB4 cells used for the *in vivo* xenograft bioluminescence approach.

The pLVX-IRES-ZsGreen1 plasmid backbone was used to clone the wild-type (WT) and mutant BCL7A (Δ27-BCL7A) variants. Since BCL7A presents two isoforms (short and long isoforms), vectors including all of the variants and isoforms possible combinations were generated:

- WT BCL7A short isoform
- Δ27-BCL7A short isoform
- WT BCL7A long isoform
- Δ27-BCL7A long isoform

The previously mentioned inserts were generated via PCR by primers designed including XbaI and BamHI restriction enzymes sites adjacent to a start codon (ATG) and a stop codon (TGA) respectively. The inserts and the recipient plasmid were double digested with XbaI/BamHI and the cohesive ends ligation was performed with T4 ligase (Cat# EL0011, Thermo Fisher Scientific, Waltham, MA, USA). The specific DNA sequence of the different inserts is detailed in the Supplementary Figure 4.

2.15 Lentiviral production

The lentiviral production was carried out in HEK293T cells, obtained from the American Type Culture Collection (Cat# CRL-11268, ATCC, Manassas, VA, USA). They were grown in Dulbecco's Modified Eagle Medium (DMEM) with L(+)-Glutamine (Cat# L0103-500, Biowest, Riverside, MO, USA) supplemented

with 10% FBS (Cat# 10,270–106, Gibco™ Thermo Fisher Scientific, Waltham, MA, USA), 100 U/mL streptomycin and penicillin using a ready-to-use solution (Cat# P0781-100ML, Sigma Aldrich / Merck KGaA, Darmstadt, Germany) and with 1% (v/v) of amphotericin B (Cat# L0009-100, VWR, Radnor, PA, USA). From now on this culture medium will be called supplemented DMEM.

The day before transfection, the HEK293T were plated in 10-cm tissue culture grade Petri dishes (Cat# SIAL0167, Sigma Aldrich / Merck KGaA, Darmstadt, Germany) to ensure exponential growth and 80% of cell confluence for the next day.

The following steps are explained for the production of only one lentivirus (then considering one vector plasmid and using only one Petri dish of HEK293T cells).

9μg of the vector plasmid, together with 6 μg of the packaging one (psPAX2) and 3 μg of the envelope (pMD2.G) plasmid (18 μg total DNA; plasmid proportions of 3:2:1, respectively) were resuspended in a total volume of 500 μL of DMEM without FBS in a 1.5mL tube. In another 1.5mL tube, a dilution of 45 μL of the LipoD293 transfection reagent (Cat# SL100668, Signagen Laboratories, Rockville, MD, USA) was prepared plus 455 μL DMEM without FBS. Then, the LipoD293 dilution was added over the plasmids' mixture, which was gently mixed by pipetting and incubated at room temperature for 20 min.

Afterwards, a Petri dish with 80% of cell confluence and 4 mL of supplemented DMEM was at hand, where the "plasmids-lipoD293" mixture was added by dripping over the cells and incubated for 5 h. Then, it was removed and replaced by gently adding 8 mL of supplemented DMEM.

Finally, the supernatant containing the lentiviral particles was collected after 48 h (first supernatant collection) and filtered using a 0.45 mm of pore size filter (Cat# FPE404030, JET Biofil, Guangzhou, China), divided in 1 mL aliquots within 1.5 mL tubes, and quickly frozen at -80°C. Then, 8 mL of supplemented DMEM were gently added to the same plate and the previously described process was repeated 24h later (second supernatant collection at 72h after transfection).

2.16 Lentiviral titration

A lentiviral titration protocol was carried out based on the use of the highly permissive K-562 cell line, obtained from the ATCC (Cat# CCL-243, ATCC, Manassas, VA, USA). This cell line was cultured in supplemented RPMI.

The following steps described belong to the titration of only one supernatant containing lentiviral particles.

In a 24 well plate (Cat# 734-2325, VWR, Radnor, PA, USA), 3 wells were seeded with 200 μL (500 cells / μL) of supplemented

RPMI containing 100,000 K-562 cells per well. Then, 5, 10 and 50 μL of the supernatant to be tittered were added in each well respectively and completed with supplemented RPMI up to 300 μL of final total volume. The next table summarizes the previous information about each well preparation:

Well	I	II	III
K-562 cells (500 cells/ μL)	200	200	200
Supernatant	5	10	50
Supplemented RPMI	95	90	50

Table 4. Volumes in μL needed to prepare the different wells in the 24 well plate for the titration of one letiviral production.

After incubating the plate 5h inside the cell culture incubator, 750 μL of supplemented RPMI was added to each well and incubated the plate for 48h in the cell culture incubator. Then, the cells were transferred to a plate with larger wells (12 or 6 well plates depending on the number of cells per well) (Cat# 734-2324 and 734-2323 respectively, VWR, Radnor, PA, USA) and added a suitable volume of supplemented RPMI to allow cell growth during 3 more days.

5 days after the addition of the supernatant, the percentage of ZsGreen1+ cells was assessed from each condition by flow cytometry using a Becton, Dickinson and Company (BD) FACSCanto II ™ Flow Cytometer (Cat# 338962, BD, Franklin

Lakes, NJ, USA). The percentage of transduced cells was determined according to ZsGreen1 reporter gene fluorescence.

Viral titers (infective units / mL, [IU]) were calculated from the percentage of ZsGreen1+ cells detected in the linear range of a serial dilution of the supernatant, taking into account the condition with the highest percentage possible just under 20% and applying the following mathematical formula:

$$IU = \frac{\left(ZsGreen1 + \% \cdot \frac{100.000\ cells}{100}\right) \cdot 1000 \frac{\mu L}{mL}}{\mu L\ added\ of\ the\ supernatant}$$

2.17 Lentiviral concentration

After a lentiviral production, if the lentiviral titer corresponding to one batch was below 10^6 IU / mL, a lentivirus concentration protocol was always performed.

Up to 15 mL of the lentivirus containing supernatant was poured over a centrifugal filter 100-K (Cat# UFC910024, Merck Life Sciences, Darmstadt, Germany), centrifuged it for 30 min 4000 rcf 4°C and the eluate was aspirated. These steps were repeated until all of the supernatant was concentrated in the upper part of the centrifugal filter.

The concentrated supernatant was homogenized by gently pipetting and then stored in 50-70 µL aliquots within 1.5 mL tubes at -80°C and it was titrated as well.

2.18 Lentiviral cell transduction and competition cell growth assay

The NB4 and M07e cell models were transduced with the lentiviral particles produced using the vector plasmid pLVX-*BCL7A*-IRES-ZsGreen1 coding for WT BCL7A, Δ27-BCL7A or the empty vector (EV). The NB4 cells were transduced with both short and long isoforms of WT BCL7A and Δ27-BCL7A variants (see Supplementary Figure 4).

The M07e cell line was transduced using only the long isoforms of the two mentioned BCL7A variants since it has been previously stated that, up to date, the phenotype produced in a cell model only depends on the variant (WT BCL7A or Δ27-BCL7A) and it is independent from the BCL7A isoform (short or long) (Carlos Baliñas-Gavira, 2020).

Three consecutive cycles of transduction were performed applying a multiplicity of infection (MOI) = 2 (MOI = 1 for the short isoform and MOI = 1 for the long one for NB4 cells; MOI = 2 for M07e including here only the long isoform, to keep equal the total MOI between cell models) with the different lentiviral particles yielding the co-expression of the BCL7A variants together with the fluorochrome ZsGreen1 in the cell lines. Afterwards, the transduced ZsGreen1+ cells were sorted using a BD FACSAria™ Fusion Flow Cytometer (Cat# 656700, BD, Franklin Lakes, NJ, USA) and subsequently mixed with sorted non-transduced cells.

The co-culture of transduced and non-transduced cells (cell growth competition culture) was tracked by measuring the percentage of ZsGreen1+ population over time using the BD FACSCanto II ™ Flow Cytometer (Cat# 338962, BD, Franklin Lakes, NJ, USA). The percentage of ZsGreen1+ cells was normalized versus the percentage of ZsGreen1+ cells at the starting point.

2.19 BCL7A immunoprecipitation and liquid chromatography with tandem mass spectrometry (LC–MS/MS) analysis

Here, the immunoprecipitation of BCL7A was performed in our facilities and the resulting samples were sent to the proteomic unit of the "Centro Nacional de Investigaciones Oncológicas" (CNIO, Madrid, Spain) to be analyzed by liquid chromatography with tandem mass spectrometry (LC–MS/MS).

2.19.1 BCL7A immunoprecipitation

The NB4 cell line was transduced with lentiviral particles packaged using the pLVX-IRES-ZsGreen1 constructs expressing the WT BCL7A or Δ27-BCL7A (only the short isoform in both cases). Cells were transduced during three consecutive cycles using a MOI=1 for each condition. After five days, the cells were

sorted using a BD FACSAria™ Fusion Flow Cytometer (Cat# 656700, BD, Franklin Lakes, NJ, USA) to obtain a pure ZsGreen1+ population and cultured until a suitable cell number was obtained.

Afterwards, total protein was extracted from the previously described cell models and quantified it following the methodology depicted in the "2.10 Western blot" methods section. For the LC/MS-MS analysis, 4mg of protein from each of the conditions was immunoprecipitated overnight at 4°C using 1μg of anti-BCL7A antibody (#HPA019762, Sigma-Aldrich) per mg of total protein. For each of the conditions, one sample that was incubated with an irrelevant anti-rabbit Immunoglobulin G (IgG) antibody was included to assess the nonspecific binding. The immunocomplexes were pulled-down adding 200μL of Dynabeads Protein G (Cat# 10004D, Thermo Fisher Scientific, Waltham, MA, USA) and incubating the samples for 3 hours at room temperature under agitation in a rotatory wheel. Subsequently, the beads were washed for 3 times in a row with PBS containing protease inhibitors. A two steps elution was performed, adding in each step 600μL of an 8M urea solution in 0.1M Tris-HCl at pH8, incubating the samples at 26°C and shaking at 1400rpm for 10 minutes.

2.19.2 Sample preparation for the proteomic analysis

The eluates were digested using the standard Filter Aided Sample Preparation (FASP) protocol (Wiśniewski et al., 2009). The

proteins were reduced (TCEP 15mM, 30 min, at room temperature), alkylated (CAA 50mM, 20 min in the dark, at room temperature) and then digested with Lys-C (FUJIFILM Wako Chemicals, Neuss, Germany) (protein:enzyme ratio 1:50, incubation overnight at room temperature) and trypsin (Promega, Madison, WI, USA) (protein:enzyme ratio 1:100, 6h at 37°C). Then, we desalted the resulting peptides using C_{18} stage-tips.

2.19.3 Mass Spectrometry (Q ExactiveTM)

The LC-MS/MS process was performed using an UltiMate 3000 High-performance liquid chromatography (HPLC) system coupled to a Q Exactive Plus mass spectrometer (both devices obtained from Thermo Fisher Scientific, Waltham, MA, USA). The peptides were loaded into a trap column (Acclaim™ PepMap™ 100 C_{18} LC Columns 5 μm, 20 mm length, Thermo Fisher Scientific, Waltham, MA, USA,) during 3 minutes at a flow rate of 10 μL/min in 0.1% Formaldehyde (FA).

Then, the peptides were transferred to an analytical column (PepMap RSLC C_{18} C18 2 μm, 75 μm x 50 cm, Thermo Fisher Scientific, Waltham, MA, USA,) and separated by a 90 min effective linear gradient (buffer A: 4% Acetonitrile (ACN), 0.1% FA; buffer B: 100% ACN, 0.1 % FA) at a flow rate of 250 nL/min. The gradient applied was: 0-5 min 4% B, 5-7.5 min 6% B, 7.5-60 min 17.5% B, 60-72.5 min 21.5% B, 72.5-80 min 25% B, 80- 94 min

42.5% B, 94-100 min 98% B, 100-104.5 min 4% B, 105-110 min 0% B.

The mass spectrometer was operated in a data-dependent mode, with automatic switching between MS scans (350-1400 m/z) and MS/MS scans and applying what is termed the "Top 15 method" (threshold signal intensity ≥ 3.9E4, z ≥2). The MS spectra were acquired on the Orbitrap at a resolution of 70,000 Full Width at Half Maximum (FWHM) (200 m/z) and MS/MS spectra at a resolution of 17,500 FWHM (200 m/z). It was applied an active exclusion time of 26.3 seconds. Peptides were isolated using a 2 Th window and fragmented using high-energy collision dissociation (HCD) with a normalized collision energy of 27. Ion target values were 3E6 for MS (maximum injection time of 25ms) and 1E5 for MS/MS (maximum injection time of 90ms).

2.19.4 Computational analysis of the LC-MS/MS generated data

The raw data was processed using the bioinformatics tool MaxQuant (v 1.6.2.6a) (Cox & Mann, 2008) with the standard configuration and using as reference a human protein database (UniProtKB / Swiss-Prot, 20,373 sequences) supplemented with contaminants. The quantification by Label-free quantification (LFQ) was performed by run-to-run matching (0.7 min matching window and 20 min alignment window). The carbamidomethylation of cysteines was set as a fixed

modification, whereas the oxidation of methionines and protein acetylation at the amino-terminal end were set as variable modifications. The minimum peptide length was set to 7 amino acids and a maximum of two missed tryptic cleavages were allowed. The obtained results were filtered applying a 0.01 FDR (at both peptide and protein level).

Subsequently, the file "proteinGroup.txt" was loaded into the software tool ProStar (v 1.12.12)(Wieczorek et al., 2017) for further statistical analysis. A minimum of two valid LFQ values per group was required for quantification. Missing values were imputed using the standard settings in ProStar (i.e. SLSA for POV and Det quantile for MEC). Analysis was then performed using Limma and p-values were adjusted using the Benjamin-Hochberg method. Only proteins with a p-value <0.05 and a sample/control ratio with log2 value > 1.5 were considered as possible interactors. In all cases, the resulting FDR was less than 5%.

2.20 Xenograft *in vivo* bioluminescence imaging

An *in vivo* bioluminescence study was carried out strictly in accordance with the recommendations in the Guide for the Care and Use of Laboratory Animals of the Bioethical Committee of the University of Granada and all of the procedures were approved by the Committee on the Ethics of Animal Experiments at the University of Granada. All of the protocols with experimentation animals (mice) were developed under isoflurane inhalation

anesthesia, and every possible effort was made to minimize animal suffering.

To generate the necessary NB4 cell models to perform this approach, the same lentiviral transduction protocol described above (methods section "2.18 Lentiviral cell transduction and competition cell growth assay") was carried out. The lentiviral particles packaged with the luciferase construct were produced using the lentiviral plasmid pUltra-Chili-Luc, which was provided by Malcom Moore's laboratory (Addgene #48688). After the NB4 cells transduction with the pUltra-Chili-Luc lentiviral particles, they were sorted using a BD FACSAria™ Fusion Flow Cytometer (Cat# 656700, BD, Franklin Lakes, NJ, USA) to generate a pure population of luciferase expressing NB4 cells. Then, these cells were transduced with wild-type BCL7A/ZsGreen1 (both short and long BCL7A isoforms) or EV pLVX-IRES-ZsGreen1 (see Supplementary Figure 4), and again sorted to provide us pure populations of the different NB4 models.

Eight-week-old male NOD.scid Il2rgtm1Wjl/SzJ (NSG) mice (provided by the Animal Experimentation Service, University of Granada) were intravenously tail vein injected with our NB4 cell models (5×10^6 cells per mice) that simultaneously steadily expressed luciferase and wild-type BCL7A/ZsGreen1 (both short and long BCL7A isoforms) or luciferase and EV pLVX-IRES-ZsGreen1. Two groups of mice were produced, including six per group.

For bioluminescence imaging, the mice were intraperitoneally injected with a D-Luciferin Monosodium Salt solution (Cat# 88292, Thermo Fisher Scientific, Waltham, MA, USA) diluted in PBS at a dose of 150 mg / kg body weight. After 5 to 8 min, the animals were anesthetized inside a dark chamber using 3% (v/v) isoflurane in the air at 1.5 L / min and O_2 at 0.2 L / min / mouse, and they were imaged in a chamber connected to a camera (IVIS Spectrum, Cat# 124262, Perkin Xenogen, Alameda, CA, USA).

The exposure time was 3 min in large binning, and the light emission quantification was obtained in photons / s using the Living Image software (Perkin Xenogen). The growth of the injected cells was monitored on days 0, 7, 14, and 21 by *in vivo* imaging and bioluminescence measurement performed in ventral and dorsal positions.

2.21 RNA sequencing

Total RNA extraction was performed using the mirVana™ miRNA Isolation Kit, with phenol (Cat# AM1560, Thermo Fisher Scientific, Waltham, MA, USA), since the RNA purity needed for RNA-seq is higher than that yielded by the described protocol in "2.11 Total RNA extraction" methods section.

Here, total RNA was extracted from 3×10^6 of NB4 cells of each condition (WT BCL7A and Δ27-BCL7A, described previously

in the "2.18 Lentiviral cell transduction and competition cell growth assay" methods section) per sample. Two samples per condition were prepared (technical duplicates). The RNA concentration and quality were measured using Qubit™ 4 Fluorometer (Cat# Q33238, Thermo Fisher Scientific, Waltham, MA, USA) and 2100 Bioanalyzer Instrument (Cat# G2939BA, Agilent Technologies, Santa Clara, CA, USA) respectively.

The total RNA samples were stored at -80°C until they were shipped to Genewiz (a division of Azenta Life Sciences) facilities, where the RNA-seq was performed using a NovaSeq (2×150 bp configuration) (Illumina, San diego, CA, USA).

The quality control of the raw FASTQ files was performed using FastQC (v0.11.8). The reads were aligned to the human genome assembly GRCh38.d1.vd1 (downloaded from https:// gdc.cancer.gov/about -data/data-harmonization -and -generation/gdc -reference -files) using STAR (version 2.7.10b) in "two-pass mode".

The annotation reference used was GENCODE v36. The multi-sample BAM was split into single-sample BAMs. The quality of the BAM files was evaluated applying Picard (v1.4.2) and QualiMap (v2.2.1) in combination with multiqc (v1.6). It was checked that the rRNA contamination was below 1% and Integrative Genomics Viewer software was used to confirm the presence of the expected *BCL7A* mutations at the RNA level.

The read counts per gene were obtained applying htseq-count (v0.6.1p1) with the following options: ‘‘-m intersectionnonempty -f bam -t exon -i gene_id -r pos -s reverse’’. Additional analyses were performed using R (version 3.6.3, Bioconductor version 3.10) and the ‘edgeR’, ‘DESeq2’ and ‘EnhancedVolcano’ packages. Hierarchical clustering and principal component analysis were performed to assess and confirm the similarities among conditions and replicates.

DESeq2 was used for the differential expression analysis testing for abs(logFC) > log2(1.5) specifying a threshold of alpha = 0.01. logFC values were shrunk using the ashr method while preserving the original p and adjusted p values. Gene ontology (GO) enrichment analysis was carried out using the gene annotation and analysis resource Metascape (http:// metas cape. org/ gp/ index. html) (Y. Zhou et al., 2019), including the top 400 differently expressed genes according to their p-adjusted value.

2.22 *Bcl7a* conditional Knock-out (KO) mouse model development

It was available in our animal facility the UBC-Cre-ERT2 (ubiquitin C [UBC] promoter, Cre recombinase fused to a G400V/M543A/L544A triple mutation of the human estrogen receptor ligand binding domain [ERT2]) mouse model (Indra et al., 1999) that was obtained from The Jackson Laboratory (Strain

#:007001, The Jackson Laboratory, Bar Harbor, ME, USA) for the development of other projects that were being developed in our research group. This model expresses Cre recombinase in its whole body upon receiving via intraperitoneal injection four doses of 100 mg tamoxifen per kg of mouse during four consecutive days (Cat# J63509.06, VWR, Radnor, PA, USA). For this purpose, a 10 mg/mL tamoxifen solution was prepared in corn oil (Cat# C8267-500ml, Merck Life Sciences, Darmstadt, Germany) to be able to inject 10 µL / g mouse (100 mg tamoxifen per kg of mouse) using a hypodermic needle 23G - stainless steel epoxy resin adhesives (Cat# 300800, BD, Franklin Lakes, NJ, USA) and a 1mL syringe (Cat# 303172, BD, Franklin Lakes, NJ, USA).

On the other hand, in response to our request Dr. Bano kindly provided us with the *Bcl7a*$^{fl/fl}$ mouse model (Wischhof et al., 2017), which presents the mouse *Bcl7a* gene exon 2 flanked by two LoxP sequences (“floxed”) in both alleles, then being able to be deleted once the Cre recombinase is present (Austin et al., 1981; Nat Sternberg & Daniel Hamilton, 1981).

Subsequently, the necessary selective breeding was performed to generate the mouse model including both features: UBC-Cre-ERT2-*Bcl7a*$^{fl/fl}$. In short, the *Bcl7a* inducible KO mouse model was generated, whose *Bcl7a* may be inactivated once its exon 2 is deleted (knocked-out) upon receiving the tamoxifen dose described above. The main background of the generated mouse model was the strain C57BL/6.

2.23 Genotyping to establish a mouse colony of the *Bcl7a* conditional KO mouse model

To generate a mouse colony of the *Bcl7a* conditional KO model it was necessary to assess which alleles of *Bcl7a* (WT or floxed) or whether the Cre-ERT2 cassette was present or not in each animal. For this purpose, the PCR products, obtained using specific primers and the mice genomic DNA as template (2 µL per PCR reaction, without previous DNA quantification), were analyzed through an agarose in TAE buffer gel electrophoresis. The polymerase used here was the DreamTaq Green PCR Master Mix (2X) (Cat# K1082, Thermo Fisher Scientific, Waltham, MA, USA).

2.23.1 Mouse genomic DNA extraction

The small ear piece taken from the mice for its labelling was used to extract mice genomic DNA. This piece was placed in a 1.5 mL tube, immersed in 250 µL of 50 mM NaOH and mixed it by vortex followed by a 30 min incubation at 98°C in a thermo block. Then, 25 µL of 1M Tris-HCl pH8 were added to neutralize the solution and the tube was centrifuged for 10 min at 13,000 rpm at 4°C. The last step was to take the supernatant (where the genomic DNA is) into a new 1.5 mL tube and the genomic DNA (ready for standard PCR amplification) was stored at -20°C. This protocol is not a "clean" DNA extraction, but the DNA quality is good enough for the standard PCR amplification needed for mice genotyping.

2.23.2 Primers and PCR conditions for mouse genotyping

The primers to evaluate the presence of the Cre-ERT2 cassette were:

- FW CRE: 5'-CCCGCAGAACCTGAAGATGT-3'
- RV CRE: 5'-GTTCGAACGCTAGAGCCTGTTT-3'

In this case, another couple of primers was added in each PCR reaction to amplify as a positive control a region which is always present in the mouse genomic DNA in order to be able to tell a negative result (absence of the Cre-ERT2 cassette) from a PCR that did not work properly. These primers were:

- FW IL2: 5'-CTAGGCCACAGAATTGAAAGATCT-3'
- RV IL2: 5'-GTAGGTGGAAATTCTAGCATCATCC-3'

This second couple of primers targets the mouse interleukin 2 gene locus yielding a larger (324 bp) PCR product compared to the one given by the FW CRE and RV CRE couple (220bp), to be able to observe the two independent amplicons from each sample.

To genotype the Cre-ERT2 cassette the PCR conditions applied were 1min 95°C and then 35 cycles of 30s 95°C, 30s at 60°C and 1 min at 72°C.

The primers used to genotype the mice *Bcl7a* locus to distinguish the floxed allele from the WT allele were:

- FW *Bcl7a* fl: 5'-GGCTTCTATCCTGTGGGAGTTTAGAG-3'
- RV *Bcl7a* fl: 5'-AACGGTCACCCATTTCTTCTCCCT-3'

The PCR conditions were: 1min 95°C and then 35 cycles of 30 s 95°C, 30 s at 55°C and 45 s at 72°C. The amplicons sizes were 474 bp for the WT *Bcl7a* allele and 532 bp for the floxed *Bcl7a* allele.

The primers used to distinguish the *Bcl7a* KO allele from the WT *Bcl7a* or floxed *Bcl7a* alleles were:

- FW *Bcl7a* KO: 5'-GGCTTCTATCCTGTGGGAGTTTAGAG-3'
- RV *Bcl7a* KO: 5'-AACGGTCACCCATTTCTTCTCCCT-3'

The PCR conditions were: 1min 95°C and then 35 cycles of 30 s 95°C, 30 s at 65°C and 1 min at 72°C. The amplicons sizes were 261 bp for the *Bcl7a* KO allele, 732 bp for the WT *Bcl7a* and 930 bp for the floxed *Bcl7a*. Here, the genomic DNA used for these PCRs was extracted from a little piece of mouse tail taken at least 10 days after the tamoxifen intraperitoneal injection.

In every case, the PCR amplicons were evaluated through a 2% (m/v) agarose in TAE buffer gel electrophoresis (85 V during 1 h). To provide these results with a reference of DNA size, the VWR® EZ-Vision®, DNA Ladder, 100 bp (Cat# N856-300UL, VWR, Radnor, PA, USA) was used.

2.24 Mice blood collection and analysis

The blood from the mouse tail was extracted, following a protocol that consisted of making a very little perpendicular cut in one of the mouse tail veins using a blade (Cat# 233-0025, VWR, Radnor, PA, USA) and collecting the blood drops up to 40 µL with a 100 µL micropipette. Mice tails were previously cleaned with a spray of ethanol 70% (v/v) and paper to avoid infections. The blade and the tip of the micropipette should have been previously dipped in 0.5 M EDTA, pH 8 (Cat# 15575020, Thermo Fisher Scientific, Waltham, MA, USA) to prevent blood coagulation while blood collection. In addition, the 40 µL of blood were placed in a 1.5 mL and mixed by pipetting with 20 µL 0.5 M EDTA, pH 8 (blood dilution 2/3) that had been previously added to the tubes.

After mice blood collection, these samples were immediately analyzed using the automated hematology analyzer Mythic 22CT C2 Diagnostics (Cat# M22/UM/SP/001, Orphée, Geneva, Switzerland).

To prevent the mice from weakening, the blood collection from each mouse was carried out only every 3 months.

2.24.1 Mice cohort details

A mice cohort was generated, including a 25 *Bcl7a* KO mice group and a 19 *Bcl7a*$^{fl/fl}$ mice group without the Cre-ERT2 cassette, so the tamoxifen injection in the latter did not generate *Bcl7a* KO

mice (control group). The total size of the study cohort included 44 mice. These two mouse models were engendered simultaneously due to mendelian segregation from the same breeding that included one *Bcl7a*$^{fl/fl}$ progenitor with the Cre-ERT2 cassette and the other *Bcl7a*$^{fl/fl}$ without it to avoid the generation of mice with more than one copy of the Cre-ERT2 cassette.

Both mice groups included males and females. The *Bcl7a* KO group had 16 males and 9 females (25 in all), and the control group had 13 males and 6 females (19 in all). Since the mice belonged to different litters, the age span was 7 months.

The tamoxifen injections were carried out approximately 2 months after the birth date of each mouse. The collection of little pieces of tail to check by genotyping the *Bcl7a* deletion was performed one month after the tamoxifen injection (in both mice groups). The first blood collection was carried out 3 months after the tamoxifen injection, and the following ones were performed every 3 months. Since some mice from both conditions randomly died sooner than it was naturally expected for unknown causes, and since the preliminary results obtained from the blood tests of the oldest litters showed non-significant differences at any time point (with a representative sample size), the corresponding blood collections were not carried out at all of the time points for all of the litters to reduce the avoidable animal suffering.

2.24.2 Data analysis

The blood test results were analyzed using the software GraphPad Prism (version 8.0.1). This software was used to perform the statistical analysis and to generate the plots including the results from the above mentioned blood tests.

Normality tests were performed and revealed that the blood tests results followed a normal distribution (when the sample size was enough to perform these tests). Then, these results were statistically analyzed assuming that characteristic.

The analyses were performed taking together males and females within each condition (*Bcl7a* KO or control), since there were similar proportions of males and females within each condition and it was observed that the little differences between the total number of white blood cells (WBC) per 1 μL between males and females are independent from the condition (*Bcl7a* KO or control). Males usually have a larger count of WBC per 1 μL than females in general (in both conditions, see Supplementary Figures 5-10). Therefore, taking the genders together in each condition would not be concealing any trend in the data.

Chapter 3.

BCL7A implications in AML

Chapter 3. *BCL7A* implications in AML

3.1 Background

In this chapter, we include the main results of this doctoral thesis. Most of them are part of the published research article related to this PhD thesis (Patiño-Mercau et al., 2023). Besides, we included here some other interesting results that were generated along but were not encompassed in the mentioned article.

These results also motivated the side project described in Chapter 5. This side project was developed during the PhD internship, that took place at Annalisa Di Ruscio's laboratory.

3.2 Results

3.2.1 The expression of *BCL7A* mRNA is modulated through promoter methylation in AML patients

First, to assess the putative involvement of the mSWI/SNF complex subunit BCL7A in AML, we examined its mutation frequency in AML patients' public data. In accordance with the known reduced mutational burden of AML, we discovered a very low frequency of *BCL7A* mutations in AML patient samples (< 1% non-synonymous coding mutations; N = 230; see methods section

2.1), thus discarding the genetic mutations as a mechanism of *BCL7A* inactivation in the context of AML.

Therefore, we evaluated whether an epigenetics mechanism might yield expression inactivation by studying the *BCL7A* genomic locus methylation levels in three independent AML patient cohorts: TCGA-LAML (N = 160), TARGET-AML (N = 188), and (Glass et al., 2017) (N = 111). We found a statistically significant inverse correlation (Pearson's correlation coefficient) between the *BCL7A* promoter methylation level and the *BCL7A* mRNA expression level in the previously mentioned AML patient cohorts (Figures 12-14), suggesting that the differential methylation of the *BCL7A* locus may impact on the *BCL7A* mRNA expression level in AML (Patiño-Mercau et al., 2023).

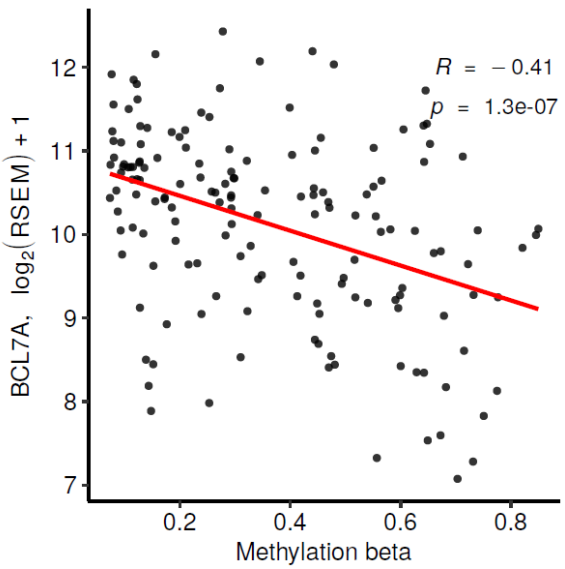

Figure 12. Significant negative correlation (Pearson's correlation coefficient) between methylation and expression of *BCL7A* in the TCGA-LAML patient cohort. Figure made by courtesy of Maria S Benitez-Cantos.

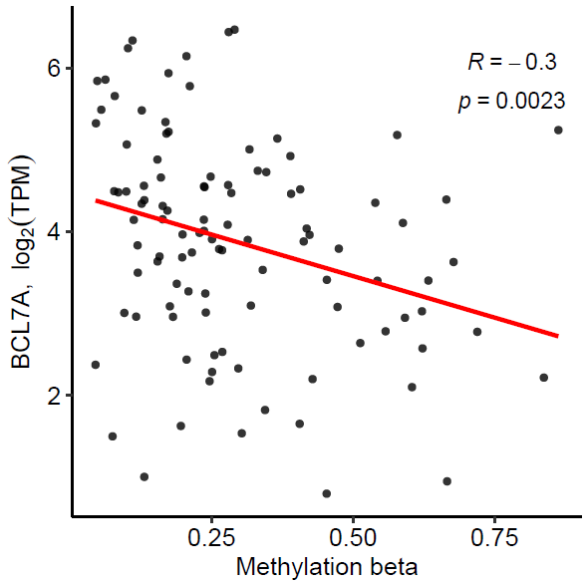

Figure 13. Significant negative correlation (Pearson's correlation coefficient) between methylation and expression of *BCL7A* in the TARGET-AML patient cohort. Figure made by courtesy of Maria S Benitez-Cantos.

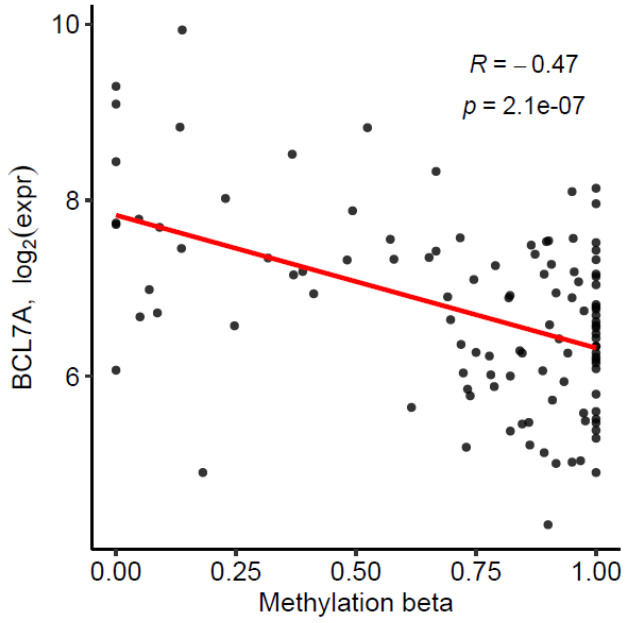

Figure 14. Significant negative correlation (Pearson's correlation coefficient) between methylation and expression of *BCL7A* in the Glass et al. patient cohort. Figure made by courtesy of Maria S Benitez-Cantos.

We also assessed *BCL7A* expression at mRNA level in the different FAB AML subtypes within the same three cohorts mentioned above. The only consistent observation across the three cohorts is the higher expression of *BCL7A* mRNA in the M1 (acute myeloblastic leukemia with minimal maturation) subtype compared to the other subtypes (Supplementary Figures 11-13). Nevertheless, due to the substantial variability in *BCL7A* levels within each subtype and the unequal sample sizes, *BCL7A* expression levels might not serve as a reliable marker for AML patients' classification here.

3.2.2 *BCL7A* mRNA expression comparison between myeloid and DLBCL cell models

The involvement of *BCL7A* in DLBCL has been already well described (Andrades et al., 2022; Baliñas-Gavira et al., 2020; Carlos Baliñas-Gavira, 2020) and the tumor suppressor genes (*BCL7A* being one of them in DLBCL) tend to be naturally downregulated during the tumor development (L. H. Wang et al., 2019). Therefore, we assessed the differences in the *BCL7A* mRNA expression levels between the AML (N = 44) and DLBCL (N = 29) cell models reanalyzing the data from the DepMap Portal (version 22Q2, cell lines detailed in Supplementary Table 2). Here, the AML cell lines consistently presented lower *BCL7A* mRNA expression than the DLBCL cell lines (Figure 15) (Patiño-Mercau et al., 2023).

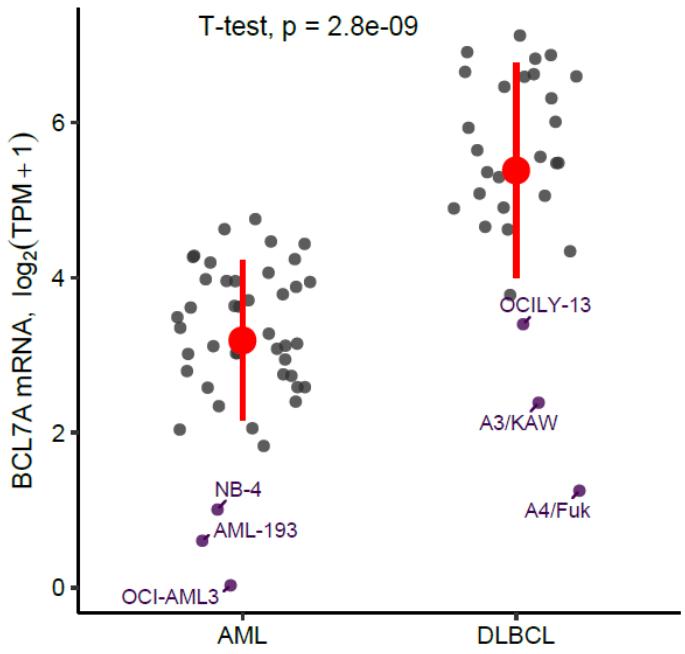

Figure 15. *BCL7A* mRNA expression level of the AML and DLBCL cell lines from the DepMap Portal database (version 22Q2). The AML cohort shows a lower *BCL7A* expression level (fold change = -4.6, $p = 2.8 \times 10^{-9}$). The three cell models of each group with the lowest expression are tagged. Cell lines detailed in Supplementary Table 2.

Moreover, to study the observed trend in a different cell lines cohort and with our own materials, we evaluated through qRTPCR the differential expression levels of the *BCL7A* mRNA between the DLBCL and myeloid leukemia (AML and CML) cell models that we had in our laboratory (Supplementary Table 3). As a result, the trend observed (Figure 16) matched the previous approach (Figure 15), showing in both cases that the myeloid models present a lower average *BCL7A* mRNA expression level compared to the DLBCL models. Here, the DLBCL cell line HBL-1 was included as a known negative control of *BCL7A* expression

since it is known that it has a homozygous deletion of the *BCL7A* gene at genomic DNA level (Baliñas-Gavira et al., 2020; Carlos Baliñas-Gavira, 2020).

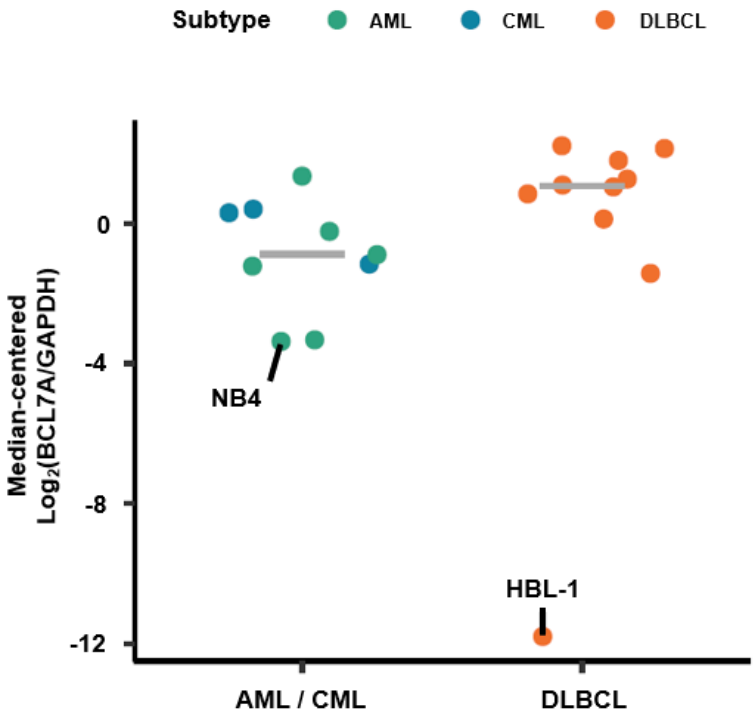

Figure 16. *BCL7A* mRNA expression levels in our cell lines cohort measured by qRTPCR. The grey horizontal bars show the median values for each group. The cell line HBL-1 (DLBCL) was included in the experiment since it is a known negative control for *BCL7A* expression to show the lowest level we could assess by our qRTPCR. The cell lines included in this graph are detailed in the Supplementary table 3. Figure made by courtesy of Alvaro Andrades.

3.2.3 The expression of *BCL7A* is inactivated in an AML cell line model by promoter methylation

Once we discovered the clear relationship between the *BCL7A* genomic methylation and its expression downregulation in

external AML patient cohorts, we searched for a suitable cell line model to study the activity of *BCL7A* in the AML context.

For this purpose, we analyzed the data from all of the AML human cell lines that have been included in the DepMap Portal database. This analysis showed that the NB4 (FAB M3: APL) human cell line model featured the highest *BCL7A* promoter methylation level as well as the third lowest *BCL7A* mRNA expression level compared to the rest of the DepMap Portal AML cell lines (Figure 17). Furthermore, during this analysis we found several CpG sites whose methylation status was significantly inversely correlated with the *BCL7A* expression (Figure 18) (Patiño-Mercau et al., 2023).

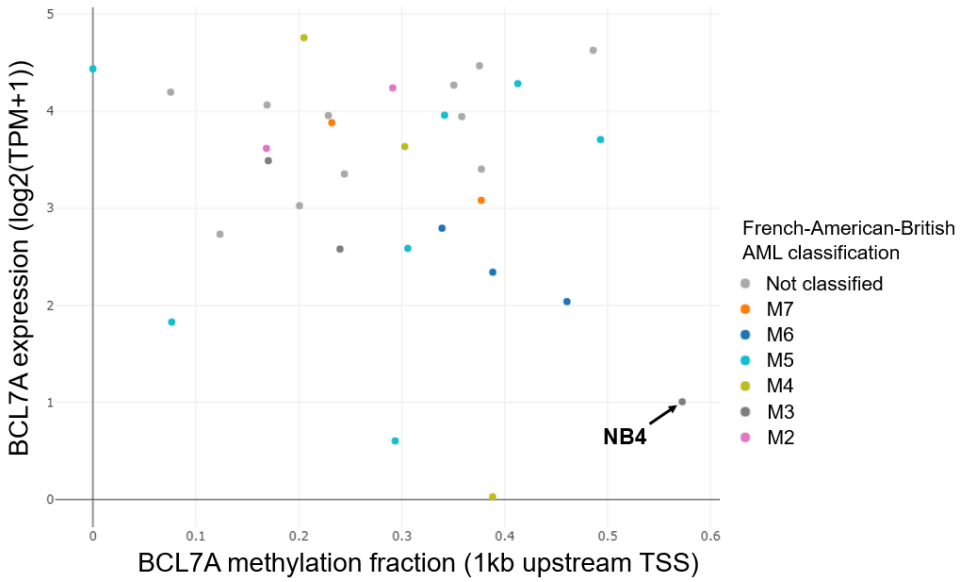

Figure 17. Methylation fraction 1 kb upstream of the *BCL7A* transcription start site (TSS) and *BCL7A* expression of the AML cell lines from the DepMap Portal database (22Q2 version). The different French-American-British (FAB) AML subtypes are shown in different colors. Here, the NB4 cell line shows the highest methylation level as well as low *BCL7A* expression.

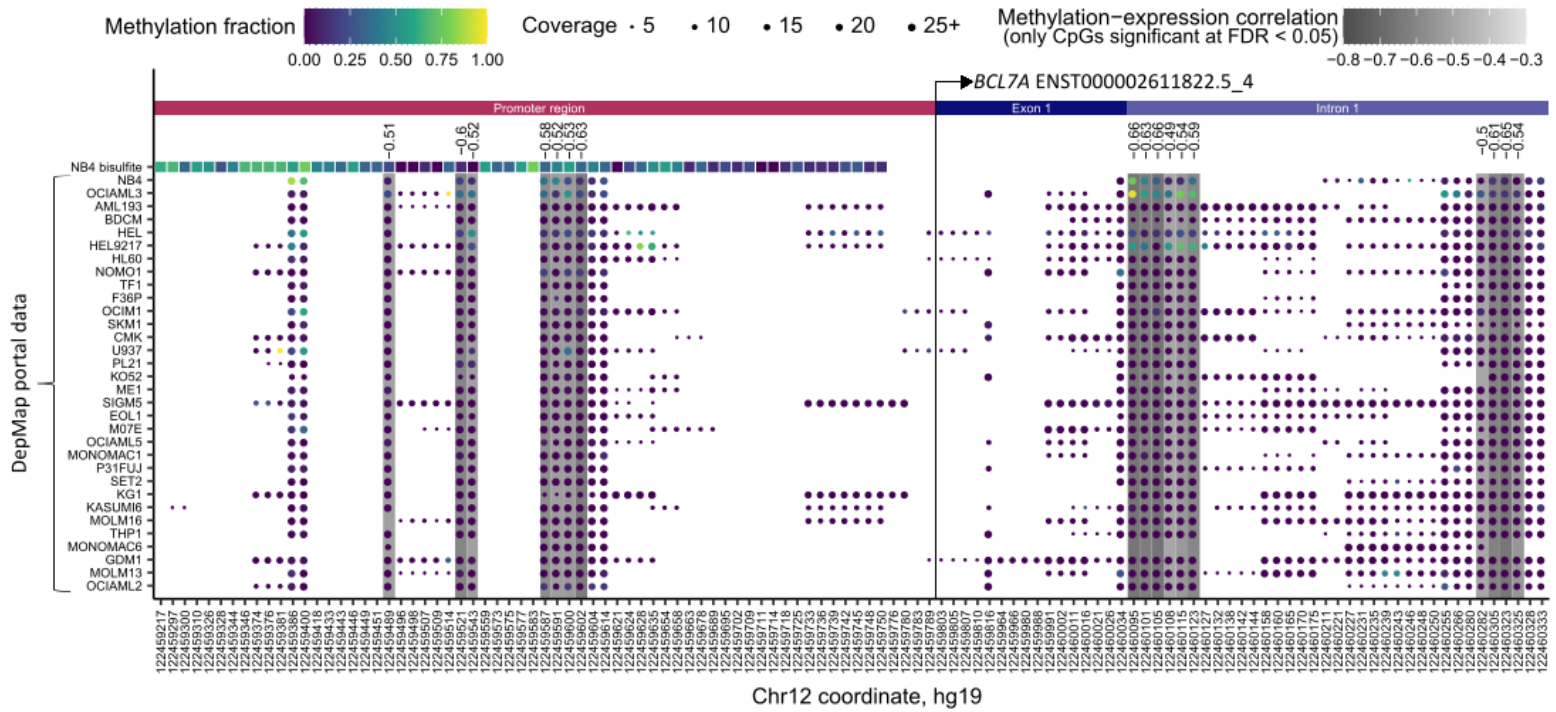

Figure 18. CpG sites methylation profile around the transcription start site (TSS) of *BCL7A* in AML cell lines. Methylation fraction measured by reduced representation bisulfite sequencing (RRBS-seq) data from the DepMap Portal is shown along with our bisulfite sequencing results of the NB4 cell line (upper row). Those CpG sites whose methylation status were inversely significantly correlated with the *BCL7A* expression (FDR < 0.05) are highlighted with a grey background and their Pearson's correlation coefficient is shown above. The transcription start site of *BCL7A* is indicated by a vertical black line. Figure made by courtesy of Maria S Benitez-Cantos.

To evaluate whether the low *BCL7A* expression observed in the NB4 cell line was related or not to a genetic alteration, we sequenced the *BCL7A* coding sequence at the genomic DNA level using previously published protocols and primers (Baliñas-Gavira et al., 2020; Carlos Baliñas-Gavira, 2020). With this approach, we did not find any mutations in the *BCL7A* coding sequence, ruling out the genomic mutations as a putative mechanism underlying *BCL7A* inactivation in this model. Then, we assessed the methylation status of the *BCL7A* promoter region in the NB4 cell model by several independent approaches.

First, as an initial step applying a quick approach, we followed a MSP protocol previously described by Okada et al. (Okada et al., 2013) (see methods section 2.7). Our MSP results showed that the *BCL7A* promoter region was methylated in NB4 cells (Figure 19).

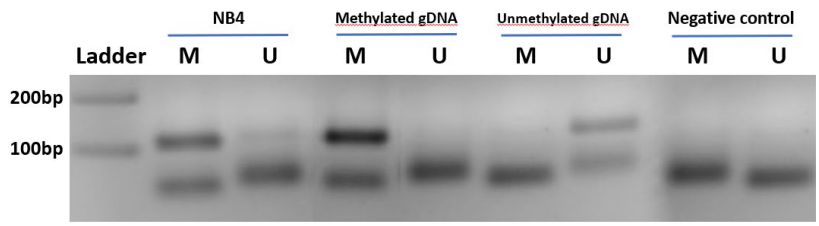

Figure 19. Agarose gel showing the MSP results. There are included the positive controls of the gDNA Meth and gDNA Unmeth (see methods section 2.6), showing in each case amplification only with the expected couple of primers. Also, there is a negative control adding no template DNA.

Afterwards, we performed bisulfite sequencing over a genomic DNA region within the *BCL7A* proximal promoter which included 61 CpG sites. The 33.52% of the sequenced CpG sites

were methylated (upper row of Figure 18 and Supplementary Figure 3).

In accordance with the DepMap Portal, our results showed that the *BCL7A* promoter is methylated in the NB4 cell line. Here, our bisulfite sequencing approach covered all of the CpG sites included within the proximal promoter region, while the DepMap Portal database coverage was not complete. Nevertheless, our experimental results closely matched the DepMap Portal data for the NB4 cell line in all CpG sites covered by the database.

Additionally, taking into account the methylation and the expression data of *BCL7A* featured in the DepMap Portal, we were also able to determine that the methylation status of 17 CpG sites presented a significant negative correlation with *BCL7A* genetic expression at mRNA level (Figure 18). Several of these CpG sites were located in the proximal promoter region while others were placed within the first intron sequence. In fact, the methylation of the first intron is a phenomenon noted to be usually negatively correlated with the gene expression (Anastasiadi et al., 2018).

To further study the relationship between promoter DNA methylation and the *BCL7A* expression silencing in NB4 cells, we evaluated whether the *BCL7A* expression can be restored by the addition of a demethylating agent such as decitabine. In fact, the expression of the *BCL7A* mRNA and protein was restored after decitabine treatment (Figure 20 and Supplementary Figure 14).

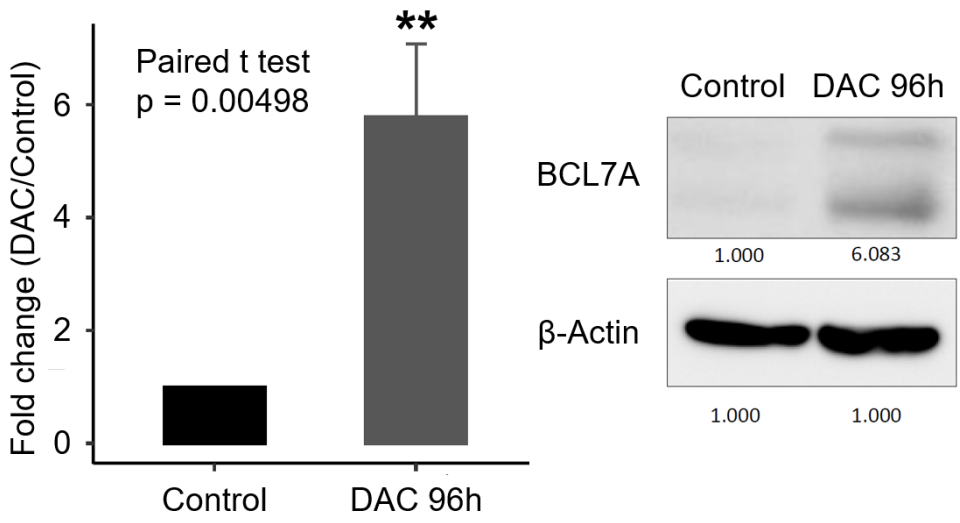

Figure 20. *BCL7A* expression restoration in NB4 cells at mRNA (left, qRTPCR results) and protein (right, WB results) levels after 2μM decitabine treatment for 96h. See Supplementary Figure 14.

Overall, all of the previously described results confirmed that the *BCL7A* silencing in NB4 cells was due to promoter methylation. Besides, when *BCL7A* expression is silenced due to DNA methylation in its genomic locus, its mRNA and protein expression can be pharmacologically restored *in vitro* (Patiño-Mercau et al., 2023).

3.2.4 BCL7A presents a tumor suppressor role in AML cell models *in vitro*

We considered whether the BCL7A protein expression restoration may restrain the tumoral phenotype in an AML cell

models. To evaluate this, we performed a cell growth competition assay upon BCL7A expression restoration.

For this purpose, we transduced the NB4 cell line with lentiviral particles packaged using constructs which lead to the co-expression of the reporter protein ZsGreen1 together with different BCL7A variants: a) WT BCL7A b) mutant BCL7A (Δ27-BCL7A) (Baliñas-Gavira et al., 2020; Carlos Baliñas-Gavira, 2020); and c) an empty vector (EV) (Supplementary Figure 4). The Δ27-BCL7A variant was used as a protein expressing control because it lacks the first 27 amino acids which are needed for BCL7A to bind to SMARCA4 (a mSWI/SNF ATPase subunit) and assemble to the mSWI/ SNFcomplex (Baliñas-Gavira et al., 2020; Carlos Baliñas-Gavira, 2020; Mashtalir et al., 2020).

The NB4 cells transduced with either of the three different constructs were co-cultured with non-transduced cells. The NB4 cell line expressing the WT BCL7A presented a reduced competitive growth capability when co-cultured with non-transduced cells compared to the cells expressing either mutant BCL7A (Δ27-BCL7A) or the EV (Figure 21). These results support that the unaltered BCL7A protein plays a tumor suppressor role in the NB4 myeloid cell line *in vitro* (Patiño-Mercau et al., 2023).

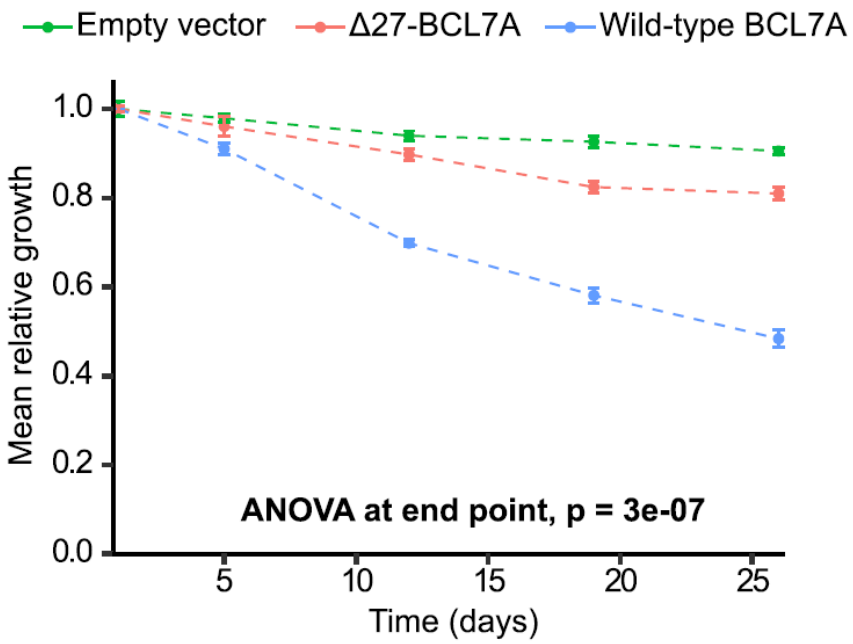

Figure 21. Competitive cell growth assay of non-transduced NB4 cells vs NB4 cells transduced with either pLVX-IRES-ZsGreen1 plasmid expressing wild-type BCL7A, mutant BCL7A (Δ27-BCL7A), or empty vector. All constructs were evaluated in a time course of ZsGreen1+ % measurements on days 1, 5, 12, 19, and 26. This assay involves the co-culture of an NB4 model transduced with one of the plasmids together with non-transduced NB4 cells.

3.2.4.1 BCL7A as tumor suppressor in another AML subtype *in vitro*

To extend the previous results to an additional cell model from a different AML subtype we used M07e (FAB M7: AMKL) which presents average levels of *BCL7A* promoter methylation ("Methylation fraction 1kb upstream TSS" dataset) and *BCL7A* expression ("Expression Public, 22Q2 version" dataset) according to the AML DepMap Portal collection (Figure 22).

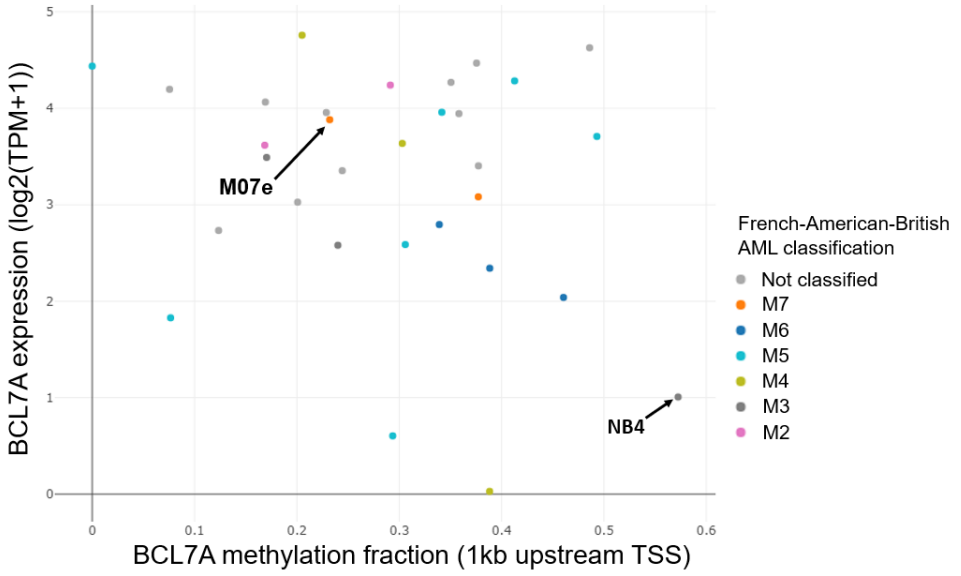

Figure 22. Methylation fraction 1 kb upstream of the *BCL7A* transcription start site (TSS) and *BCL7A* expression of the AML cell lines from the DepMap Portal database (22Q2 version). The different French-American-British (FAB) AML subtypes are shown in different colors. Here, the M07e cell line displays average levels of *BCL7A* promoter methylation and of *BCL7A* expression.

Then, we assessed in our laboratory the M07e *BCL7A* mRNA expression level and whether BCL7A protein expression may be restored treating these cells with decitabine since we found several differentially methylated CpG sites around the *BCL7A* intron one region in the "BCL7A/ CpG Methylation/ Context: Acute Myeloid Leukemia" dataset from DepMap Portal. We found a similar *BCL7A* mRNA expression level compared to NB4 in our qRTPCR approach (Supplementary Figure 15 and Supplementary Table 3), and we observed a strong BCL7A protein expression restoration after both 2μM and 4μM decitabine treatments for 96h (Figure 23 and Supplementary Figure 16).

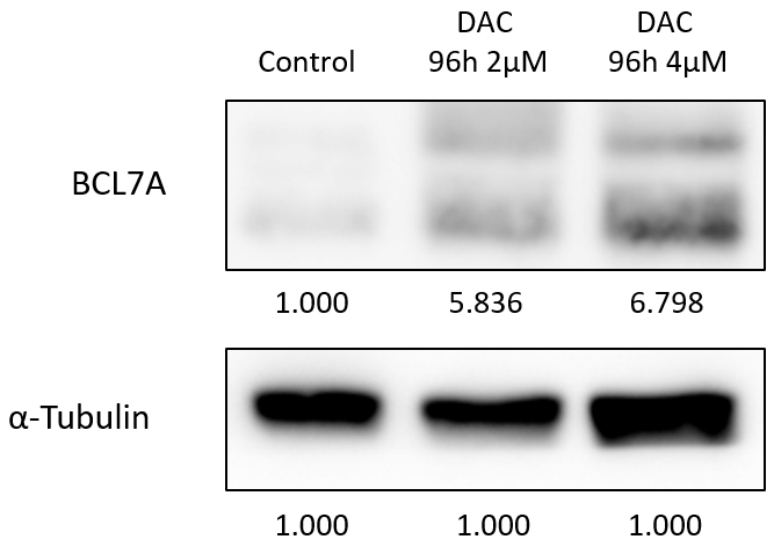

Figure 23. WB results showing the BCL7A expression restoration in M07e cells at protein level after 2µM and 4µM decitabine treatment for 96h in both cases. See Supplementary Figure 16.

These results revealed that the M07e cell line is an AML model from a different subtype compared to NB4, but that shares some similarities with NB4 cells regarding the *BCL7A* expression downregulation, that might be due to *BCL7A* genomic locus DNA methylation.

Furthermore, we performed a competition cell growth assay with the M07e cell line. This experiment showed very similar results to those observed in NB4: the expression of WT BCL7A in M07e cells significantly decreased its competitive growth capability in comparison with the EV and mutant BCL7A (Δ27-BCL7A) (Figure 24) (Patiño-Mercau et al., 2023).

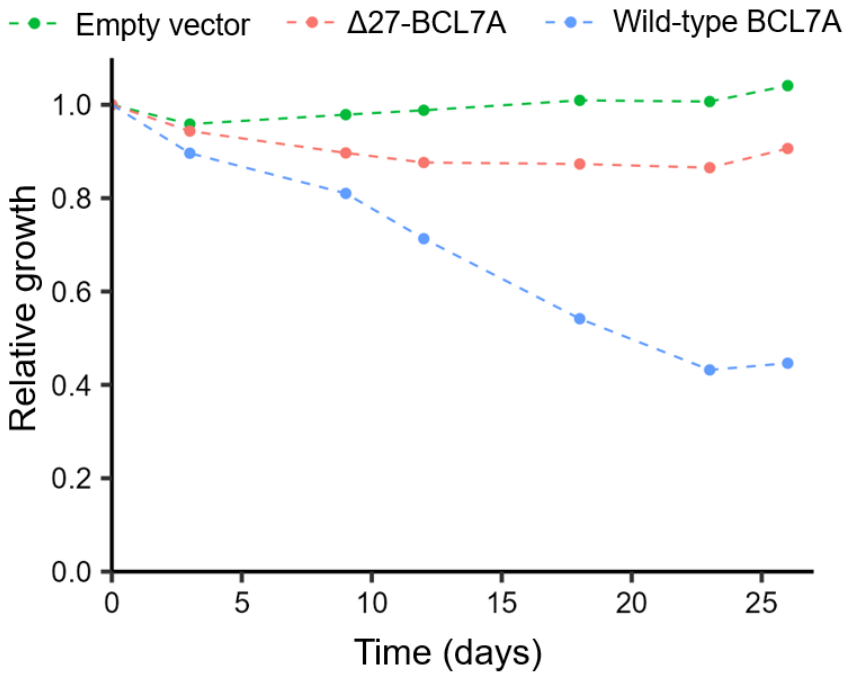

Figure 24. Competition cell growth assay after BCL7A variants expression restoration *in vitro*. Competition cell growth assay of non-transduced M07e cells vs M07e cells transduced with either pLVX-IRES-ZsGreen1 plasmid expressing wild-type BCL7A, mutant BCL7A (Δ27-BCL7A), or empty vector. All constructs were evaluated in a time course of ZsGreen1+ % measurements on days 0, 3, 9, 12, 18, 23 and 26. This assay consists of a co-culture of an M07e model transduced with one of the plasmids together with non-transduced M07e cells. Here, we were not able to carry out a statistics analysis since we have only one replicate.

3.2.4.2 The BCL7A subunit binds to the mSWI/SNF complex through its amino-terminal domain in NB4 cells

In a previous project developed in our research group, we demonstrated that the BCL7A subunit binds the rest of the mSWI/SNF complex through its N-terminal in the DLBCL cell model HBL-1, which does not have any endogenous BCL7A expression since this cell line presents a homozygous deletion of

the BCL7A genomic locus (Baliñas-Gavira et al., 2020; Carlos Baliñas-Gavira, 2020).

Therefore, we assessed whether the N-terminal domain of BCL7A was also crucial for its binding to the mSWI/SNF complex in the NB4 cell model, being the main cell model used in this doctoral thesis project. For this purpose, we performed a BCL7A immunoprecipitation followed by a LC-MS/MS analysis with the NB4 cells transduced with WT BCL7A and Δ27-BCL7A.

Our approach showed that the WT BCL7A presents more interactions (higher Z-score) with the rest of the mSWI/SNF complex subunits compared to the Δ27-BCL7A mutant variant condition (Figure 25), which is known to be unable to bind the mSWI/SNF complex in a DLBCL model (Baliñas-Gavira et al., 2020). Therefore, these results show that BCL7A depends on its N-terminal to bind the rest of the mSWI/SNF complex also in this myeloid cell model.

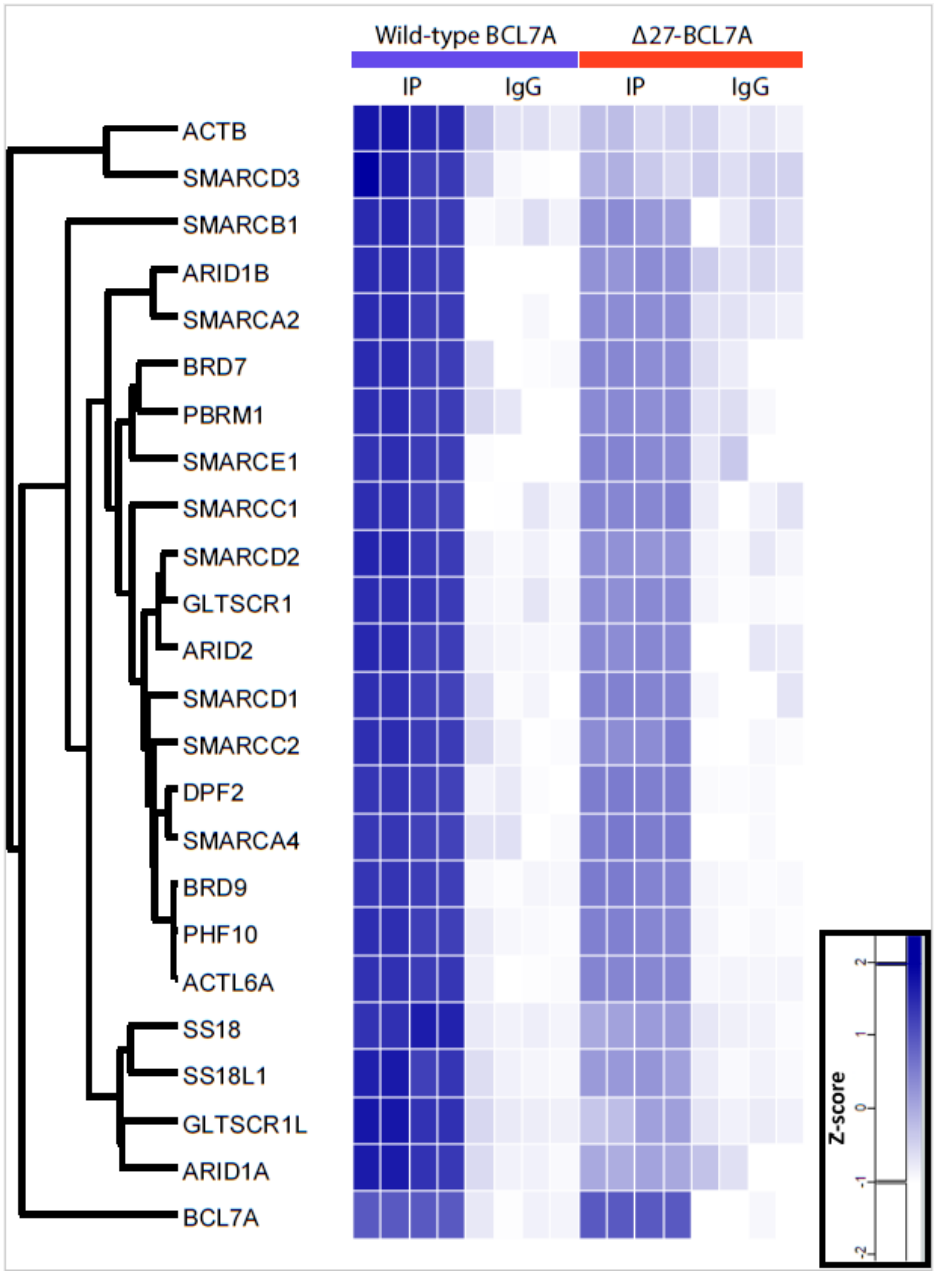

Figure 25. LC/MS-MS analysis of the mSWI/SNF complex subunits. Immunoprecipitates were purified using anti-BCL7A in NB4 cells transduced with wild-type BCL7A or Δ27-BCL7A (only short isoforms). Two biological replicates were performed for each condition (immunoprecipitation [IP] and irrelevant IgG), with each replicate run twice. "Label-free Quantification" (LFQ) values were represented after Z-Score normalization. Adapted figure, made by the proteomic unit of the "Centro Nacional de Investigaciones Oncológicas" (CNIO, Spain).

3.2.5 BCL7A presents a tumor suppressor role in an AML cell model in an *in vivo* context

Since the *in vivo* approaches provide more reliable results to the scientific community because they reproduce better the natural conditions compared to the *in vitro* ones, we designed an *in vivo* xenograft approach to assess the putative tumor suppressor activity of BCL7A.

At the ontset, we generated sorted pure populations of two different NB4 cell models that simultaneously stably co-expressed luciferase and wild-type BCL7A/ZsGreen1 (both short and long BCL7A isoforms) or luciferase and EV pLVX-IRES-ZsGreen1.

Then, we intravenously injected five million of NB4 cells per mouse, giving rise to two groups of six NSG immunodeficient mice: one group with NB4 cells co-expressing luciferase and WT BCL7A, and the other one of NB4 expressing luciferase and carrying the EV (control cells).

Then, we applied *in vivo* imaging technologies (IVIS-Spectrum) to evaluate the bioluminescence. 21 days after the injection, the mice group injected with the luciferase and WT BCL7A co-expressing NB4 cells presented a significantly lower bioluminescence compared to the mice group injected with control cells (Figures 26-27).

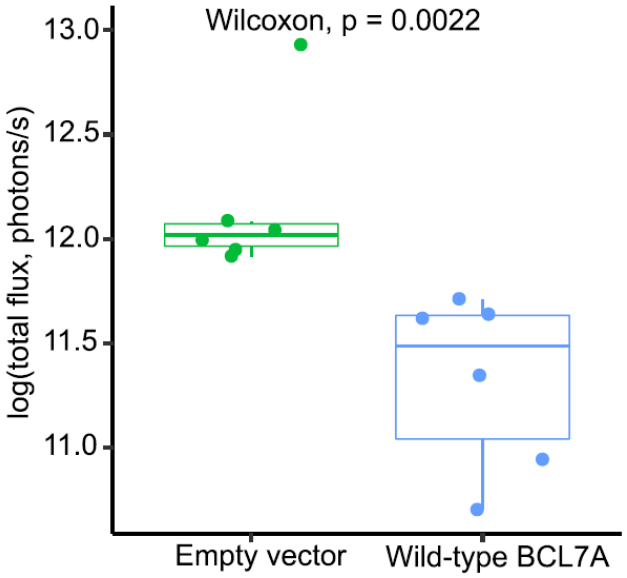

Figure 26. Mice bioluminescence signal captured 21 days after the injection of the NB4-luciferase-transduced cell models. The wild-type BCL7A NB4 injected mice group (n = 6) shows a significant ($p < 0.05$, Wilcoxon test, N = 12) bioluminescence reduction compared to the empty vector-transduced NB4 mice group (n = 6; control group).

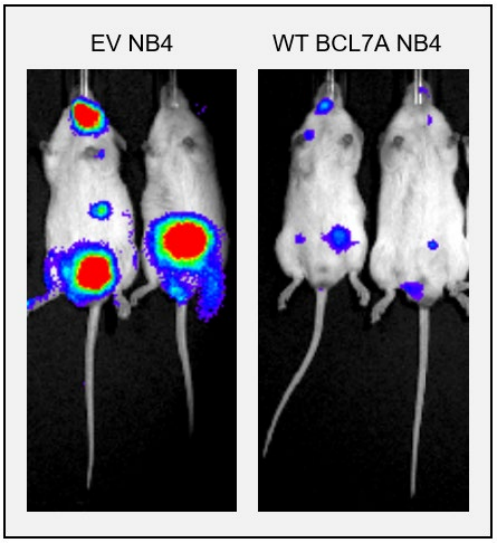

Figure 27. Bioluminiscence signal captured from two representative mice of each group of the *in vivo* xenograft approach. Image obtained using *in vivo* imaging technologies (IVIS-Spectrum).

The bioluminescence signal reduction in the WT BCL7A mice group revealed a lower tumorigenic ability of the NB4 cells in the presence of WT BCL7A, confirming its tumor suppressor role in an *in vivo* context too. Consequently, our *in vivo* approach endorsed that the BCL7A expression restoration promotes a tumor suppressor phenotype in NB4 cells (Patiño-Mercau et al., 2023).

3.2.6 The restoration of BCL7A expression in NB4 cells affects to the expression of key AML genes

To study in greater depth the molecular changes yielded by restoring BCL7A expression, we performed RNA-seq in the NB4 cell line.

Here, we compared the transcriptomes from the WT BCL7A and Δ27-BCL7A transduced NB4 cell models. We identified 1151 differentially expressed genes (adjusted p-value < 0.001; Figure 28).

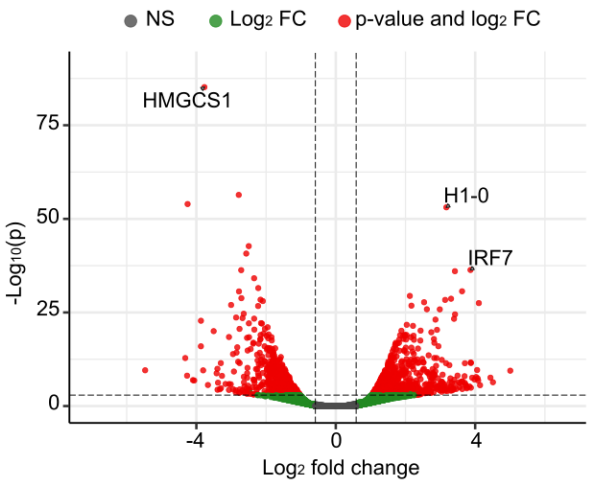

Figure 28. Volcano plot showing the differentially expressed genes in NB4 cell line in the comparison between NB4 transfected with WT BCL7A and Δ27-BCL7A. NS: non-significant. The established thresholds are: FC: +log2(1.5) and -log2(1.5); and p: -log10(0.01). Figure made by courtesy of Maria S Benitez-Cantos.

To know whether the previously mentioned genes cluster in any functional pathway, we performed a GO enrichment analysis including the top 400 genes with better-adjusted p-value and using the algorithm Metascape (Y. Zhou et al., 2019). Those most significantly enriched pathways ($p < 1 \times 10^{-10}$) were related to protein synthesis, cell cycle, and mitotic cell cycle (Figure 29), which may underlie the molecular explanation of the tumor suppressor phenotype observed in the WT BCL7A transduced NB4 cells.

In the comparison between the NB4 cells transduced with WT BCL7A vs Δ27-BCL7A, the most differentially downregulated gene according to its adjusted p-value was 3-Hydroxy-3-Methylglutaryl-CoA Synthase 1 (*HMGCS1*) (p-adjusted value = 9.12×10^{-82}, 13.63-fold change of downregulation; Figures 28 and 30). In fact, the *HMGCS1* gene codes for a key enzyme of the mevalonate pathway of the cholesterol synthesis and it has been found dysregulated in AML patients, where it was also observed to be overexpressed in recently diagnosed and relapsed/refractory patients (C. Zhou et al., 2021). Moreover, these authors hypothesized that *HMGCS1* can potentially be involved in the survival of AML cells.

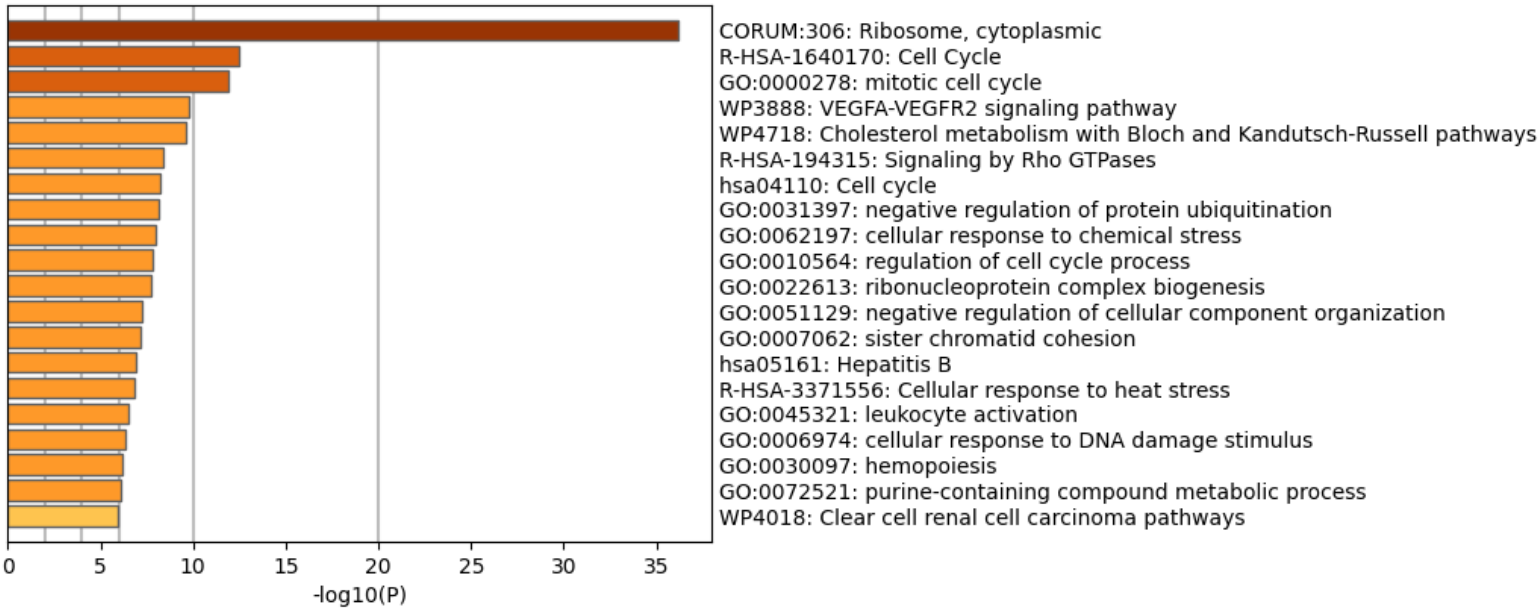

Figure 29. Enriched terms across the top significant (p adjusted) 400 differentially expressed genes when comparing NB4 transduced with WT BCL7A and Δ27-BCL7A.

Besides, the most differentially upregulated genes according to their adjusted p-value were the H1.0 Linker Histone (*H1-0*) (p-adjusted value = 8.36×10^{-54}, 9.02-fold change; Figures 28 and 30) and the Interferon regulatory factor 7 (*IRF7*) (p-adjusted value = 8.75×10^{-34}, 14.58-fold change; Figures 28 and 30).

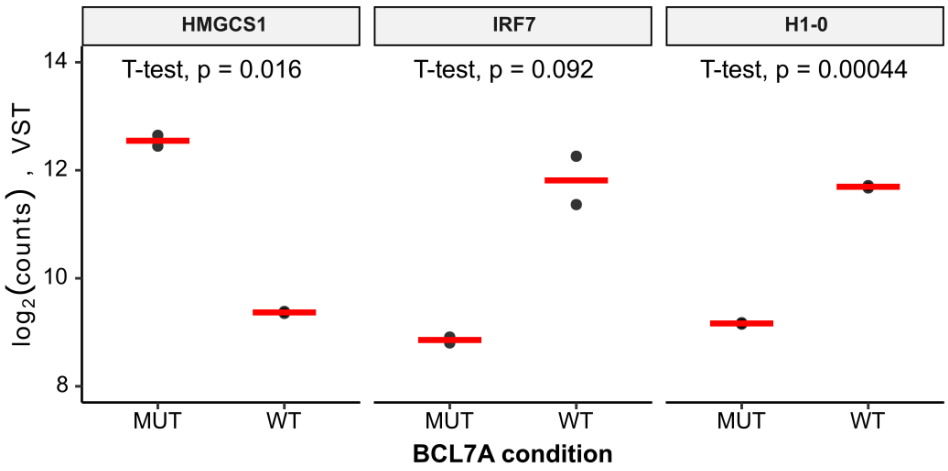

Figure 30. Gene expression values from our RNA-seq data of three selected genes: *HMGCS1*, *IRF7*, and *H1-0*. Log_2 of variance-stabilized transformed (VST) gene counts was obtained with DESeq2 in R. The mean value is represented with the red horizontal lines.

The *H1-0* gene encodes a linker histone (H1.0) involved in the formation of supra-nucleosomal chromatin higher-order structures. Here, the detected changes in *H1-0* expression levels may be related to alterations in cell proliferation and differentiation, since H1-0 has been found to act as an epigenetic regulator of gene expression (Di Liegro et al., 2018).

On the other hand, the *IRF7* gene has been described to have a tumor suppressor role in *in vivo* AML models. In fact, the *IRF7* loss enhances AML progression while *IRF7* overexpression

decreases the leukemia stem cell levels and cell proliferation (H. Wang et al., 2022).

Overall, our results suggest that BCL7A modulates the expression of key genes that can be linked to a tumor suppressor phenotype in the AML context (Patiño-Mercau et al., 2023).

3.3 Discussion

BCL7A has previously been widely described in the context of lymphoid lineage disorders (Baliñas-Gavira et al., 2020; Carbone et al., 2008; Gao, 2007; Litvinov et al., 2013; Ramos-Medina et al., 2013; Van Doorn et al., 2005), but despite the article describing the case of a single patient with *BCL7A*-associated CML (Yu et al., 2017), our results included in this chapter confirm that *BCL7A* also plays a tumor suppressor role in the myeloid lineage through experimental evidences (Patiño-Mercau et al., 2023).

When we analyzed the data from the external cohorts of AML patients: TCGA-LAML (N = 160), TARGET-AML (N = 188) and (Glass et al., 2017) (N = 111); we found too few mutations and even that the expression of *BCL7A* was inversely correlated with its methylation level (Figures 12-14). This inverse correlation between methylation and gene expression is the most common trend, as DNA methylation controls gene expression either by attracting proteins associated with gene repression or by blocking the binding of transcription factors to DNA (Moore et al.,

2013). However, in certain circumstances DNA hypermethylation has been found to be associated with increased gene expression, challenging the conventional view where DNA methylation is consistently associated with the inhibition of gene expression (Rauluseviciute et al., 2020). Despite that, our results here determined that *BCL7A* follows the usual trend between its DNA locus methylation and gene expression downregulation which is a common feature of tumor suppressors (Lopez-Serra & Esteller, 2012).

Moreover, when analyzing *BCL7A* expression between the different AML subtypes in the same cohorts mentioned above (Supplementary Figures 11-13), we observed that the M1 FAB subtype (acute myeloblastic leukemia with minimal maturation) presented a slightly higher *BCL7A* expression compared to the rest of the subtypes, but considering the large variability in *BCL7A* levels within each subtype and the uneven distribution of sample sizes, using *BCL7A* expression levels for classification of AML patients might not be accurate.

Based on our experience and knowledge about *BCL7A* in DLBCL models, we as well studied the comparison of *BCL7A* mRNA expression between AML and DLBCL cell models. Here, the results from the external data and our own cell models showed the same trend: the AML models showed a lower *BCL7A* expression level compared to the DLBCL models (Figures 15-16). In fact, the tumor suppressor genes are often downregulated in cancer (Gregory & Copple, 2023). Thus, the lower *BCL7A* expression in

the AML models supported our hypothesis about the putative tumor suppressor role of *BCL7A* in AML, as this role had been previously determined in B-cell derived hematologic malignancies (Baliñas-Gavira et al., 2020). However, the different hematologic lineages (myeloid and lymphoid) exhibit different genetic expression profiles (Miyamoto et al., 2002), which may even provide an explanation to this lower *BCL7A* expression in myeloid models as a physiological characteristic.

Then, when looking for suitable AML models to study *BCL7A* in this hematologic disorder, we searched for a model with reduced or absent *BCL7A* expression, since the *BCL7A*-deficient cell lines may be used to restore the expression of this gene and to evaluate the functional impact of *BCL7A* on the tumor phenotype. Among the models included in the DepMap Portal database and in our own collection, we first found the NB4 (FAB M3) and then the M07e (FAB M7) cell lines. Both showed *BCL7A* expression downregulation compared to other myeloid lineage cell lines (Figure 16), due to methylation of the *BCL7A* genomic locus. We evaluated this feature in both cell lines by treatment with decitabine (HMA) followed by analysis of the expected restoration of BCL7A protein expression (Figures 20 and 23). In NB4, we were also able to assess this feature by MSP and bisulfite sequencing, giving us a more detailed view for this cell model (Figures 18-19). We then used these two models for our study as they were already present in our collection.

Since the NB4 cell line (FAB M3, APL) was initially our main cell model, we looked for other AML subtype cell models because APL (about 10-15% of all AML cases) has a very specific cytogenetic feature: the reciprocal translocation between chromosomes 15 and 17: t(15:17). This made our APL model controversial for some authors, since this feature makes APL behave differently compared to other AML subtypes. Therefore, we chose M07e (FAB M7), which belongs to a different AML subtype, as a secondary model for this project. Acute megakaryoblastic leukemia (FAB M7) does not have a high incidence among AML patients. It represents about 1% of adult leukemia cases, and 3% to 10% of childhood leukemia cases (Dima et al., 2017). Nevertheless, the M07e cell line had the necessary characteristics (in common with NB4) to be suitable for our project.

The t(15:17) translocation results in a fusion between the *PML* and *RARA* genes, giving rise to the *PML-RARA* fusion gene. This defines the current generalized APL treatment, which consists of the combination therapy of All-Trans Retinoic Acid (ATRA) and Arsenic Trioxide (ATO). These agents induce the differentiation of leukemic promyelocytes present in the BM of APL patients, thereby preventing the accumulation of these leukemic promyelocytes. Historically, APL has the highest mortality rate among leukemia subtypes due to severe coagulopathies. However, with the introduction of combined ATRA-ATO therapy, APL now has a more favorable outcome

compared to other AML subtypes (Chale et al., 2019; H. Y. Wang et al., 2022; Z.-Y. Wang & Chen, 2008).

In fact, NB4 cells have been shown to be differentiated by ATRA *in vitro* (Idres et al., 2001; Khanna-Gupta et al., 1994). The underlying metabolic changes in ATRA-treated NB4 appear to be the activation of the aerobic glycolysis pathway and the reduction of oxidative phosphorylation dependent ATP production. These changes may be related to the differentiation of these APL cells *in vitro*. Then, further study of these metabolic changes may provide new insights for the development of modern therapeutic approaches (Albanesi et al., 2020).

Furthermore, during our analysis of the AML cell models present in the DepMap Portal, we found that the OCI-AML3 cell line (FAB M4, acute myelomonocytic leukemia) was the cell model with the lowest *BCL7A* mRNA expression level. These data focused our attention on this model of another AML subtype to plan further research on the role of *BCL7A* in AML using this cell line.

The decitabine treatment of the NB4 and M07e cell lines showed that *BCL7A* expression at the protein level can be restored *in vitro* while using this HMA, which has already been approved by the United States Food and Drug Administration (FDA) for the treatment of certain AML patients in the clinic (Kantarjian et al., 2021). Therefore, this restoration of BCL7A expression revealed a part of the metabolic changes that may be responsible for the improvement in the condition of AML patients. In fact, the BCL7A

expression restoration is supposed to lead to the assembly of a functional SWI/SNF (including BCL7A) that might infer in several metabolic pathways. However, it is important to note that these HMAs are non-specific demethylating agents that act genome-wide and that can promote the activation of some proto-oncogenes as it has been previously noted (Grimm & Binder, 2022; Y.-C. Liu et al., 2022).

Then, our experimental approaches performed with the two selected cell lines, NB4 and M07e, showed that restoration and overexpression of WT BCL7A protein resulted in a competitive growth reduction compared to both the mutant variant Δ27-BCL7A and the EV (Figures 21 and 24). These results suggested that BCL7A plays a tumor suppressor role in AML cell models *in vitro*.

To provide a broader perspective, we also performed an *in vivo* xenograft approach using the NB4 cell line, which again showed that restoration of WT BCL7A protein overexpression promoted decreased growth of NB4 cells *in vivo* compared to the EV condition, supporting that BCL7A plays a tumor suppressor role not only *in vitro* but even *in vivo* (Figures 26-27). Although animal models have some drawbacks, such as the ethical implications, variations in biokinetic parameters and the challenge of extrapolating results to humans, they are generally considered more reliable than *in vitro* approaches (Saeidnia et al., 2016). For this reason, *in vivo* support of *in vitro* results is currently preferred to provide sound research information.

Regarding the results obtained by immunoprecipitation followed by LC-MS/MS of the BCL7A subunit from protein extracts of the NB4 models (WT BCL7A and Δ27-BCL7A), we have here confirmed that the BCL7A subunit binds the rest of the mSWI/SNF complex through its N-terminal domain (Figure 25). This confirmed that this fact also occurs in the context of a myeloid lineage cell model (NB4), as this phenomenon has been previously described in lymphoid models (HBL-1 cell line, DLBCL) (Baliñas-Gavira et al., 2020). Moreover, this finding was as well observed by another research group using a different technique (cross-linking mass-spectrometry: CX-MS) and model (HEK293F cells) (Figure 31) (Mashtalir et al., 2020). Therefore, we hypothesize that the binding of BCL7A to the rest of the mSWI/SNF complex occurs through its N-terminal domain in a tissue-independent manner.

Figure 31. Protein-protein interactions between the SWI/SNF subunits BCL7A and SMARCA4 as determined by Mashtalir et al. (Mashtalir et al., 2020). There are numbers indicating the positions of each amino acid that interact with each other (solid lines). The region from BCL7A exon 1 that is deleted in splice site mutant BCL7A (Δ27-BCL7A) variant (Baliñas-Gavira et al., 2020) is marked in dark red. There are also marked the already known domains of SMARCA4 as described in UniProt.

Furthermore, the fact that the mSWI/SNF subunits BCL7A, BCL7B and BCL7C share the same N-terminal domain (see Supplementary Figure 2) suggests a common function for this

domain, which may be the binding of these three subunits to the mSWI/SNF complex (Carlos Baliñas-Gavira, 2020).

An interesting comparison arises from the results of BCL7A subunit immunoprecipitation followed by LC-MS/MS in the NB4 (Figure 25) and HBL-1 cell models (Baliñas-Gavira et al., 2020). While in NB4 *BCL7A* is strongly downregulated by genomic DNA methylation, the HBL-1 cell line has a homozygous deletion of the *BCL7A* gene. Therefore, in the HBL-1 results, there are no differences between the immunoprecipitation and irrelevant IgG (negative control) signals in the Δ27-BCL7A transduced HBL-1 cells. However, in the Δ27-BCL7A transduced NB4 cells, there is a slight signal in the immunoprecipitation compared to the irrelevant IgG, which may be explained by the existence of a residual expression of BCL7A. This means that the methylation might not lead to a complete silencing of the gene expression in NB4. This observation is consistent with the expression of BCL7A at the mRNA level (see Figure 16) in our qPCR results, where HBL-1 has a much lower expression than NB4.

In addition, we analyzed and compared the transcriptomes of both WT BCL7A and Δ27-BCL7A transduced NB4 cell models and identified 1151 genes with differential expression (Figures 28). Also, the most altered metabolic pathways were related to protein synthesis and cell cycle (Figure 29), which may provide a molecular explanation for the tumor suppressor phenotype observed in the WT BCL7A transduced NB4 cells. Among the most differentially expressed genes, we found *HMGCS1*, *H1-0* and *IRF7*

(Figure 30), which have been observed to be involved in AML (Di Liegro et al., 2018; H. Wang et al., 2022; C. Zhou et al., 2021). Thus, their altered expression levels may explain, at least in part, the tumor suppressor phenotype conferred by restoration of WT BCL7A protein expression in NB4 cells (Figures 21, 26 and 27).

Besides, for the future scope of this project, which aims to provide a complete description of the mSWI/SNF complex BCL7A subunit in models of AML (NB4) (Patiño-Mercau et al., 2023) and DLBCL (OciLy1) (Baliñas-Gavira et al., 2020), we have recently planned to perform ChIP-seq and ATAC-seq approaches. We expect that these techniques will provide additional data about the specific genomic binding sites of the mSWI/SNF complex as well as information about relevant changes in chromatin accessibility at different genomic loci in the presence or absence of WT BCL7A. Subsequently, these results may further explain the tumor suppressor phenotypes observed in NB4 and OciLy1 upon restoration of WT BCL7A protein expression.

Currently, the clinical interest in the activity of the mSWI/SNF complexes has increased due to the identification of several synthetic lethal interactions among its subunits, paving the way for targeted therapies (Michel et al., 2018; Santiago Schiaffino-Ortega et al., 2014; Sasaki & Ogiwara, 2020). In addition, there has been significant research about precision therapies targeting mSWI/SNF subunits in AML. In fact, a recent report has supported the notion of targeting the mSWI/SNF catalytic subunits (SMARCA4 and SMARCA2) as a potential

therapeutic strategy in AML (Rago et al., 2022). Additionally, a specific targeted drug that inhibits the BRD9 subunit has been developed, which yields an anti-tumor phenotype in AML in both cell models and *in vivo* models (Martin et al., 2016). While these findings suggest potential, further research is needed to determine the full impact of the mSWI/SNF complexes on AML and their potential clinical significance.

Here, our results provide the first experimental evidence that *BCL7A* plays a role in AML models in *in vitro* and *in vivo* models, acting as a tumor suppressor gene in this context. However, further research is needed to increase the knowledge of *BCL7A* involvement in AML. These studies may clarify whether the expression level of *BCL7A* can be considered as a diagnostic or prognostic biomarker for the classification of AML patients.

Chapter 4.

Bcl7a conditional knock-out mouse model

Chapter 4. *Bcl7a* conditional knock-out mouse model

4.1 Background

In this chapter we show the results from a long-term *in vivo* approach in which we generated in our animals facility an original *Bcl7a* inducible KO mouse model.

Here, since the SWI/SNF chromatin remodeling complexes subunits are a remarkably conserved set of proteins present in a wide range of eukaryotic organisms (Hernández-García et al., 2022), and since the mouse Bcl7a protein has a very high sequence homology with the human BCL7A protein (see Supplementary Figure 17), we expected that the mouse *Bcl7a* gene has identical or very similar biological functions compared to the human *BCL7A* gene. However, we can not discard the putative functional differences among these two orthologous genes.

Our main aim in this *in vivo* approach was to study the possible alterations in hematologic cells (not only myeloid lineage cells) and tissues yielded by *Bcl7a* inactivation, since *BCL7A* alterations have been found very related to hematologic disorders (Baliñas-Gavira et al., 2020; Carlos Baliñas-Gavira, 2020; Kadoch et al., 2013; Patiño-Mercau et al., 2023).

In a previous external study, it was reported that a ubiquitous *Bcl7a* KO mouse model (C57BL/6 background), in which *Bcl7a* was deleted already during the mouse embryonic development, resulted in pre-weaning mortality and the researchers speculated that this phenotype might be related to a failure in the initiation of a proper feeding or a normal respiration (Wischhof et al., 2017).

Therefore, we knew that to study the effects of *Bcl7a* inactivation in a mouse model in this same background (C57BL/6), we needed the *Bcl7a* gene to be functional during the embryonic development and then have the possibility to inactivate this gene to develop our project. For this purpose, we generated our *Bcl7a* inducible KO mouse model, to be able to delete *Bcl7a* once the mice were already weaned and close to the adulthood and thus preventing them from dying before weaning.

4.2 Results

These results have not been published yet.

4.2.1 *Bcl7a* inducible KO mouse model generation

We performed the necessary selective breeding between our UBC-Cre-ERT2 (ubiquitous Cre expression inducible by tamoxifen) mouse model (Indra et al., 1999) and the *Bcl7a*$^{fl/fl}$ mouse model (Wischhof et al., 2017) to generate the desired

model including both features: UBC-Cre-ERT2-*Bcl7a*$^{fl/fl}$ (the *Bcl7a* inducible KO mouse model).

In addition, we checked that this model worked as expected, yielding the whole body *Bcl7a* inactivation only after the intraperitoneal injection of the corresponding tamoxifen dose. For this purpose, we genotyped 5 UBC-Cre-ERT2-*Bcl7a*$^{fl/fl}$ mice where 4 were intraperitoneally injected with tamoxifen and one was not injected (control mouse) (see methods section 2.23) (Figure 32).

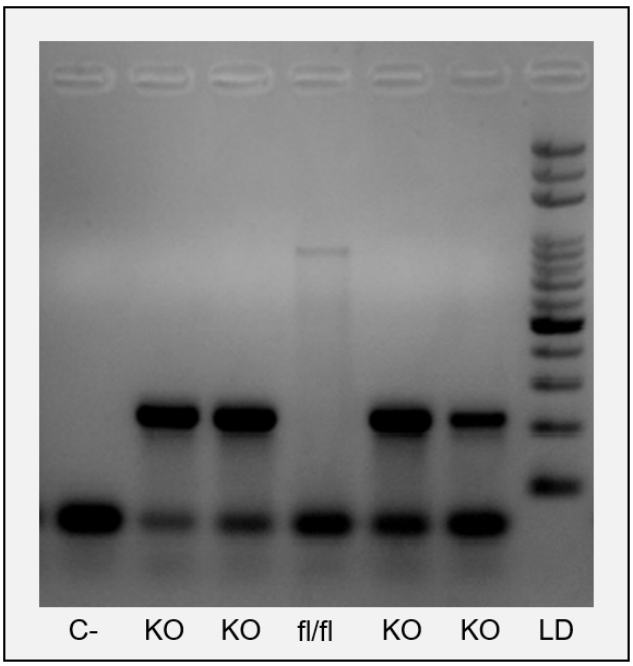

Figure 32: Example of an agarose gel electrophoresis results from mice genotyping PCRs showing the expected amplicons when our UBC-Cre-ERT2-*Bcl7a*$^{fl/fl}$ mice models are given the suitable dose of tamoxifen. C-: PCR negative control without template DNA; fl/fl: *Bcl7a* floxed allele (930 bp amplicon) of the control mouse; KO: *Bcl7a* KO allele (261 bp amplicon), LD: 100 bp DNA ladder.

4.2.3 Blood tests results of the *Bcl7a* KO mice models

Some phenotypical effects given by a hematologic cells disorder are visible to the naked eye, such as weight loss, a reduction of the physical activity or an abdominal enlargement (as a result of splenomegaly or a swollen lymph node) among other features.

Indeed, we visited our animals facility weekly and evaluated each mouse conditions. We monitored mice weigh, behavior, abdominal size and whether they presented any other visible anomaly. However, we did not find any differences in the simple view phenotype between the two mice groups (*Bcl7a* KO and control) up until they were approximately two years old and all of them were getting weaker due to the age.

Simultaneously, we performed blood collections and blood tests of each mouse to assess whether they presented differences in the count of WBC per 1 μL in the peripheral blood, since the previous knowledge showed that *Bcl7a* has been seen usually related to hematologic disorders associated with this subgroup of blood cells (Baliñas-Gavira et al., 2020; Carlos Baliñas-Gavira, 2020; Patiño-Mercau et al., 2023).

Our results showed non-significant differences in the WBC count between the two conditions (*Bcl7a* KO and control) at any timepoint (Figures 33-35). Also, we observed a slightly higher WBC count in male mice than in female mice in general

(Supplementary Figures 5-10) and a decrease in total WBC per 1 μL as the age of the mice increased (Figures 33-35).

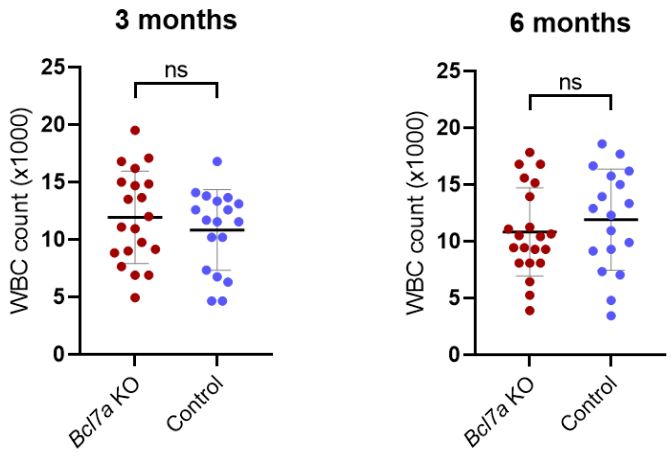

Figure 33. White blood cells (WBC) count per 1 μL 3 and 6 months after tamoxifen injection. No significant (ns) differences were found between the control and *Bcl7a* KO mice groups ($p > 0.05$, unpaired T-test, N = 38 at 3 months, N = 39 at 6 months).

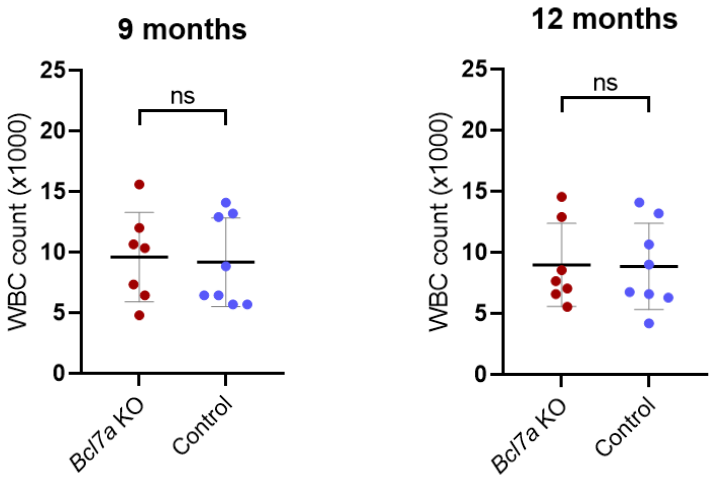

Figure 34. White blood cells (WBC) count per 1 μL 9 and 12 months after tamoxifen injection. No significant (ns) differences were found between the control and *Bcl7a* KO mice groups ($p > 0.05$, unpaired T-test, N = 15 at 9 months, N = 15 at 12 months).

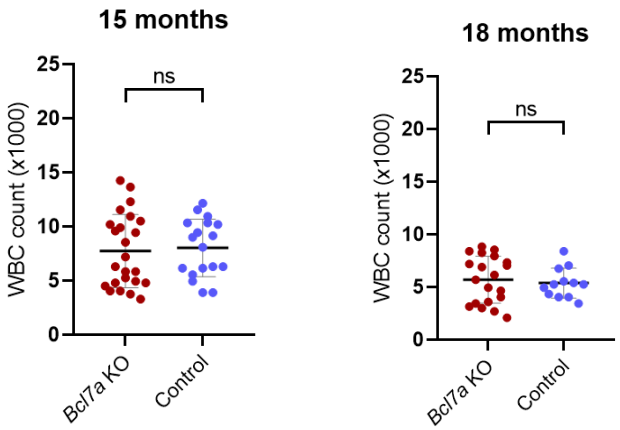

Figure 35. White blood cells (WBC) count per 1 µL 15 and 18 months after tamoxifen injection. No significant (ns) differences were found between the control and *Bcl7a* KO mice groups ($p > 0.05$, unpaired T-test, N = 42 at 15 months, N = 32 at 18 months).

Besides, we analyzed the WBC / red blood cells (RBC) proportion (Figures 36-38) and the count of total platelets per 1 µL (Figures 39-41). We did not find any significant differences between the two conditions for these two parameters.

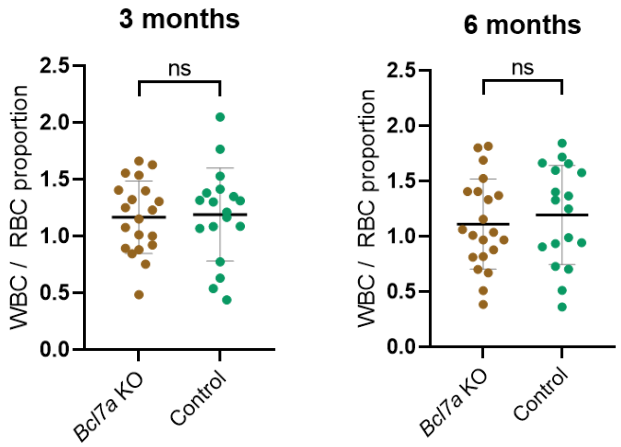

Figure 36. White blood cells (WBC) / Red blood cells (RBC) proportion 3 and 6 months after tamoxifen injection. No significant (ns) differences were found between the control and *Bcl7a* KO mice groups ($p > 0.05$, unpaired T-test, N = 38 at 3 months, N = 39 at 6 months).

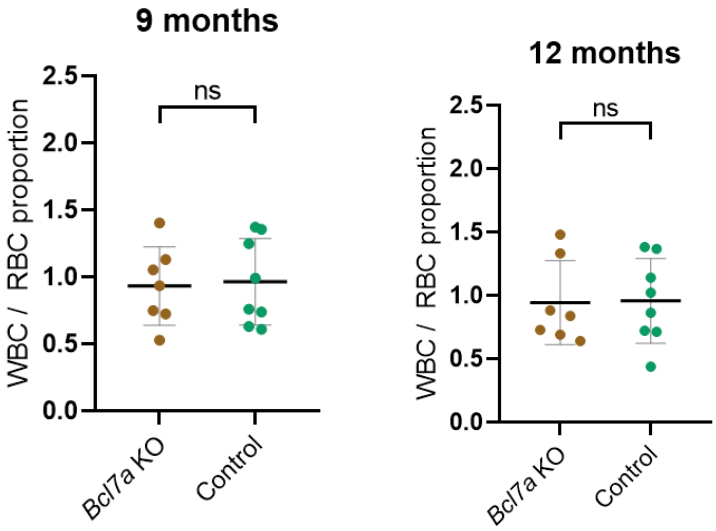

Figure 37. White blood cells (WBC) / Red blood cells (RBC) proportion 9 and 12 months after tamoxifen injection. No significant (ns) differences were found between the control and *Bcl7a* KO mice groups ($p > 0.05$, unpaired T-test, N = 15 at 9 months, N = 15 at 12 months).

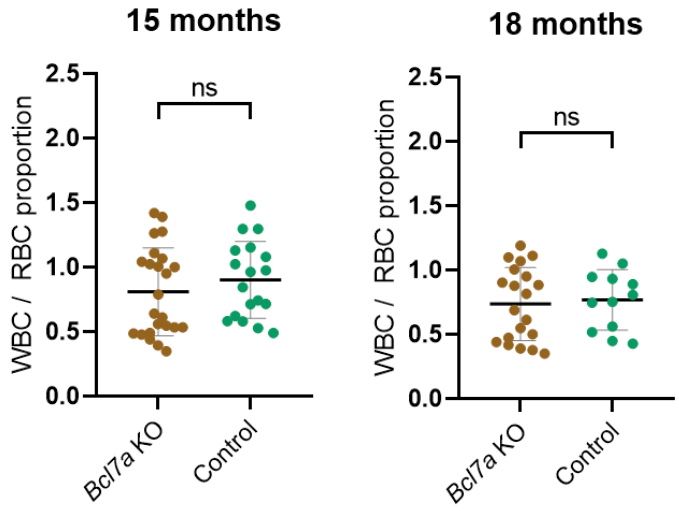

Figure 38. White blood cells (WBC) / Red blood cells (RBC) proportion 15 and 18 months after tamoxifen injection. No significant (ns) differences were found between the control and *Bcl7a* KO mice groups ($p > 0.05$, unpaired T-test, N = 42 at 15 months, N = 32 at 18 months).

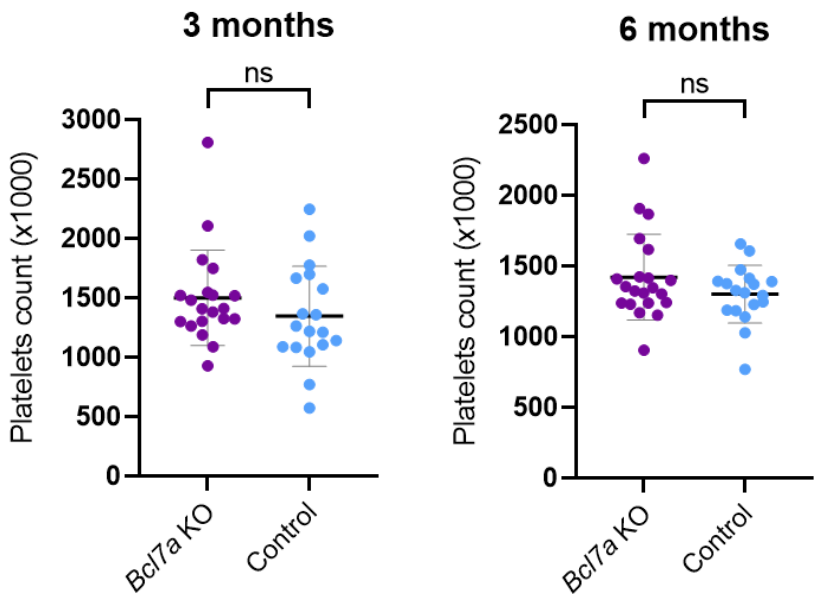

Figure 39. Platelets count per 1 µL 3 and 6 months after tamoxifen injection. No significant (ns) differences were found between the control and *Bcl7a* KO mice groups ($p > 0.05$, unpaired T-test, N = 38 at 3 months, N = 39 at 6 months).

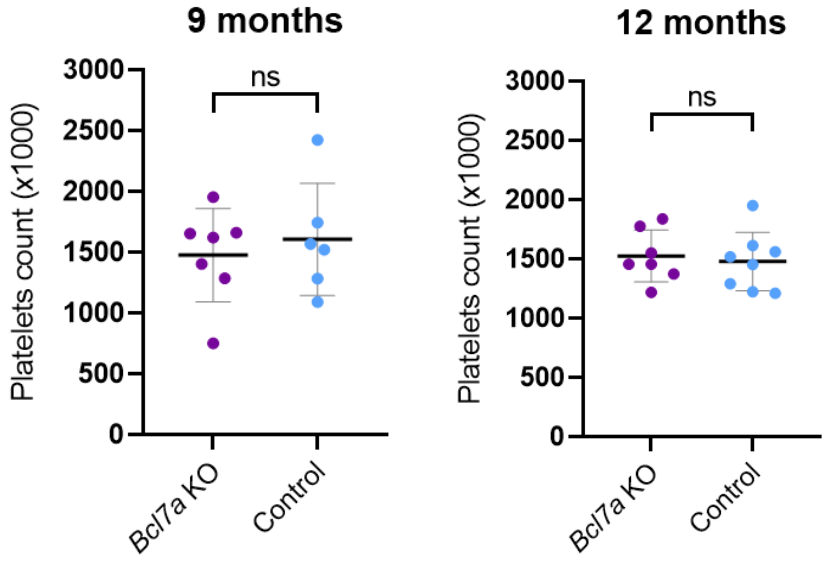

Figure 40. Platelets count per 1 µL 9 and 12 months after tamoxifen injection. No significant (ns) differences were found between the control and *Bcl7a* KO mice groups ($p > 0.05$, unpaired T-test, N = 13 at 9 months, N = 15 at 12 months).

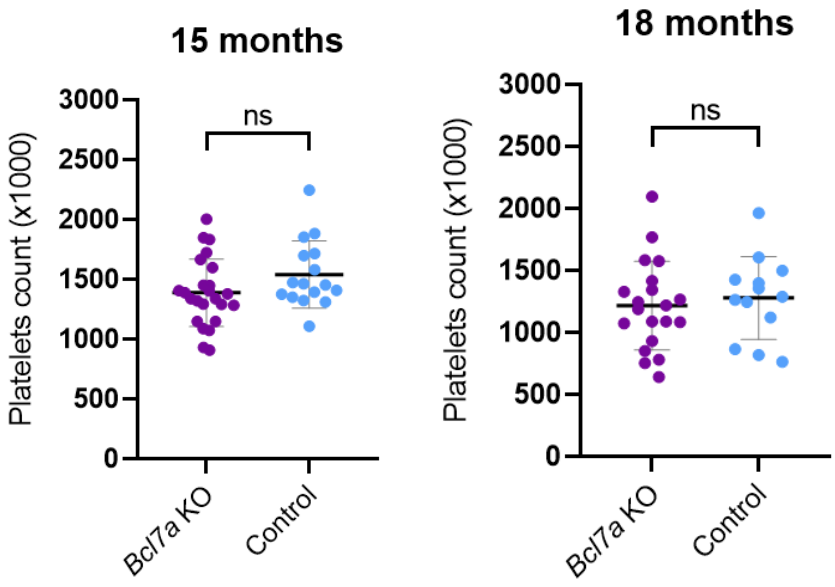

Figure 41. Platelets count per 1 µL 15 and 18 months after tamoxifen injection. No significant (ns) differences were found between the control and *Bcl7a* KO mice groups ($p > 0.05$, unpaired T-test, N = 40 at 15 months, N = 33 at 18 months).

Overall, there were no significant differences between the *Bcl7a* KO and control mice groups between the 3 months and 18 months time points when assessing the WBC counts per microliter, the WBC / RBC proportion and the platelets counts per microliter.

4.3 Discussion

As mentioned above, we developed an inducible *Bcl7a* KO mouse model because in the C57BL/6 strain, a previous study showed that *Bcl7a* inactivation during the embryonic development lead to pre-weaning lethality. The authors of this

study generated the *Bcl7a* KO mouse model through a gene targeting method that incorporated LoxP sites flanking exon 2 of the *Bcl7a* gene ("floxed" *Bcl7a*) and applying the Cre-LoxP recombination system, deleting the mentioned exon and therefore avoiding the synthesis of any transcript that can produce a functional Bcl7a protein in the mouse whole body (Wischhof et al., 2017).

Therefore, when inducing *Bcl7a* ablation (tamoxifen mediated) in our inducible *Bcl7a* KO mice, once they were already weaned and close to entering into adulthood (around 2 months after birth), all of them were able to survive as much as the control mice. Nevertheless, all of the results presented above suggested that the deletion of *Bcl7a* in our mice study cohort did not yield any clear phenotype related to hematologic disorders that we could detect in mice peripheral blood in this mouse background (or strain: C57BL/6).

Since the SWI/SNF subunits are highly conserved among eukaryotic organisms (Hernández-García et al., 2022), and mouse Bcl7a and the human BCL7A protein sequences are very similar (see Supplementary Figure 17) we were expecting that the inactivation of mouse *Blc7a* may have promoted any hematological disorder related to the lymphoid lineage, because human *BCL7A* has been seen clearly related to B-cell and T-cell derived lymphomas (Baliñas-Gavira et al., 2020; Carbone et al., 2008; Litvinov et al., 2013; Ramos-Medina et al., 2013; Van Doorn et al., 2005). More specifically, the results from previous projects

developed in our laboratory suggested that *BCL7A* inactivation might be very related to B-cell lymphomas, more specifically, to the DLBCL progression, in *in vitro* and *in vivo* when performing experiments using human DLBCL cell models (Baliñas-Gavira et al., 2020; Carlos Baliñas-Gavira, 2020).

On the other hand, another study harbored within a doctoral thesis project carried out in Dr. Riccardo Dalla-Favera research group (Columbia University, NY, U.S.) used a different mouse strain (129Sv/Ev) and even a different *Bcl7a* inactivation molecular mechanism. Technically speaking, it means that it is a different *in vivo* model that yields a *Bcl7a* KO mouse model (named *Bcl7a*$^{-/-}$ by the authors). These mice were born at the expected mendelian rate and showed normal development (Gao, 2007) instead of dying at early ages, as it was seen in the C57BL/6 background *Bcl7a* KO mouse model (Wischhof et al., 2017).

The different phenotypes shown by the two mouse strains mentioned above might be due to the several generations of inbreeding that have led to significant variations among the different mouse strains used in *in vivo* research approaches. In fact, the diversity in strains implies that each one may respond differently to an introduced mutation, which may subsequently interact uniquely with the mouse's surroundings (Doetschman, 2009).

In the research project developed at Columbia University mentioned above, they as well studied *Bcl7a* in the lymphoid

lineage. The *Bcl7a* deficient mouse model developed by these authors (*Bcl7a*$^{-/-}$), was generated to study *Bcl7a* in normal development and specifically in B-cells. However, these *Bcl7a*$^{-/-}$ mice exhibited typical development and functionality of lymphoid organs. This included regular formation of GCs and immune responses dependent on T-cells. Thus, the role of *Bcl7a* in the lymphoid lineage might be subtle, not readily detectable through standard tests, or substituted by an alternative pathway in *Bcl7a*$^{-/-}$ mice (Gao, 2007).

Getting back to our study, the UBC-Cre-ERT2-*Bcl7a*$^{fl/fl}$ mouse model without tamoxifen injection (without the *Bcl7a* induced deletion) could have been an appropriate model to use as a negative control since it is genetically identical to the study condition mouse model (*Bcl7a* KO). However, due to time constraints we used the *Bcl7a*$^{fl/fl}$ without Cre-ERT2 cassette as the negative control for our experiments, since it was expected to have the *Bcl7a* expression unaltered and it was generated simultaneously (and hence faster) by the same breeding, that produced both UBC-Cre-ERT2-*Bcl7a*$^{fl/fl}$ and *Bcl7a*$^{fl/fl}$ mouse models.

Besides, the research group that provided us with the *Bcl7a*$^{fl/fl}$ mouse model, after observing the pre-weaning lethality phenotype, they generated a mouse model where Cre recombinase expression was controlled by the neuronal-specific Synapsin promoter. This model was generated to try to prevent the pre-weaning lethality and hence to be able to have adult mice

to study the phenotype given when inactivating *Bcl7a* only in neurons. In fact, they observed that *Bcl7a* plays a role in Purkinje cell function and motor coordination (Wischhof et al., 2017).

Some other previous *in vivo* studies, in which the authors were assessing the predicted role of a gene using KO mouse models for that specific gene, the results found did not confirm those predicted activities, which is a similar outcome to ours, that may be related to the huge multiparametric complexity inherent to the research involving mouse models. For instance, the G-Patch Domain Containing 2 (*Gpatch2*) KO mouse model showed that *Gpatch2* ablation is not critical for the control of Tumor Necrosis Factor (*Tnf*) expression, when this gene was predicted to act as a putative *Tnf* expression repressor by a CRISPR screen using a *Tnf* reporter system (Dalseno et al., 2023). Also, the DnaJ Heat Shock Protein Family (Hsp40) Member B4 (*Hlj1*) was found to be expressed in platelets and megakaryocytes, but the *Hlj1* KO mouse model, which had *Hlj1* inactivated did not show any role as a regulator of blood coagulation under physiological conditions (Hsu et al., 2022).

Based on the information we have from the literature and our own results, we suggest that in this *in vivo* context (C57BL/6 mouse strain harboring the UBC-Cre-ERT2-*Bcl7a*$^{fl/fl}$ genetic characteristics detailed in methods section 2.22), when *Bcl7a* function is ablated, it might be replaced by some other metabolic pathway avoiding any hematologic disorder development.

Since no clear phenotypic changes in our *Bcl7a* KO mice were observed, the future perspectives in our research group regarding this *in vivo* project comprise the combination of this mouse model with other models which present a specific oncogenic stimulation of the hematologic lineage. Then, this approach may "enhance" the putative phenotypic alterations (and make them detectable) when inactivating *Bcl7a*, hence allowing us to understand in which pathways *Bcl7a* may be involved in. In fact, since *Bcl7a* is expected to play a tumor suppressor role, it may be subjected to the two-hit hypothesis (Knudson, 1971). Therefore, an additional genetic alteration might be necessary to generate a pathological mouse phenotype, not produced when only *Bcl7a* was inactivated.

These additional mouse models to combine with our inducible Bcl7a KO are VavP-*Bcl2*, which undergoes an onset of follicular lymphoma after presenting GC hyperplasia (Egle et al., 2004); Eμ-*myc*, that carries the *myc* oncogene linked to the immunoglobulin heavy-chain enhancer (Eμ) and displays aberrant B-lymphocyte development and eventually develop B lymphoid tumors (Alexander et al., 1987); and the conditional *Ezh2*^{Y641N} knockin. In this last one, when the mutant *Ezh2*^{Y641N} variant is expressed, it triggers GC hyperplasia and enhances the development of lymphoma in collaboration with *Bcl2* (Béguelin et al., 2013). Moreover, with these combined models and with the uncombined UBC-Cre-ERT2-*Bcl7a*$^{fl/fl}$, further experiments are planned to evaluate the putative effects of *Bcl7a* ablation from additional perspectives. For instance, sheep red blood cells

(SRBC) mice immunizations will be performed with all of the mentioned above mouse models to evaluate whether or not the GC formed in the spleen and lymph nodes are developed normally.

Chapter 5.

BCL7A targeted demethylation *in vitro* in an AML cell model

Chapter 5. *BCL7A* targeted demethylation *in vitro* in an AML cell model

5.1 Background

In this chapter it is described the project carried out during my internship at Dr. Annalisa Di Rusio's laboratory, located at Beth Israel Deaconess Medical Center / Harvard Medical School (Boston, MA, U.S.).

The Clustered regularly interspaced short palindromic repeats (CRISPR)/CRISPR-associated (Cas) systems provide bacteria and archaea with adaptive immunity against viruses and plasmids since it specifically silences the invading nucleic acids. After this discovery, researchers developed a molecular tool based on CRISPR-Cas which includes its corresponding single guide RNA (sgRNA) whose sequence allow the targeted genome editing. So far, this technology is considered among the most relevant tools for genome editing and engineering, with such a huge impact on basic biomedical research that it has been applied in several clinical trials (Jinek et al., 2012; T. Li et al., 2023; Mojica et al., 2005). In fact, the Nobel Prize in Chemistry 2020 was awarded to the developers of this genome editing molecular tool based on CRISPR-Cas.

At Di Ruscio's laboratory we worked with a CRISPR-dead Cas9 (dCas9) based platform called CRISPR-DiR (DNMT1-interacting RNA) (Di Ruscio et al., 2013), whose specially edited sgRNAs (sgDiRs) inhibit the DNA methyltransferase 1 (DNMT1) activity in a locus-specific manner, therefore promoting a targeted genomic locus demethylation (Y. V Liu et al., 2020). The CRISPR-DiR platform methods belong to the authors and Harvard University's intellectual property, hence we are not allowed to disclose the detailed methods here. Despite this, the methods can be extrapolated from (Y. V Liu et al., 2020).

Since the *BCL7A* locus in the NB4 cell line is methylated yielding its gene expression silencing, here we designed sgDiRs targeting 3 regions (3 sgDiRs per region) around *BCL7A*'s TSS to apply the CRISPR-DiR platform to study the phenotype given upon the expected BCL7A protein expression restoration in NB4 cells. Also, we designed an additional a scrambled sgDiR (without any specific targeting) to include a negative control in our experiments.

5.2 Results

Due to a time limitation, the experiments carried out during this internship provided us with a screening of the CRISPR-DiR activity over *BCL7A* expression restoration in NB4 cells at different time points. Thus, we were able to perform only one biological

replicate of each experiment, preventing us to make any statistical analyses here.

The qRTPCR, WB and cell competitive assays were performed following protocols much alike those described in the methods section of this PhD dissertation.

5.2.1 NB4 CRISPR-DiR models

We generated 5 different cell models from the NB4 cell line:

- NB4 scrambled: NB4 with the scrambled sdDiR (negative control).
- NB4 PreTSS: NB4 with three sgDiRs targeting the region close upstream *BCL7A* TSS.
- NB4 5'UTR-Exon 1: NB4 with three sgDiRs targeting a region that encompasses the 5' Untranslated Region (5'UTR) and the Exon 1 of *BCL7A*.
- NB4 Intron 1: with three sgDiRs targeting the beginning of *BCL7A*'s Intron 1.
- NB4 ALL: NB4 with the combination of the 9 sgDiRs of the previous three models (NB4 PreTSS, NB4 5'UTR-Exon1 and NB4 Intron1).

5.2.2 *BCL7A* expression level evaluation upon application of CRISPR-DiR

To determine when the CRISPR-DiR showed the highest activity in NB4 cells (the highest *BCL7A* expression restoration), we assessed the *BCL7A* expression level at mRNA and protein levels through qRTPCR and WB respectively in the five NB4 cell models described above at different time points (Figures 42-48).

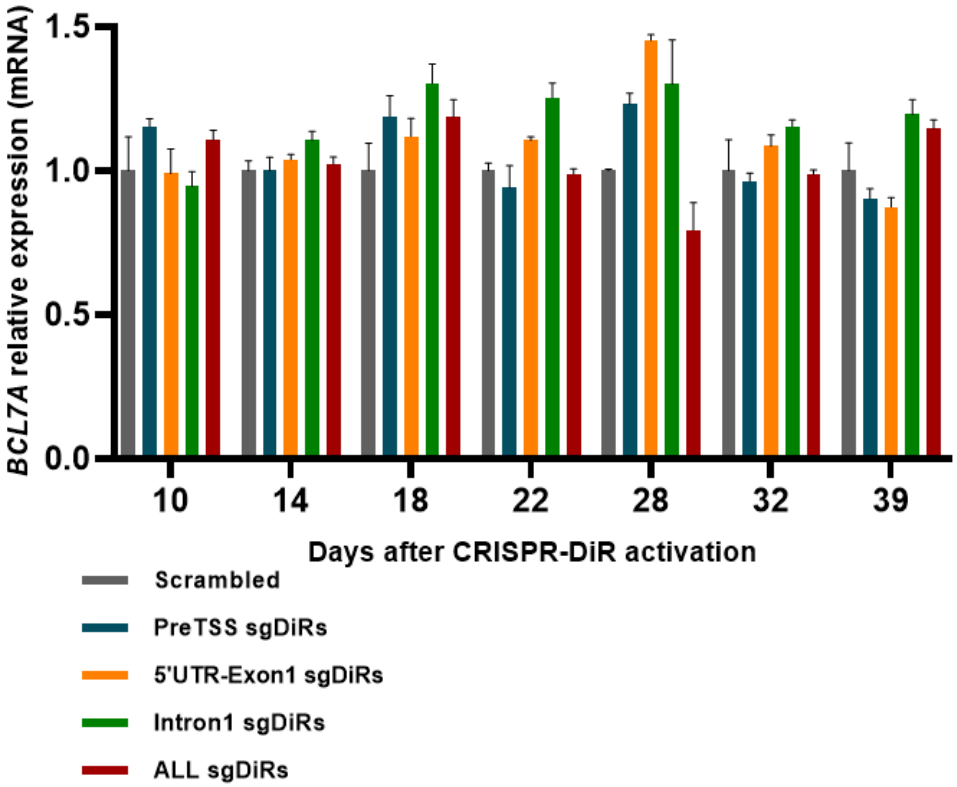

Figure 42. *BCL7A* relative expression at mRNA level normalized versus the Scrambled condition assessed via qRTPCR. *GAPDH* was used as endogenous reference for data normalization of each sample. Samples from the same time point were normalized versus the scrambled condition. CRISPR-DiR seems to promote the highest *BCL7A* mRNA expression restoration at 18 and 28 days after its activation compared to the scrambled condition. We had only one biological replicate, so no statistics were performed. The standard deviation among each two technical replicates are shown by the thin grey error bars.

In the following WB results (Figures 43-48), the different samples are named by their abbreviated name: SCR (NB4 scrambled), PT (NB4 PreTSS), EX (NB4 5'UTR-Exon1), INT (NB4 Intron 1) and ALL (NB4 ALL).

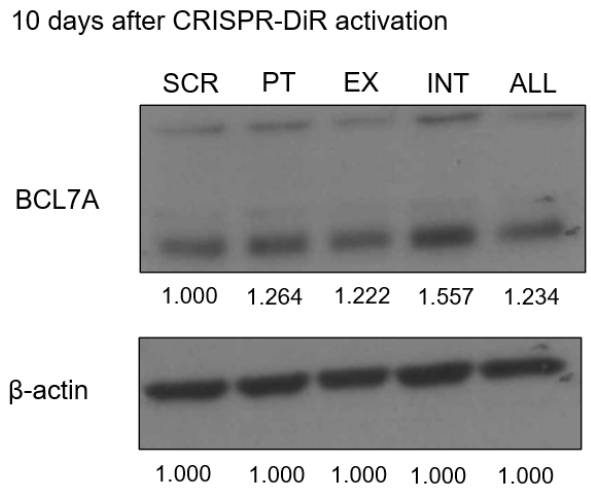

Figure 43. WB results showing *BCL7A* expression in NB4 cells at protein level 10 days after CRISPR-DiR activation.

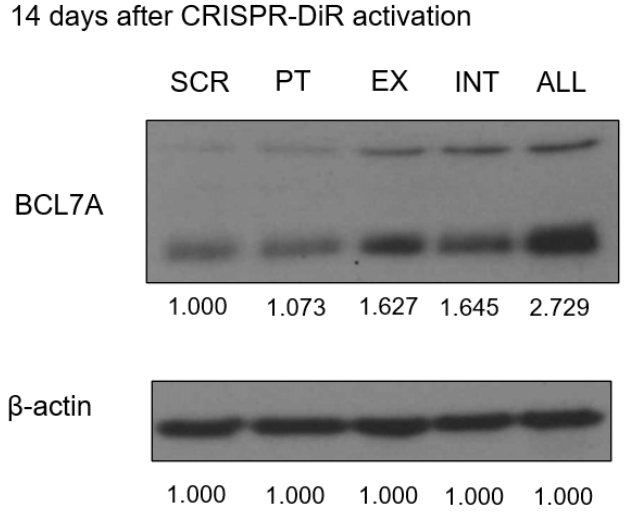

Figure 44. WB results showing *BCL7A* expression in NB4 cells at protein level 14 days after CRISPR-DiR activation.

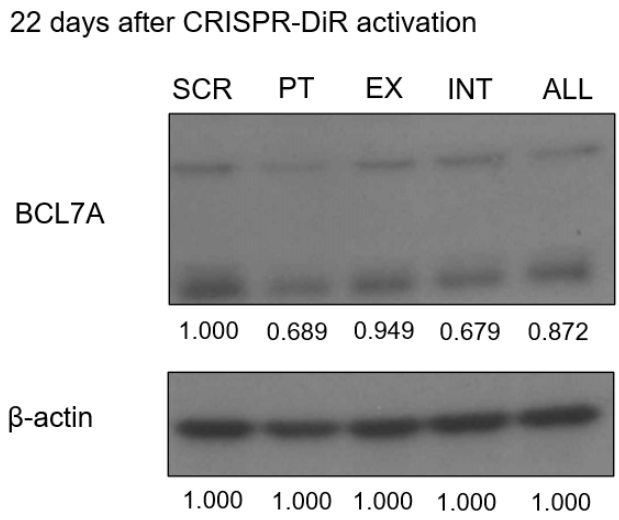

Figure 45. WB results showing *BCL7A* expression in NB4 cells at protein level 22 days after CRISPR-DiR activation.

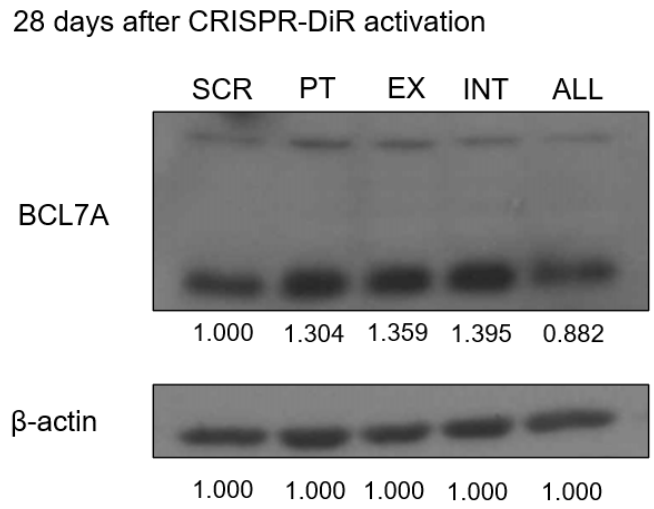

Figure 46. WB results showing *BCL7A* expression in NB4 cells at protein level 28 days after CRISPR-DiR activation.

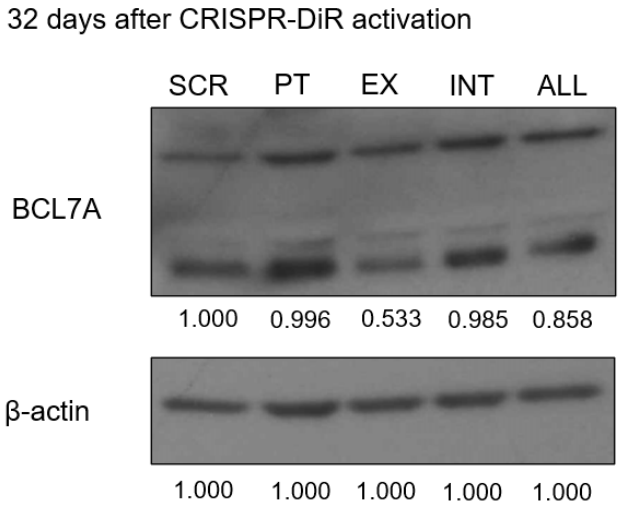

Figure 47. WB results showing *BCL7A* expression in NB4 cells at protein level 32 days after CRISPR-DiR activation.

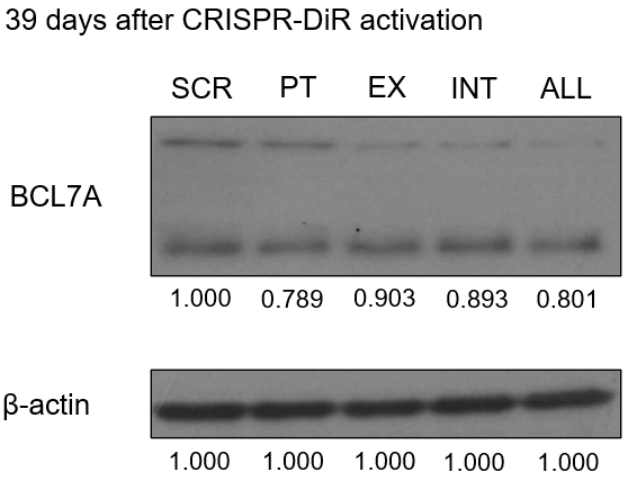

Figure 48. WB results showing *BCL7A* expression in NB4 cells at protein level 39 days after CRISPR-DiR activation.

At protein level, *BCL7A* showed the highest expression levels (compared to the scrambled condition) at days 10, 14 and 28 after CRISPR-DiR activation.

In general, we observed a light restoration of *BCL7A* expression both at mRNA and protein levels after CRISPR-DiR activation at several time points. However, at day 28 we found the common highest expression level of the mRNA and protein levels.

5.2.3 Cell competition assay of NB4 CRISPR-DiR models

Ten days after CRISPR-DiR activation we set a cell growth competition assay including the 5 NB4 models described above (Figure 49).

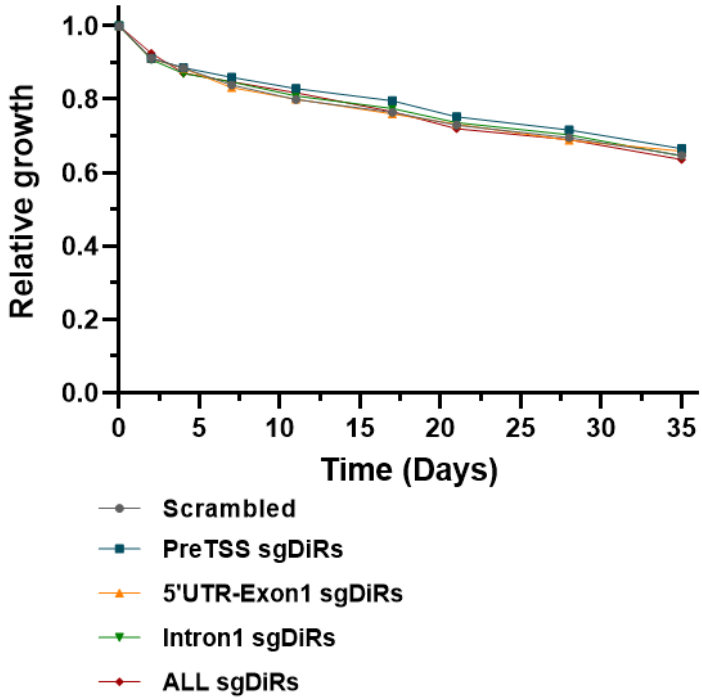

Figure 49. Competition cell growth assay of the 4 different CRISPR-DiR NB4 cell models including the scrambled NB4 model as negative control. This competitive assay was performed following the protocol described in the methods section. We performed only one biological replicate due to time constraints, so no statistics were performed.

Here, all of the different cell models (including the negative control, the scrambled condition) showed very similar competitive growth capabilities. Therefore, it seems that the expected CRISPR-DiR activity over the *BCL7A* genomic locus in NB4 was not able to yield any differences in cell competitive growth.

5.3 Discussion

The approach described in this section aimed to replicate better the "natural" *BCL7A* expression level after its expected locus demethylation by CRISPR-DiR, compared to the overexpression models that are usually used in basic biomedical research, like those that were mainly used for the development of the main research article related to this PhD dissertation (Patiño-Mercau et al., 2023); which usually yield a larger expression level compared to the physiological levels (Prelich, 2012).

However, we observed little fluctuations of the *BCL7A* mRNA and protein expression levels yielded by CRISPR-DiR in NB4. The highest expression levels of *BCL7A* mRNA were detected at days 18 and 28 after CRISPR-DiR activation. Regarding the BCL7A protein, the top levels were found at 10, 14 and 28 days after the platform activation. Therefore, the time point of the common highest expression level of both mRNA and protein was 28 days.

Also, we did not observe any phenotypic changes among experimental conditions (including CRISPR-DiR) and controls in the cell growth competition assay (see Figure 49). This might be due to the little fluctuations over time of the *BCL7A* mRNA and protein expression levels (shown in section 5.2.2) after using CRISPR-DiR over the *BCL7A* locus of NB4 cells.

There are several DNA HMAs, such as decitabine or Azacitidine, that are now standard clinical use for AML and MDS patients. However, their exact mode of action, off-targets due to the genome-wide demethylation such as oncogene upregulation (Grimm & Binder, 2022; Y.-C. Liu et al., 2022), and the knowledge about the mechanisms of resistance to them are not fully described. In fact, a current research line is aiming to find treatment combinations (including HMAs) to overcome the disadvantages mentioned above when applying HMAs alone (Stomper et al., 2021). Thus, CRISPR-DiR may overcome the off-targets effects disadvantage mostly, since it is an artificial targeted demethylating molecular platform.

In addition, several other experimental tools for targeted DNA demethylation based on CRISPR-Cas have been developed to date. They differ in their design and thus in their mode of action to achieve targeted DNA locus demethylation (Choudhury et al., 2016; Hanzawa et al., 2020; Tejedor et al., 2023; Xu et al., 2016).

Nevertheless, despite the fact that there is an increasing number of studies trying to develop targeted therapies for cancer

based on CRISPR-Cas, this technology still presents much trouble to use in patients. One of the most relevant inconveniences is the high immunogenicity caused by the foreign materials needed for this system activity. This is a critical difficulty that needs to be overcome to be able to apply this system in patients' treatment in a safe manner (W. Liu et al., 2021).

On the other hand, due to time constraints, we were not able to perform any approach, like bisulfite sequencing or combined bisulfite restriction analysis: COBRA (Xiong & Laird, 1997); to directly reveal the methylation status of the CpG sites surrounding the sgDiRs binding regions within the *BCL7A* genomic locus in the different NB4 CRISPR-DiR cell models. Indeed, this is one of the main points to carry on with this project in the future, together with additional biological replicates of the experiments depicted in the previous sections 5.2.2 and 5.2.3. The results provided by these approaches might allow us to find compelling conclusions regarding the use of CRISPR-DiR over the *BCL7A* locus of NB4 cells.

Conclusions / Conclusiones

Conclusions

1. In three independent AML cohorts, *BCL7A* showed a significant inverse correlation between its locus methylation degree and its expression at the mRNA level.

2. Based on the information obtained from external datasets (DepMap Portal) and also from our own models, the AML cell models showed a lower *BCL7A* expression at mRNA level compared to the DLBCL cell models.

3. *BCL7A* mRNA expression in NB4, and BCL7A protein expression in NB4 and M07e, can be restored *in vitro* by decitabine treatment, as *BCL7A* expression is expected to be downregulated in both models due to DNA methylation at the *BCL7A* genomic locus.

4. Restoration of WT BCL7A protein expression resulted in a competitive growth defect in both NB4 and M07e *in vitro* when compared to the mutant variant Δ27-BCL7A and to the empty vector control conditions. This result demonstrated the tumor suppressor role played by BCL7A *in vitro*.

5. The binding of the BCL7A subunit to the mSWI/SNF complex occurs through its N-terminal domain in NB4 cells. Together with previous results, this suggests that this fact is not cell lineage or tissue dependent.

6. Restoration of WT BCL7A protein expression in NB4 cells yielded a reduced growth in an *in vivo* mouse xenograft model compared to the empty vector control condition, suggesting a tumor suppressor role for WT BCL7A in this *in vivo* model.

7. Our *Bcl7a* conditional knock-out mouse model showed no clear phenotypic alteration upon *Bcl7a* ubiquitous deletion when assessing mouse hematologic parameter from mouse peripheral blood.

8. Targeted demethylation by CRISPR-DiR within the genomic locus of *BCL7A* in the NB4 cell line resulted in a slight upregulation of both *BCL7A* mRNA and protein at some time points. This small increase in expression with fluctuations over time was not sufficient to reduce the competitive cell growth compared to the control condition.

Conclusiones

1. En tres cohortes independientes de AML, *BCL7A* presentó una correlación inversa significativa entre el grado de metilación de su locus y su expresión a nivel de ARNm.

2. Basándonos en la información obtenida de conjuntos de datos externos (DepMap Portal) y también de nuestros propios modelos, los modelos de células de AML mostraron una menor expresión de *BCL7A* a nivel de ARNm en comparación con los modelos de células de DLBCL.

3. La expresión del ARNm de *BCL7A* en NB4, y la expresión de la proteína BCL7A en NB4 y M07e, pueden restaurarse *in vitro* mediante el tratamiento con decitabine, ya que la expresión de *BCL7A* parece estar regulada a la baja en ambos modelos debido a la metilación del ADN en el locus genómico de *BCL7A*.

4. La restauración de la expresión de proteína BCL7A WT resultó en un defecto competitivo de crecimiento tanto en NB4 como en M07e *in vitro* en comparación con la variante mutante Δ27-BCL7A y con la condición control de vector vacío. Este resultado manifestó el papel de supresor tumoral desempeñado por BCL7A *in vitro*.

5. La unión de la subunidad BCL7A al complejo mSWI/SNF ocurre a través de su dominio N-terminal en las células NB4. Junto con resultados previos, esto sugiere que este hecho no depende del linaje celular o del tejido.

6. La restauración de la expresión de proteína BCL7A WT en células NB4 produjo un crecimiento reducido en un modelo de xenotrasplante en ratones *in vivo* en comparación con la condición control de vector vacío, lo que sugiere un papel de supresor tumoral para BCL7A WT en este modelo *in vivo*.

7. Nuestro modelo de ratón *Bcl7a* knock-out condicional no mostró ninguna alteración fenotípica clara tras la supresión en todo el organismo de *Bcl7a* al evaluar parámetros hematológicos en la sangre periférica de ratón.

8. La desmetilación dirigida por CRISPR-DiR dentro del locus genómico de *BCL7A* en la línea celular NB4 produjo un ligero aumento tanto del ARNm como de la proteína BCL7A en algunos puntos temporales. Este pequeño aumento de la expresión con fluctuaciones en el tiempo no fue suficiente para reducir el crecimiento celular competitivo en comparación con la condición control.

Supplementary material

Supplementary material

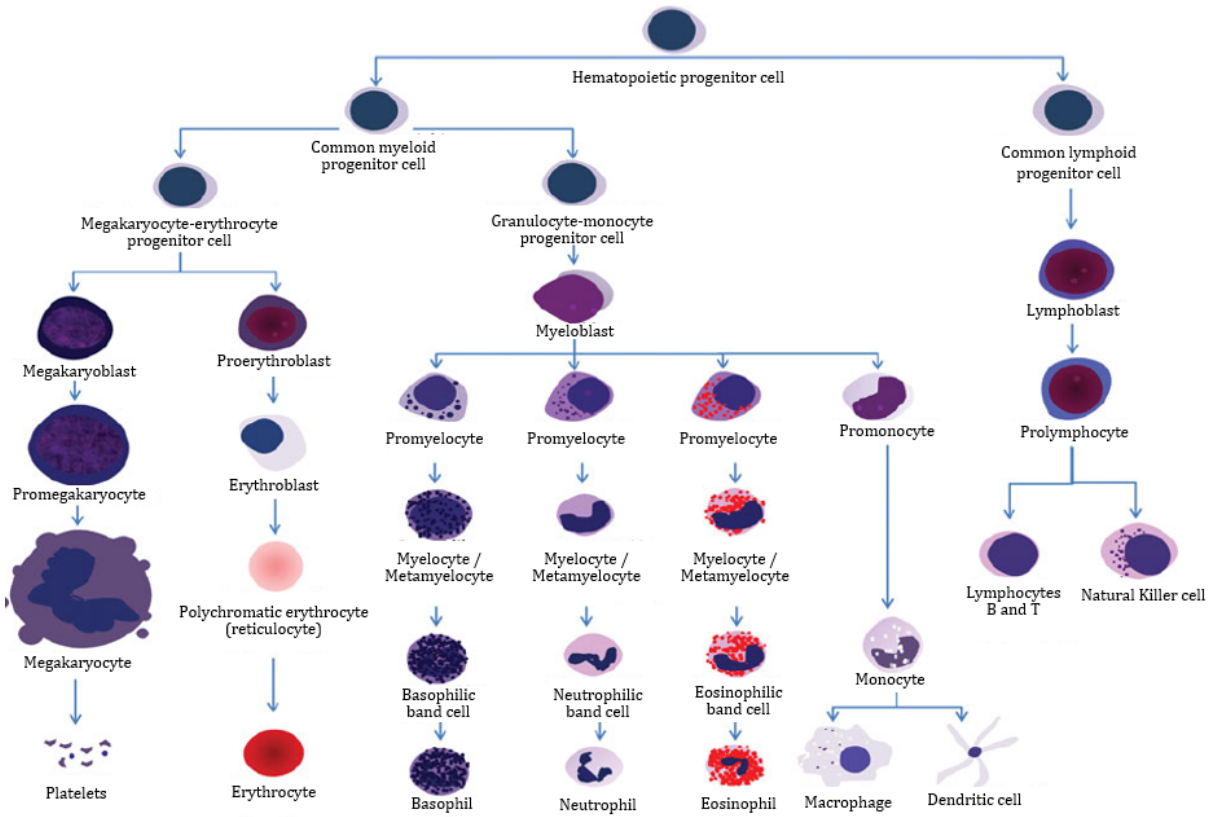

Supplementary Figure 1. Simplified schematic representation of the hematological cells differentiation. Adapted from (Mahalingaiah et al., 2018).

Shared subunits
SMARCC1 (BAF155)
SMARCC2 (BAF170)
SMARCA4 (BRG1 or BAF190A)
SMARCA2 (BRM, BAF190B or SNF2L2)
SMARCB1 (BAF47, INI1 or SNF5)
SMARCE1 (BAF57)
SMARCD1, SMARCD2 and SMARCD3 (BAF60A, BAF60B and BAF60C, respectively)
ACTB
ACTL6A and ACTL6B (BAF53A and BAF53B, respectively)
BCL7A, BCL7B and BCL7C
SS18 (SYT or SSXT)
cBaF subunits
ARID1A (BAF250A or SMARCF1)
ARID1B (BAF250B)
DPF2 and DPF3 (BAF45D and BAF45C, respectively)
BCL11A and BCL11B
PBaF subunits
ARID2 (BAF200)
PBRM1 (BAF180)
BRD7
PHF10 (BAF45A)
ncBaF subunits
BRD9
BICRA and BICRAL (GLTSCR1 and GLTSCR1L)

Supplementary Table 1. SWI/SNF- related, matrix- associated, actin-dependent regulator of chromatin (SMARC) nomenclature by the Human Genome Organization (HUGO). Adapted from (Mittal & Roberts, 2020).

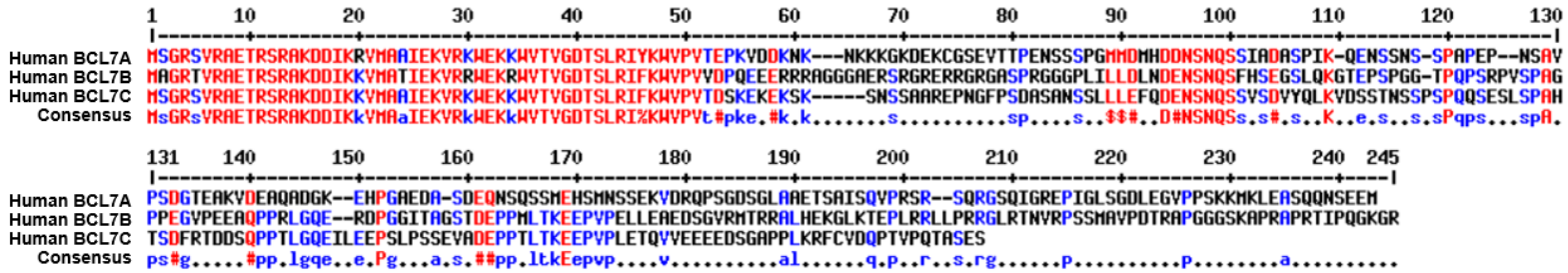

Supplementary Figure 2. Alignment of human BCL7A, BCL7B and BCL7C protein sequences, including only the longest isoform variant of each protein. Red and blue letters highlight sequences' identity. Alignment performed using the online software tool "MultAlin" (Corpet, 1988). Protein sequences obtained from the UniProt database (http://www.uniprot.org/) (Bateman et al., 2015).

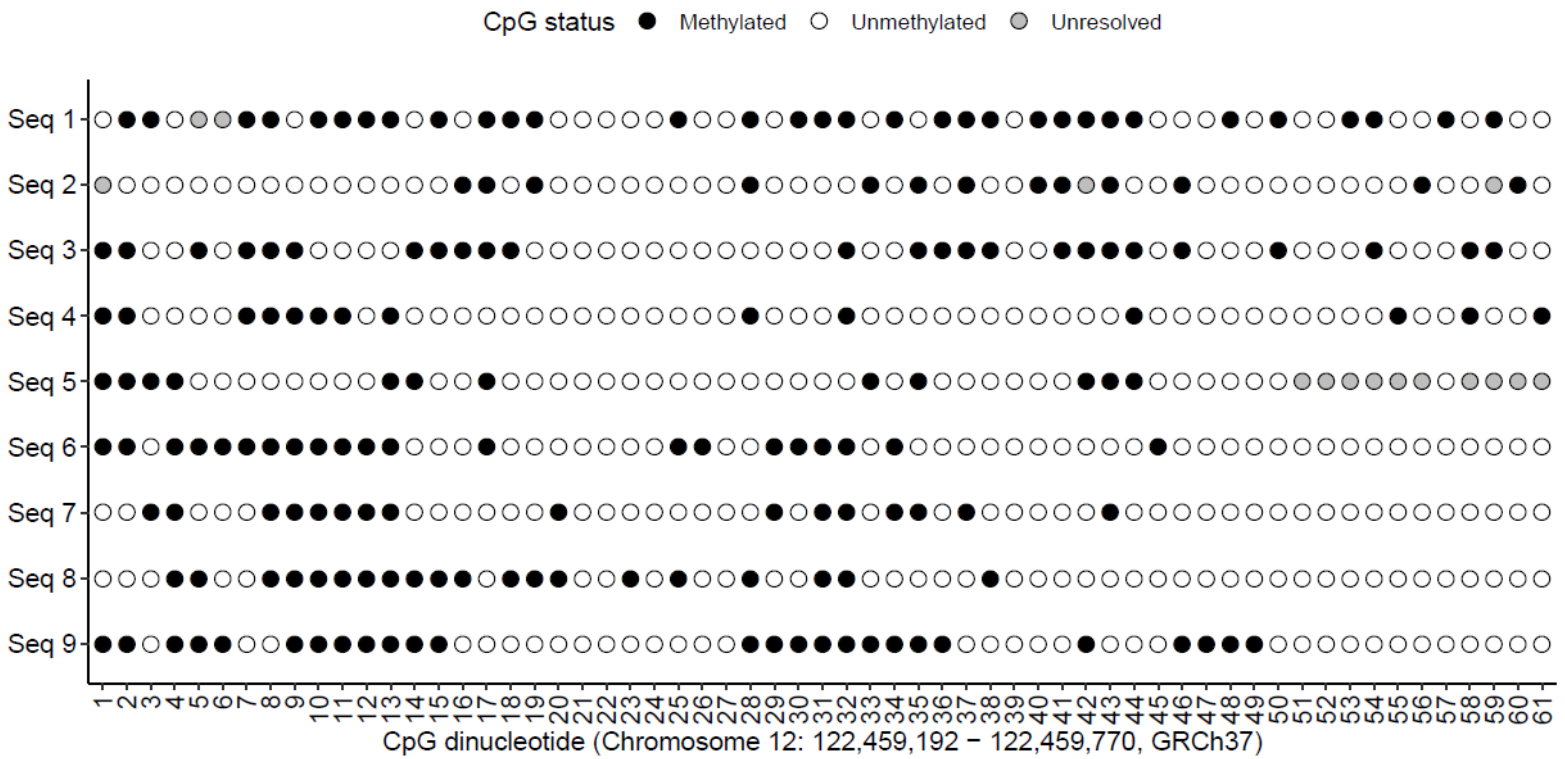

Supplementary Figure 3. Diagram displaying CpG-methylation status around the *BCL7A* transcription start site (TSS). Genomic DNA from the NB4 cell line was subjected to bisulfite conversion and used for subsequent TA-cloning. Then, nine independent amplicons were analyzed by Sanger sequencing. 61 CpG sites included in the 579 bp amplicon (chr12:122,459,192 - 122,459,770 GRCh37; hg19 genome assembly) were assessed. Figure made by courtesy of Maria S Benitez-Cantos.

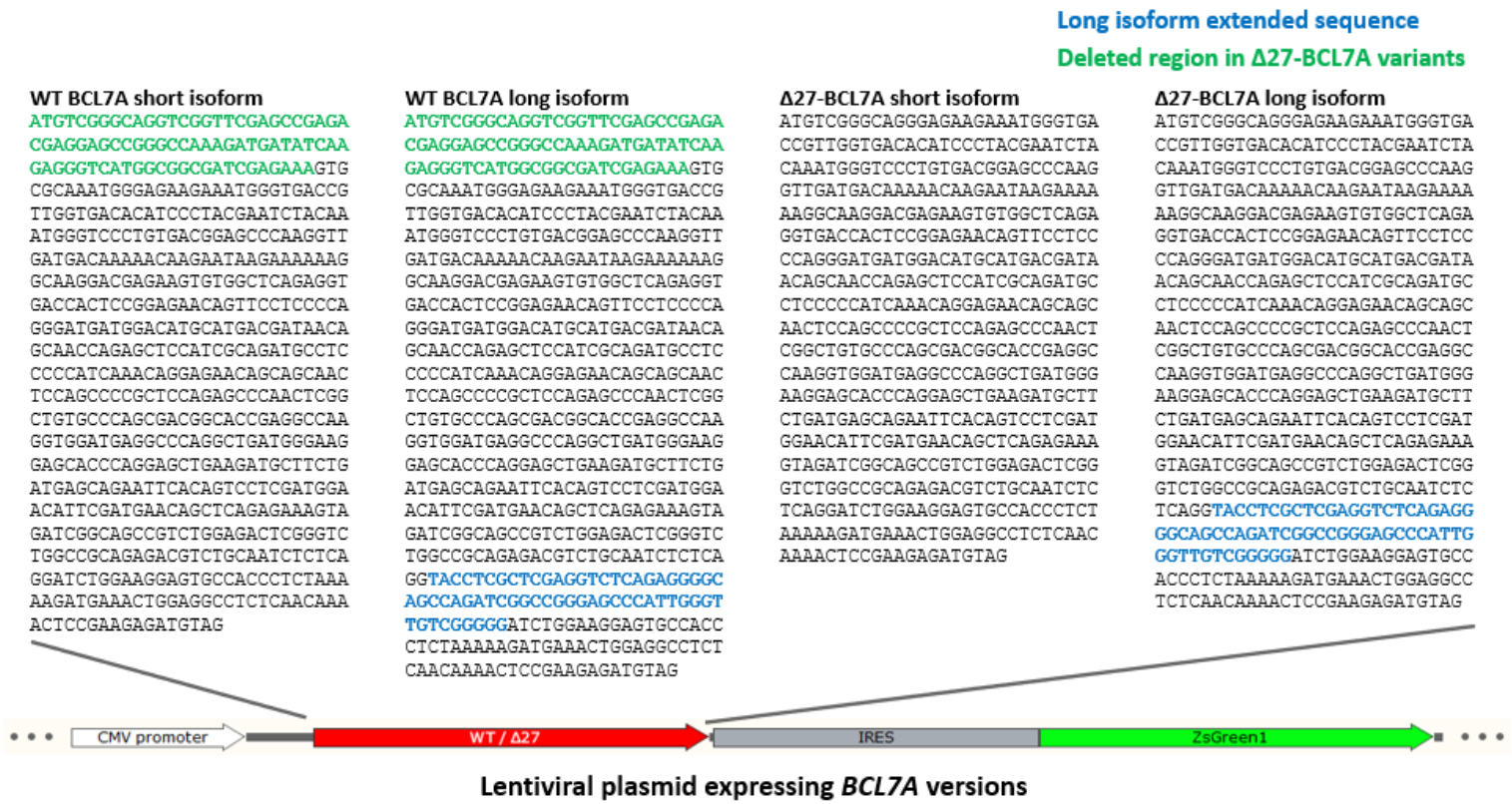

Supplementary Figure 4. Schematic representation of the different lentiviral plasmids used in the experimental procedures. The specific region of the long isoform of BCL7A is colored in blue. The specific region that is deleted in the BCL7A mutant (Δ27-BCL7A) is colored in green. The Empty Vector (EV) has the pLVX-IRES-ZsGreen1 structure without any insert.

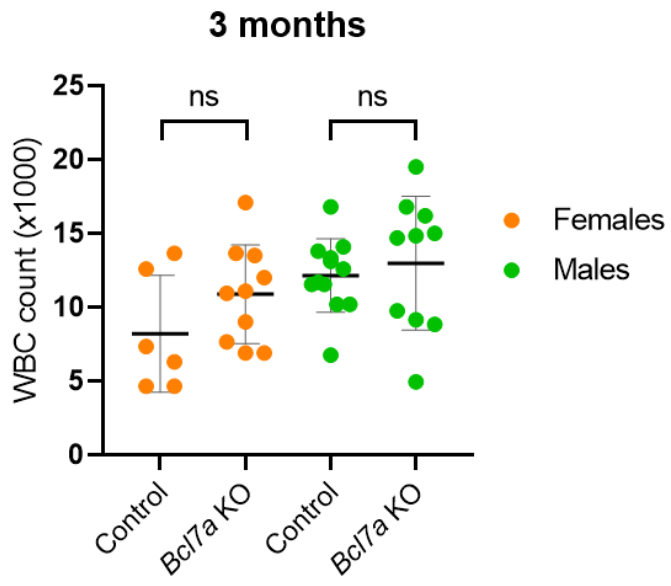

Supplementary Figure 5. White blood cells (WBC) count per 1 µL 3 months after tamoxifen injection. No significant (ns) differences were found between the control and *Bcl7a* KO mice groups within each gender ($p > 0.05$, unpaired T-test, N = 38).

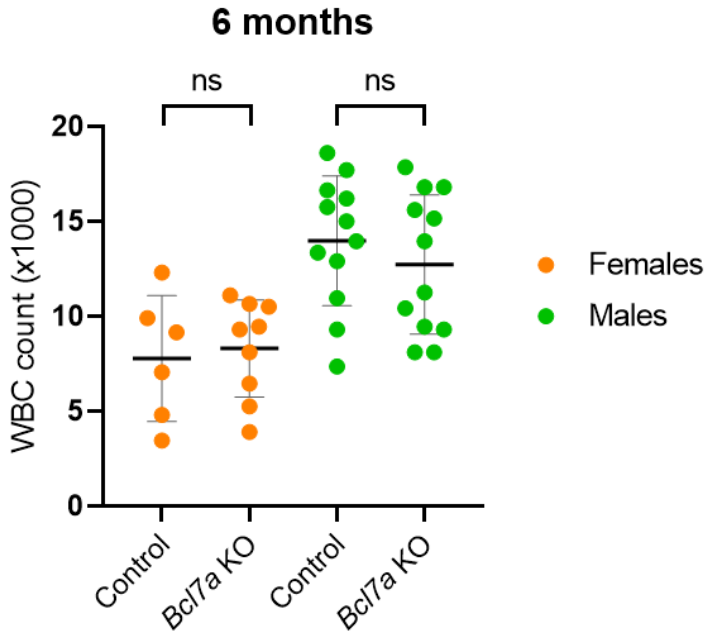

Supplementary Figure 6. White blood cells (WBC) count per 1 µL 6 months after tamoxifen injection. No significant (ns) differences were found between the control and *Bcl7a* KO mice groups within each gender ($p > 0.05$, unpaired T-test, N = 39).

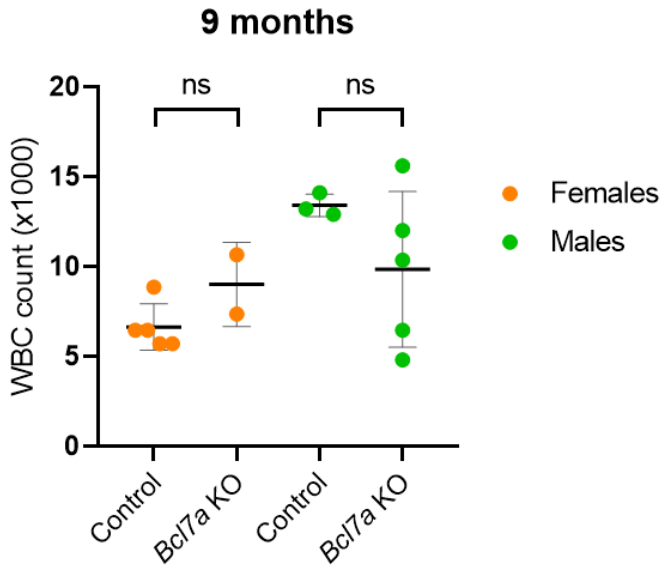

Supplementary Figure 7. White blood cells (WBC) count per 1 μL 9 months after tamoxifen injection. No significant (ns) differences were found between the control and *Bcl7a* KO mice groups within each gender ($p > 0.05$, unpaired T-test, N = 15).

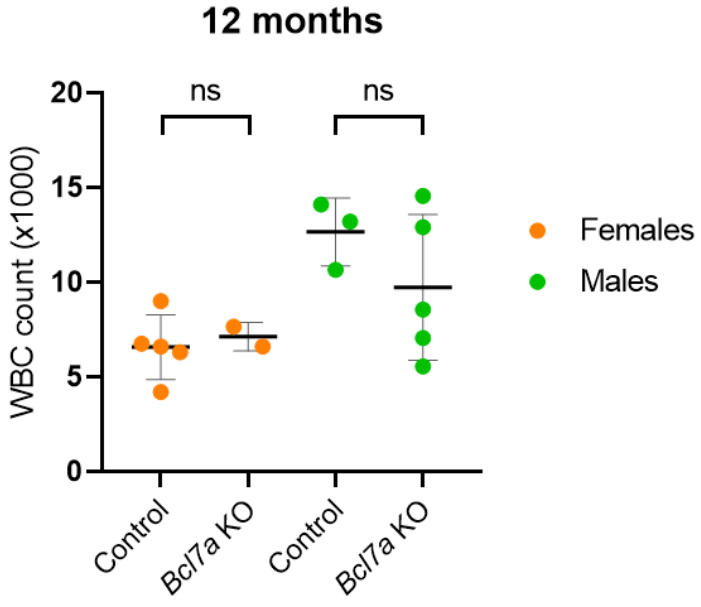

Supplementary Figure 8. White blood cells (WBC) count per 1 μL 12 months after tamoxifen injection. No significant (ns) differences were found between the control and *Bcl7a* KO mice groups within each gender ($p > 0.05$, unpaired T-test, N = 15).

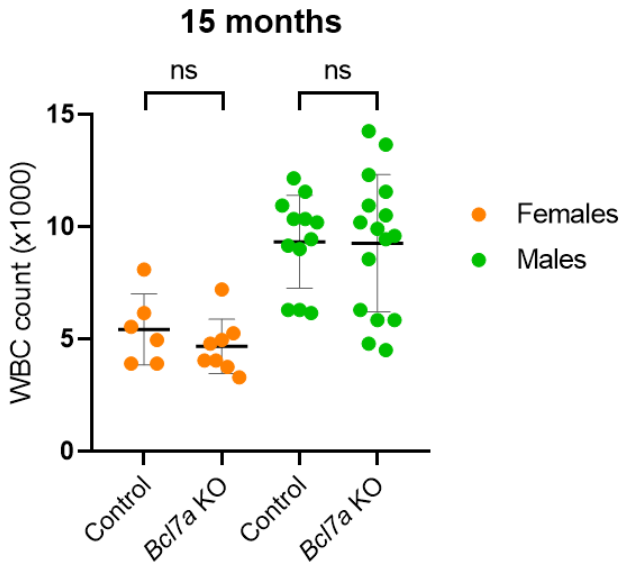

Supplementary Figure 9. White blood cells (WBC) count per 1 µL 15 months after tamoxifen injection. No significant (ns) differences were found between the control and *Bcl7a* KO mice groups within each gender ($p > 0.05$, unpaired T-test, N = 42).

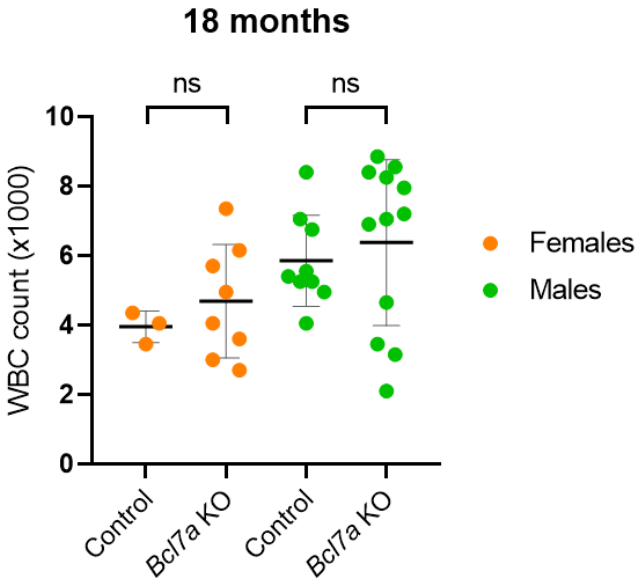

Supplementary Figure 10. White blood cells (WBC) count per 1 µL 18 months after tamoxifen injection. No significant (ns) differences were found between the control and *Bcl7a* KO mice groups within each gender ($p > 0.05$, unpaired T-test, N = 32).

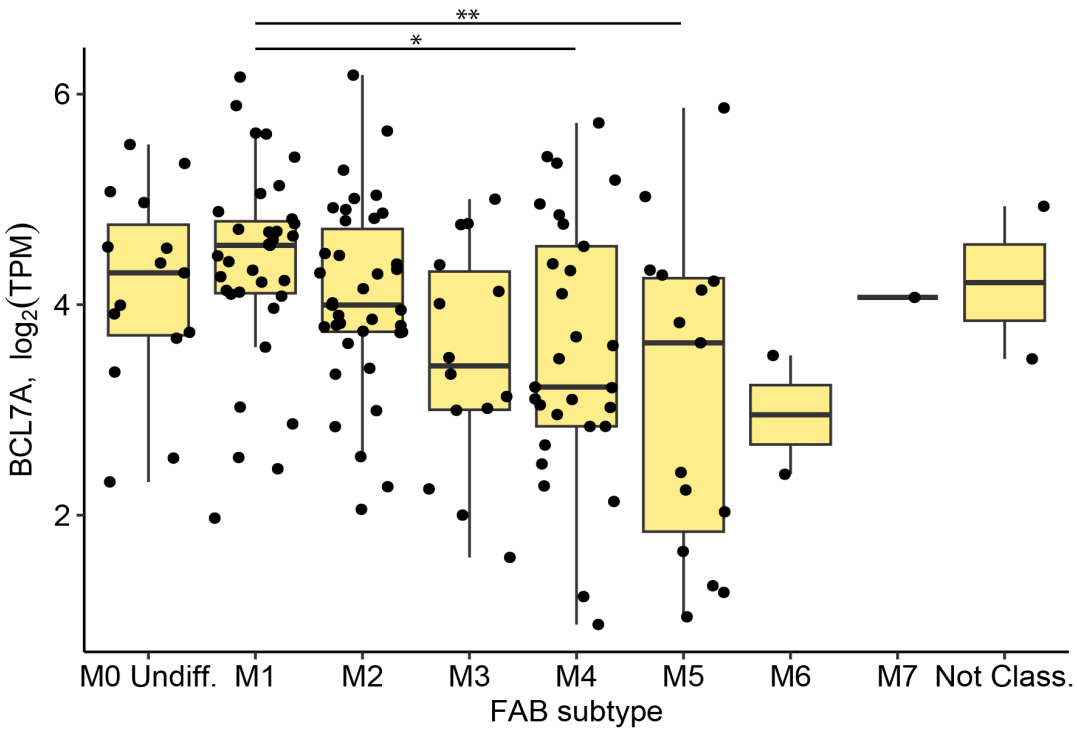

Supplementary Figure 11. Differential expression of *BCL7A* mRNA among AML subtypes in TCGA-LAML. Significant differences based on Student's t tests are marked with asterisks. **: FDR-adjusted $p < 0.01$; *: FDR-adjusted $p < 0.05$. Not Class: not classified. Figure made by courtesy of Alvaro Andrades.

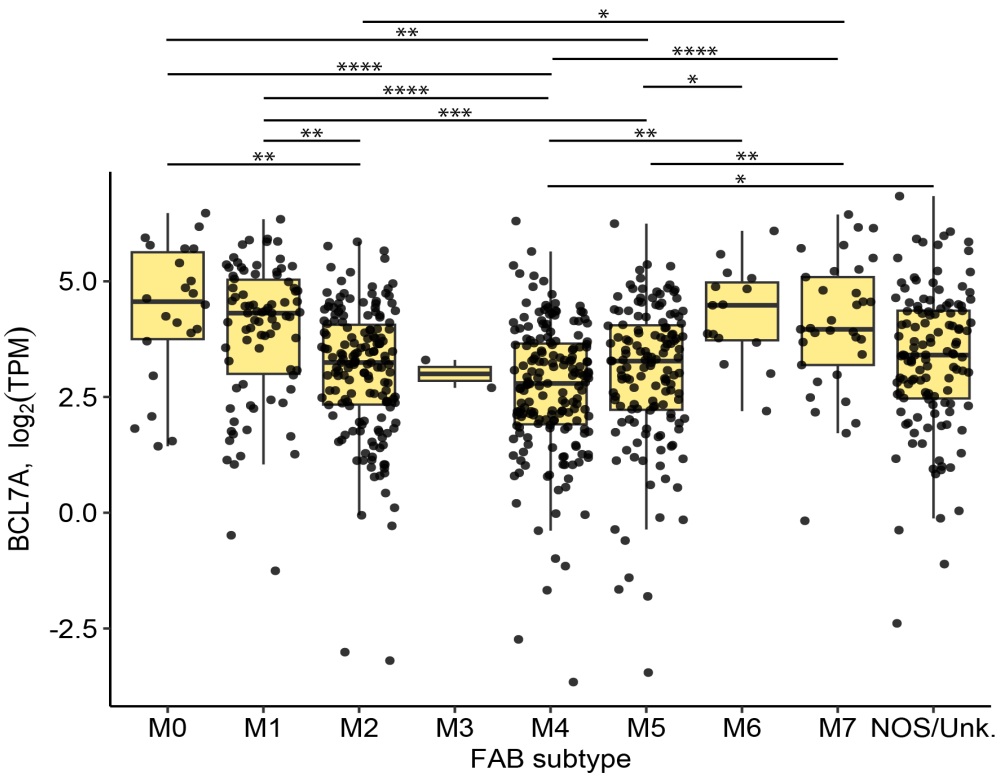

Supplementary Figure 12. Differential expression of *BCL7A* mRNA among AML subtypes in TARGET-AML. Significant differences based on Student's t tests are marked with asterisks. ****: FDR-adjusted p < 10-4; ***: FDR-adjusted p < 10-3; **: FDR-adjusted p < 0.01; *: FDR-adjusted p < 0.05. NOS/Unk: Not Otherwise Specified / unknown. Figure made by courtesy of Alvaro Andrades.

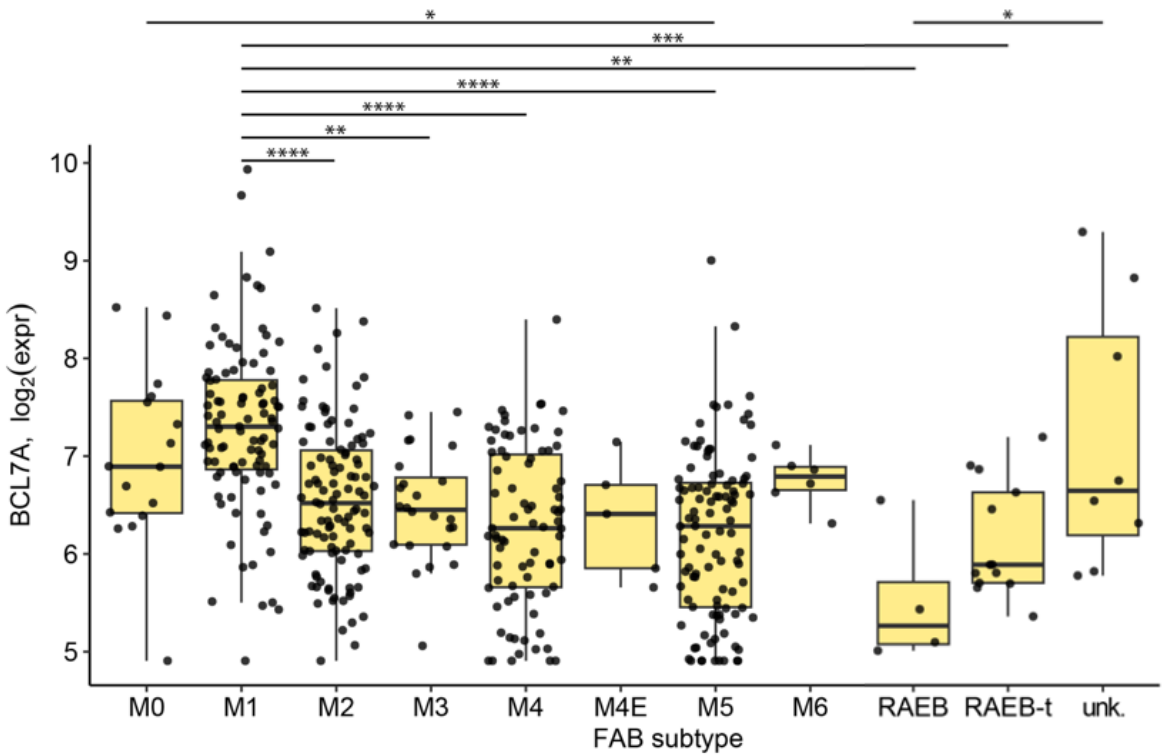

Supplementary Figure 13. Differential expression of *BCL7A* mRNA among AML subtypes in (Glass et al., 2017). Significant differences based on Student's t tests are marked with asterisks. ****: FDR-adjusted p < 10-4; ***: FDR-adjusted p < 10-3; **: FDR-adjusted p < 0.01; *: FDR-adjusted p < 0.05. RAEB: refractory anemia with excess blasts; RAEB-t: Refractory anemia with excess of blasts in transformation. unk: unknown. Figure made by courtesy of Alvaro Andrades.

Cell line	Subtype	BCL7A mRNA, log2(TPM+1)
OCI-AML3	AML	0,029
AML-193	AML	0,604
NB4	AML	1,007
BDCM	AML	1,828
HEL	AML	2,039
OCI-M2	AML	2,057
HEL 92.1.7	AML	2,342
NA	AML	2,401
HL-60	AML	2,580
MUTZ-8	AML	2,587
NOMO-1	AML	2,587
TF-1	AML	2,733
F-36P	AML	2,753
OCI-M1	AML	2,795
MOLM-14	AML	2,945
SHI-1	AML	3,016
OCI-AML4	AML	3,025
SKM-1	AML	3,027
CMK	AML	3,082
NA	AML	3,116
CMK-11-5	AML	3,123
SKNO-1	AML	3,149
MV4;11	AML	3,278
U-937	AML	3,353
PL-21	AML	3,491
KO52	AML	3,615
KASUMI-1	AML	3,626
ME-1	AML	3,636
SIG-M5	AML	3,708
EOL-1	AML	3,787
M-07e	AML	3,882
OCI-AML5	AML	3,945
MONO-MAC-1	AML	3,956
P31/FUJ	AML	3,958
NA	AML	3,980
Set-2	AML	4,064
KG-1	AML	4,196
Kasumi-6	AML	4,240
MOLM-16	AML	4,268
THP-1	AML	4,283
MONO-MAC-6	AML	4,437
GDM-1	AML	4,468
MOLM-13	AML	4,627
OCI-AML2	AML	4,757

Cell line	Subtype	BCL7A mRNA, log2(TPM+1)
A4/Fuk	DLBCL	1,251
A3/KAW	DLBCL	2,387
OCILY-13	DLBCL	3,399
KML-1	DLBCL	3,777
SU-DHL-8	DLBCL	4,341
RC-K8	DLBCL	4,623
HT	DLBCL	4,657
NU-DHL-1	DLBCL	4,895
OCI-LY3	DLBCL	4,905
WSU-NHL	DLBCL	5,058
RL	DLBCL	5,086
SU-DHL-5	DLBCL	5,298
OCI-LY-19	DLBCL	5,362
OCI-LY7	DLBCL	5,480
Farage	DLBCL	5,482
OCI-LY18	DLBCL	5,561
NU-DUL-1	DLBCL	5,647
SU-DHL-4	DLBCL	5,935
Pfeiffer	DLBCL	6,013
SU-DHL-10	DLBCL	6,316
DB	DLBCL	6,465
WSU-DLCL2	DLBCL	6,594
Toledo	DLBCL	6,599
VAL	DLBCL	6,628
SU-DHL-6	DLBCL	6,657
DOHH-2	DLBCL	6,828
U-2904	DLBCL	6,874
KARPAS-422	DLBCL	6,913
RI-1	DLBCL	7,127

Supplementary Table 2. Expression of *BCL7A* at mRNA level in log2(TPM+1) and subtype (AML or DLBCL) of the cell lines included in Figure 15. Data from DepMap Portal database (22Q2).

Cell line	Subtype	Median-centered Log_2(BCL7A/GAPDH)
NB4	AML	-3,6776
M07e	AML	-3,6311
HL60	AML	-1,5233
U937	AML	-1,1944
THP-1	AML	-0,5316
MOLM-13	AML	1,0485
Ku812	CML	-1,4647
K-562	CML	0,0000
HAP1	CML	0,1057
HBL-1	DLBCL	-12,1130
Karpas-422	DLBCL	-1,7313
RL	DLBCL	-0,1764
DB	DLBCL	0,5422
U-2932	DLBCL	0,7400
SU-DHL-4	DLBCL	0,7936
OciLy7	DLBCL	0,9639
OciLy3	DLBCL	1,4982
OciLy1	DLBCL	1,8377
Ri-1	DLBCL	1,9173

Supplementary Table 3. *BCL7A* mRNA expression level (normalized versus *GAPDH*, median-centered, and log_2-transformed) and subtype (AML, CML or DLBCL) of the cell lines included in Figure 16. Table made by courtesy of Alvaro Andrades.

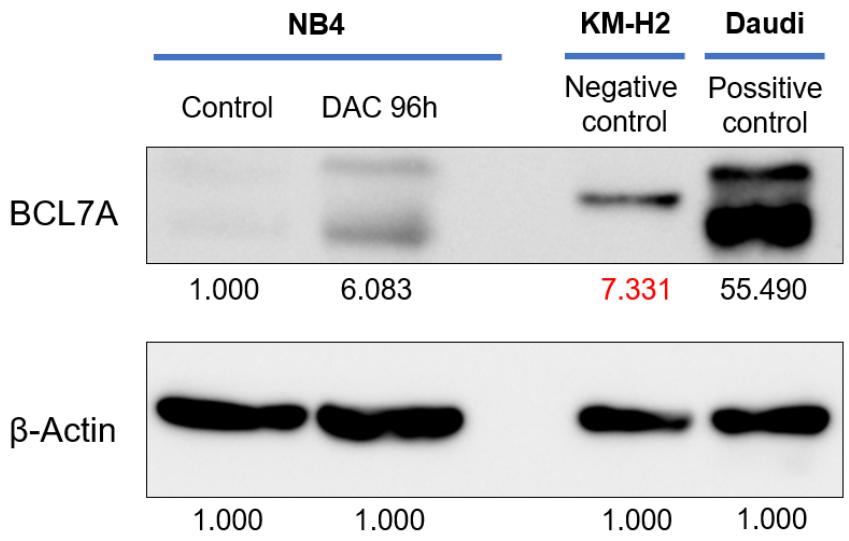

Supplementary Figure 14. Western blot including the decitabine (DAC) treatment over the NB4 cell line shown in Figure. 20. In this image, we have also shown the remaining lanes of this WB experiment that included a negative control for BCL7A expression (KM-H2 cell line, which has no BCL7A expression), and a positive control (Daudi cell line) which expresses average BCL7A levels. The band appearing in the KM-H2 (quantification in red) sample is a nonspecific band due to nonspecific binding of the anti-BCL7A (Cat# HPA019762) that we used (Carlos Baliñas-Gavira, 2020).

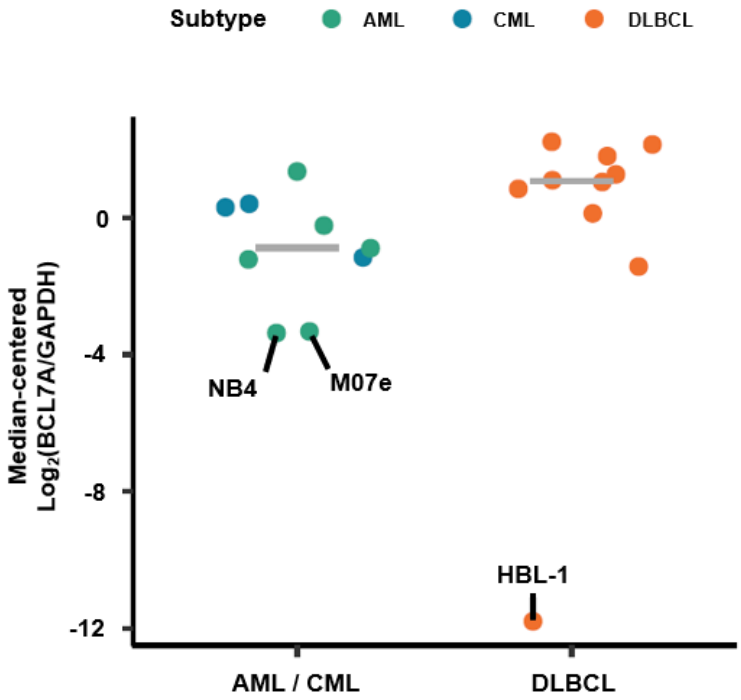

Supplementary Figure 15. *BCL7A* mRNA expression levels in our cell lines cohort using qRTPCR pointing out the M07e cell model too. The median values for each group are represented by the grey horizontal bars. To illustrate the lowest level that our qRTPCR could detect, we included the HBL-1 cell line (DLBCL) as a known negative control for *BCL7A* expression. Detailed information about the cell lines featured in this graph can be found in Supplementary Table 3. Figure made by courtesy of Alvaro Andrades.

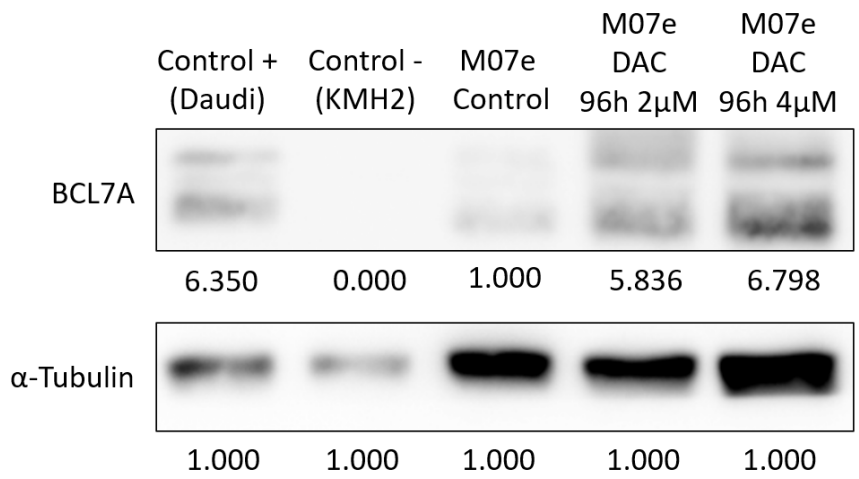

Supplementary Figure 16. Western blot including the decitabine (DAC) treatment over the M07e cell line shown in Figure 23. In this image, we have also included the remaining lanes of this WB experiment that included a negative control for BCL7A expression (KM-H2 cell line, which has no BCL7A expression), and a positive control (Daudi cell line) which expresses average BCL7A levels. The nonspecific band observed in the previous Supplementary Figure 14 is not shown here in the KM-H2 sample lane because M07e cells express higher basal BCL7A protein levels than NB4. Therefore, the intensity of the chemioluminescence captured here was lower compared to the previous Supplementary Figure 14.

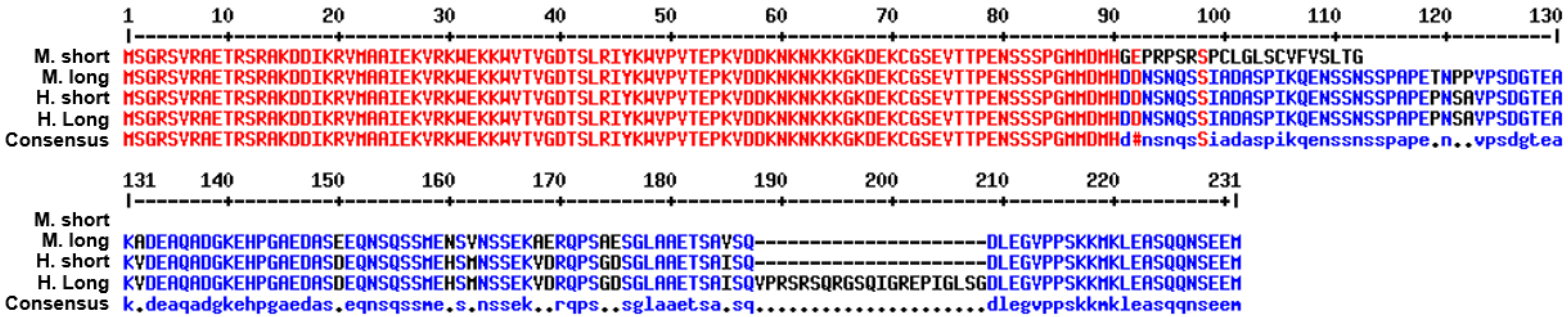

Legend

M. short: Mouse Bcl7a short isoform protein sequence
M. long: Mouse Bcl7a long isoform protein sequence
H. short: Human Bcl7a short isoform protein sequence
H. Long: Human Bcl7a long isoform protein sequence
Consensus: Consensus protein sequence

Supplementary Figure 17. Alignment of mouse Bcl7a protein vs human BCL7A protein sequences, including both short and long isoforms from both species. Red and blue letters highlight sequences' identity. Alignment performed using the online software tool "MultAlin" (Corpet, 1988). Protein sequences obtained from the UniProt database (http://www.uniprot.org/) (Bateman et al., 2015).

References

References

Alaggio, R., Amador, C., Anagnostopoulos, I., Attygalle, A. D., Araujo, I. B. de O., Berti, E., Bhagat, G., Borges, A. M., Boyer, D., Calaminici, M., Chadburn, A., Chan, J. K. C., Cheuk, W., Chng, W. J., Choi, J. K., Chuang, S. S., Coupland, S. E., Czader, M., Dave, S. S., … Xiao, W. (2022). The 5th edition of the World Health Organization Classification of Haematolymphoid Tumours: Lymphoid Neoplasms. In *Leukemia* (Vol. 36, Issue 7, pp. 1720–1748). Springer Nature. https://doi.org/10.1038/s41375-022-01620-2

Albanesi, J., Noguera, N. I., Banella, C., Colangelo, T., De Marinis, E., Leone, S., Palumbo, O., Voso, M. T., Ascenzi, P., Nervi, C., Bianchi, F., & Di Masi, A. (2020). Transcriptional and metabolic dissection of atra-induced granulocytic differentiation in NB4 acute promyelocytic leukemia cells. *Cells*, *9*(11). https://doi.org/10.3390/cells9112423

Alexander, W. S., Schrader, J. W., Adams, J. M., & Hall, E. (1987). Expression of the c-myc Oncogene under Control of an Immunoglobulin Enhancer in Eμ-myc Transgenic Mice. *Molecular and Cellular Biology*, *7*(4), 1436–1444. https://journals.asm.org/journal/mcb

Allis, C. D., & Jenuwein, T. (2016). The molecular hallmarks of epigenetic control. In *Nature Reviews Genetics* (Vol. 17, Issue 8, pp. 487–500). Nature Publishing Group. https://doi.org/10.1038/nrg.2016.59

Anastasiadi, D., Esteve-Codina, A., & Piferrer, F. (2018). Consistent inverse correlation between DNA methylation of the first intron and gene expression across tissues and species. *Epigenetics and Chromatin*, *11*(1). https://doi.org/10.1186/s13072-018-0205-1

Andrades, A., Álvarez-Pérez, J. C., Patiño-Mercau, J. R., Cuadros, M., Baliñas-Gavira, C., & Medina, P. P. (2022). Recurrent splice site mutations affect key diffuse large B-cell lymphoma genes. *Blood*, *139*(15), 2406–2410. https://doi.org/10.1182/blood.2021011708

Antequera, F., & Bird, A. (1999). CpG islands as genomic footprints of promoters that are associated with replication origins. *Current Biology*, *9*(17), R661–R667. http://biomednet.com/elecref/09609822009R0661

Aster, J. C., Pear, W. S., & Blacklow, S. C. (2017). The Varied Roles of Notch in Cancer. *Annual Review of Pathology: Mechanisms of Disease*, *12*, 245–275. https://doi.org/10.1146/annurev-pathol-052016-100127

Austin, S., Ziese, M., & Sternberg, N. (1981). A novel role for site-specific recombination in maintenance of bacterial replicons. *Cell*, *25*(3), 729–736. https://doi.org/https://doi.org/10.1016/0092-8674(81)90180-X

Baker, S. J., Markowitz, S., Fearon, E. R., Willson, J. K. V., & Vogelstein, B. (1990). Suppression of Human Colorectal Carcinoma Cell Growth by Wild-Type p53. *Science*, *249*(4971), 912–915. www.sciencemag.org

Baliñas-Gavira, C., Rodríguez, M. I., Andrades, A., Cuadros, M., Álvarez-Pérez, J. C., Álvarez-Prado, Á. F., de Yébenes, V. G., Sánchez-Hernández, S., Fernández-Vigo, E., Muñoz, J., Martín, F., Ramiro, A. R., Martínez-Climent, J. A., & Medina, P. P. (2020). Frequent mutations in the amino-terminal domain of BCL7A impair its tumor suppressor role in DLBCL. *Leukemia*, *34*(10), 2722–2735. https://doi.org/10.1038/s41375-020-0919-5

Bateman, A., Martin, M. J., O'Donovan, C., Magrane, M., Apweiler, R., Alpi, E., Antunes, R., Arganiska, J., Bely, B., Bingley, M., Bonilla, C., Britto, R., Bursteinas, B., Chavali, G., Cibrian-Uhalte, E., Da Silva, A., De Giorgi, M., Dogan, T., Fazzini, F., … Zhang, J. (2015). UniProt: A hub for protein information. *Nucleic Acids Research*, *43*(D1), D204–D212. https://doi.org/10.1093/nar/gku989

Béguelin, W., Popovic, R., Teater, M., Jiang, Y., Bunting, K. L., Rosen, M., Shen, H., Yang, S. N., Wang, L., Ezponda, T., Martinez-Garcia, E., Zhang, H., Zheng, Y., Verma, S. K., McCabe, M. T., Ott, H. M., VanAller, G. S., Kruger, R. G., Liu, Y., … Melnick, A. M. (2013). EZH2 Is Required for Germinal Center Formation and Somatic EZH2 Mutations Promote Lymphoid Transformation. *Cancer Cell*, *23*(5), 677–692. https://doi.org/10.1016/j.ccr.2013.04.011

Blenk, S., Engelmann, J., Weniger, M., Schultz, J., Dittrich, M., Rosenwald, A., Müller-Hermelink, H. K., Müller, T., & Dandekar, T. (2007). Germinal Center B Cell-Like (GCB) and Activated B Cell-Like (ABC) Type of Diffuse Large B Cell Lymphoma (DLBCL): Analysis of Molecular Predictors, Signatures, Cell Cycle State and Patient Survival. *Cancer Informatics*, 3–399. http://www.microarrays.

Bracken, A. P., Brien, G. L., & Verrijzer, C. P. (2019). Dangerous liaisons: Interplay between SWI/SNF, NURD, and polycomb in chromatin regulation and cancer. *Genes and Development*, *33*(15–16), 936–959. https://doi.org/10.1101/gad.326066.119

Bradford, M. M. (1976). A Rapid and Sensitive Method for the Quantitation of Microgram Quantities of Protein Utilizing the Principle of Protein-Dye Binding. In *ANALYTICAL BIOCHEMISTRY* (Vol. 72).

Buscarlet, M., Krasteva, V., Ho, L., Simon, C., Josée, J. J., Wilhelm, B., Crabtree, G. R., Sauvageau, G., Thibault, P., & Lessard, J. A. (2014). Essential role of BRG, the ATPase subunit of BAF chromatin remodeling complexes, in leukemia maintenance. *Blood*, *123*(11), 1720–1728. https://doi.org/10.1182/blood-2013-02

Carbone, A., Bernardini, L., Valenzano, F., Bottillo, I., De Simone, C., Capizzi, R., Capalbo, A., Romano, F., Novelli, A., Dallapiccola, B., & Amerio, P. (2008). Array-based comparative genomic hybridization in early-stage mycosis fungoides: Recurrent deletion of tumor suppressor genes BCL7A, SMAC/DIABLO, and RHOF. *Genes Chromosomes and Cancer*, *47*(12), 1067–1075. https://doi.org/10.1002/gcc.20601

Carlos Baliñas-Gavira. (2020). *Estudio de las implicaciones de BCL7A en el desarrollo tumoral* [University of Granada]. http://hdl.handle.net/10481/65386

Centore, R. C., Sandoval, G. J., Soares, L. M. M., Kadoch, C., & Chan, H. M. (2020). Mammalian SWI/SNF Chromatin Remodeling Complexes: Emerging Mechanisms and Therapeutic Strategies. *Trends in Genetics*, *36*(12), 936–950. https://doi.org/10.1016/j.tig.2020.07.011

Chale, R., Abad, A., & Jimenez, J. (2019). Acute Promyelocytic Leukemia – A Review of the Literature. *Clinical Lymphoma, Myeloma & Leukemia*, *19*(S1), S236–S237.

Chapman, M. A., Lawrence, M. S., Keats, J. J., Cibulskis, K., Sougnez, C., Schinzel, A. C., Harview, C. L., Brunet, J. P., Ahmann, G. J., Adli, M., Anderson, K. C., Ardlie, K. G., Auclair, D., Baker, A., Bergsagel, P. L., Bernstein, B. E., Drier, Y., Fonseca, R., Gabriel, S. B., … Golub, T. R. (2011). Initial genome sequencing and analysis of multiple myeloma. *Nature*, *471*(7339), 467–472. https://doi.org/10.1038/nature09837

Choudhury, S. R., Cui, Y., Lubecka, K., Stefanska, B., & Irudayaraj, J. (2016). CRISPR-dCas9 mediated TET1 targeting for selective DNA demethylation at BRCA1 promoter. *Oncotarget*, *7*, 46545–46556. https://doi.org/https://doi.org/10.18632/oncotarget.10234

Ciccia, A., & Elledge, S. J. (2010). The DNA Damage Response: Making It Safe to Play with Knives. *Molecular Cell*, *40*(2), 179–204. https://doi.org/10.1016/j.molcel.2010.09.019

Clapier, C. R., Iwasa, J., Cairns, B. R., & Peterson, C. L. (2017). Mechanisms of action and regulation of ATP-dependent chromatin-remodelling complexes. *Nature Reviews Molecular Cell Biology*, *18*(7), 407–422. https://doi.org/10.1038/nrm.2017.26

Clapier, C. R., Kasten, M. M., Parnell, T. J., Viswanathan, R., Szerlong, H., Sirinakis, G., Zhang, Y., & Cairns, B. R. (2016). Regulation of DNA Translocation Efficiency within the Chromatin Remodeler RSC/Sth1 Potentiates Nucleosome Sliding and Ejection. *Molecular Cell*, *62*(3), 453–461. https://doi.org/10.1016/j.molcel.2016.03.032

Corpet, F. (1988). Multiple sequence alignment with hierarchical clustering. *Nucleic Acids Research*, *16*(22), 10881–10890. https://doi.org/10.1093/nar/16.22.10881

Cox, J., & Mann, M. (2008). MaxQuant enables high peptide identification rates, individualized p.p.b.-range mass accuracies and proteome-wide protein quantification. *Nature Biotechnology*, *26*(12), 1367–1372. https://doi.org/10.1038/nbt.1511

Cumming, A. J., Khananisho, D., Harris, R., Bayer, C. N., Nørholm, M. H. H., Jamshidi, S., Ilag, L. L., & Daley, D. O. (2022). Antibiotic-Efficient Genetic Cassette for the TEM-1 β-Lactamase That Improves Plasmid Performance. *ACS Synthetic Biology*, *11*(1), 241–253. https://doi.org/10.1021/acssynbio.1c00393

Dalseno, D., Anderton, H., Kueh, A., Herold, M. J., Silke, J., Strasser, A., & Bouillet, P. (2023). Deletion of Gpatch2 does not alter Tnf expression in

mice. *Cell Death and Disease*, *14*. https://doi.org/10.1038/s41419-023-05751-x

Daniel A. Arber, Attilio Orazi, Robert P. Hasserjian, Michael J. Borowitz, Katherine R. Calvo, Hans-Michael Kvasnicka, Sa A. Wang, Adam Bagg, Tiziano Barbui, Susan Branford, Carlos E. Bueso-Ramos, Jorge E. Cortes, Paola Dal Cin, Courtney D. DiNardo, Hervé Dombret, Eric J. Duncavage, Benjamin L. Ebert, Elihu H. Estey, Fabio Facchetti, … Ayalew Tefferi. (2022). International Consensus Classification of Myeloid Neoplasms and Acute Leukemias: integrating morphologic, clinical, and genomic data. *Blood*, *140*(11), 1200–1228. https://doi.org/10.1182/BLOOD.2019000962

Di Liegro, C. M., Schiera, G., & Di Liegro, I. (2018). H1.0 linker histone as an epigenetic regulator of cell proliferation and differentiation. In *Genes* (Vol. 9, Issue 6). MDPI AG. https://doi.org/10.3390/genes9060310

Di Ruscio, A., Ebralidze, A. K., Benoukraf, T., Amabile, G., Goff, L. A., Terragni, J., Figueroa, M. E., De Figueiredo Pontes, L. L., Alberich-Jorda, M., Zhang, P., Wu, M., D'Alò, F., Melnick, A., Leone, G., Ebralidze, K. K., Pradhan, S., Rinn, J. L., & Tenen, D. G. (2013). DNMT1-interacting RNAs block gene-specific DNA methylation. *Nature*, *503*(7476), 371–376. https://doi.org/10.1038/nature12598

Dima, D., Oprita, L., Rosu, A. M., Trifa, A., Selicean, C., Moisoiu, V., Frinc, I., Zdrenghea, M., & Tomuleasa, C. (2017). Adult acute megakaryoblastic leukemia: Rare association with cytopenias of undetermined significance and p210 and p190 BCR–ABL transcripts. *OncoTargets and Therapy*, *10*, 5047–5051. https://doi.org/10.2147/OTT.S146973

Doetschman, T. (2009). *Influence of Genetic Background on Genetically Engineered Mouse Phenotypes (Gene Knockout Protocols)* (Vol. 530). www.springer.com/series/7651

Döhner, H., Estey, E. H., Amadori, S., Appelbaum, F. R., Bü, T., Burnett, A. K., Dombret, H., Fenaux, P., Grimwade, D., Larson, R. A., Lo-Coco, F., Naoe, T., Niederwieser, D., Ossenkoppele, G. J., Sanz, M. A., Sierra, J., Tallman, M. S., Lö, B., & Bloomfield, C. D. (2010). Diagnosis and management of acute myeloid leukemia in adults: recommendations from an international expert panel, on behalf of the European LeukemiaNet. *Blood*, *115*(3), 453–474. https://doi.org/10.1182/blood-2009-07

Doug Chung, D. W., & Le Roch, K. G. (2013). Genome-wide analysis of gene expression. In *Encyclopedia of Biological Chemistry: Second Edition* (pp. 369–374). Elsevier Inc. https://doi.org/10.1016/B978-0-12-378630-2.00634-4

Egle, A., Harris, A. W., Bath, M. L., O'Reilly, L., & Cory, S. (2004). VavP-Bcl2 transgenic mice develop follicular lymphoma preceded by germinal center hyperplasia. *Blood*, *103*(6), 2276–2283. https://doi.org/10.1182/blood-2003-07-2469

Esteller, M. (2007). Epigenetic gene silencing in cancer: The DNA hypermethylome. *Human Molecular Genetics*, *16*(R1), R50–R59. https://doi.org/10.1093/hmg/ddm018

Falini, B., Brunetti, L., Sportoletti, P., & Martelli, M. P. (2020). NPM1-mutated acute myeloid leukemia: from bench to bedside. *Blood*, *136*(15), 1707–1721. http://ashpublications.org/blood/article-pdf/136/15/1707/1760541/bloodbld2019004226c.pdf

Fan, Y., Liao, L., Liu, Y., Wu, Z., Wang, C., Jiang, Z., Wang, S., & Liu, Y. (2021). Risk factors affect accurate prognosis in ASXL1-mutated acute myeloid leukemia. *Cancer Cell International*, *21*. https://doi.org/10.1186/s12935-021-02233-y

Fennell, K. A., Bell, C. C., & Dawson, M. A. (2019). Epigenetic therapies in acute myeloid leukemia: where to from here? *Blood*, *134*(22), 1891–1901. http://ashpublications.org/blood/article-pdf/134/22/1891/1543146/bloodbld2019003262.pdf

Ferrone, C. K., Blydt-Hansen, M., & Rauh, M. J. (2020). Age-associated TET2 mutations: Common drivers of myeloid dysfunction, cancer and cardiovascular disease. *International Journal of Molecular Sciences*, *21*(2). https://doi.org/10.3390/ijms21020626

Gao, J. (2007). *Studies on the Function and Regulation of BCL7A and BCL6 in Germinal Center B cells*. Columbia University.

Gardiner-Garden, M., & Frommer, M. (1987). CpG Islands in vertebrate genomes. *Journal of Molecular Biology*, *196*(2), 261–282.

Ghashghaeinia, M., Köberle, M., Mrowietz, U., & Bernhardt, I. (2019). Proliferating tumor cells mimick glucose metabolism of mature human erythrocytes. *Cell Cycle*, *18*(12), 1316–1334. https://doi.org/10.1080/15384101.2019.1618125

Gibson, B. A., Blaukopf, C., Lou, T., Chen, L., Doolittle, L. K., Finkelstein, I., Narlikar, G. J., Gerlich, D. W., & Rosen, M. K. (2023). In diverse conditions, intrinsic chromatin condensates have liquid-like material properties. *Proceedings of the National Academy of Sciences of the United States of America*, *120*(118). https://doi.org/10.1073/pnas.2218085120

Glass, J. L., Hassane, D., Wouters, B. J., Kunimoto, H., Avellino, R., Garrett-Bakelman, F. E., Guryanova, O. A., Bowman, R., Redlich, S., Intlekofer, A. M., Meydan, C., Qin, T., Fall, M., Alonso, A., Guzman, M. L., Valk, P. J. M., Thompson, C. B., Levine, R., Elemento, O., … Figueroa, M. E. (2017). Epigenetic identity in AML depends on disruption of nonpromoter regulatory elements and is affected by antagonistic effects of mutations in epigenetic modifiers. *Cancer Discovery*, *7*(8), 868–883. https://doi.org/10.1158/2159-8290.CD-16-1032

Goyama, S., Schibler, J., Cunningham, L., Zhang, Y., Rao, Y., Nishimoto, N., Nakagawa, M., Olsson, A., Wunderlich, M., Link, K. A., Mizukawa, B., Grimes, H. L., Kurokawa, M., Liu, P. P., Huang, G., & Mulloy, J. C. (2013). Transcription factor RUNX1 promotes survival of acute myeloid leukemia cells. *Journal of Clinical Investigation*, *123*(9), 3876–3888. https://doi.org/10.1172/JCI68557

Greenberg, M. V. C., & Bourc'his, D. (2019). The diverse roles of DNA methylation in mammalian development and disease. *Nature Reviews Molecular Cell Biology*, *20*, 590–607. https://doi.org/10.1038/s41580-019-0159-6

Gregory, G. L., & Copple, I. M. (2023). Modulating the expression of tumor suppressor genes using activating oligonucleotide technologies as a therapeutic approach in cancer. *Molecular Therapy - Nucleic Acids*, *31*, 211–223. https://doi.org/10.1016/j.omtn.2022.12.016

Grimm, J., & Binder, M. (2022). Curse and blessing: upregulation of oncogenes upon treatment with hypomethylating agents in myelodysplastic syndrome. *Signal Transduction and Targeted Therapy*, *7*(1). https://doi.org/10.1038/s41392-022-01143-3

Grimwade, D., Hills, R. K., Moorman, A. V., Walker, H., Chatters, S., Goldstone, A. H., Wheatley, K., Harrison, C. J., & Burnett, A. K. (2010). Refinement of cytogenetic classification in acute myeloid leukemia: Determination of prognostic significance of rare recurring chromosomal abnormalities among 5876 younger adult patients treated in the United Kingdom Medical Research Council trials. *Blood*, *116*(3), 354–365. https://doi.org/10.1182/blood-2009-11-254441

Grimwade, D., Ivey, A., & Huntly, B. J. P. (2016). Molecular landscape of acute myeloid leukemia in younger adults and its clinical relevance. *Blood*, *127*(1), 29–41. https://doi.org/10.1182/blood-2015-07

Grob, T., Al Hinai, A. S. A., Sanders, M. A., Kavelaars, F. G., Rijken, M., Gradowska, P. L., Biemond, B. J., Breems, D. A., Maertens, J., Kooy, M. van M., Pabst, T., de Weerdt, O., Ossenkoppele, G. J., van de Loosdrecht, A. A., Huls, G. A., Cornelissen, J. J., Beverloo, H. B., Löwenberg, B., Jongen-Lavrencic, M., & Valk, P. J. M. (2022). Molecular characterization of mutant TP53 acute myeloid leukemia and high-risk myelodysplastic syndrome. *Blood*, *139*(15), 2347–2354. https://doi.org/10.1182/BLOOD.2019000962

Hanahan, D. (2022). Hallmarks of Cancer: New Dimensions. *Cancer Discovery*, *12*(1), 31–46. https://doi.org/10.1158/2159-8290.CD-21-1059

Hanahan, D., & Weinberg, R. A. (2000). The Hallmarks of Cancer Review evolve progressively from normalcy via a series of pre. *Cell*, *100*(1), 57–70. https://doi.org/https://doi.org/10.1016/S0092-8674(00)81683-9

Hanahan, D., & Weinberg, R. A. (2011). Hallmarks of cancer: The next generation. *Cell*, *144*(5), 646–674. https://doi.org/10.1016/j.cell.2011.02.013

Hanzawa, N., Hashimoto, K., Yuan, X., Kawahori, K., Tsujimoto, K., Hamaguchi, M., Tanaka, T., Nagaoka, Y., Nishina, H., Morita, S., Hatada, I., Yamada, T., & Ogawa, Y. (2020). Targeted DNA demethylation of the Fgf21 promoter by CRISPR/dCas9-mediated epigenome editing. *Scientific Reports*, *10*. https://doi.org/10.1038/s41598-020-62035-6

Haschek, W. M., Rousseaux, C. G., & Wallig, M. A. (2010). Manifestations of Toxic Cell Injury. In *Fundamentals of Toxicologic Pathology* (pp. 9–42). Elsevier. https://doi.org/10.1016/b978-0-12-370469-6.00002-7

Herman, J. G., Graff, J. R., Myohanen, S., Nelkin, B. D., & Baylin, S. B. (1996). Methylation-specific PCR: a novel PCR assay for methylation status of CpG islands. *Proc Natl Acad Sci U S A*, *93*(18), 9821–9826. https://doi.org/https://doi.org/10.1073/pnas.93.18.9821

Hernández-García, J., Diego-Martin, B., Kuo, P. H., Jami-Alahmadi, Y., Vashisht, A. A., Wohlschlegel, J., Jacobsen, S. E., Blázquez, M. A., & Gallego-Bartolomé, J. (2022). Comprehensive identification of SWI/SNF complex subunits underpins deep eukaryotic ancestry and reveals new plant components. *Communications Biology*, *5*(1). https://doi.org/10.1038/s42003-022-03490-x

Heshmati, Y., Türköz, G., Harisankar, A., Kharazi, S., Boström, J., Dolatabadi, E. K., Krstic, A., Chang, D., Månsson, R., Altun, M., Qian, H., & Walfridsson, J. (2018). The chromatin-remodeling factor CHD4 is required for maintenance of childhood acute myeloid leukemia. *Haematologica*, *103*(7), 1169–1181. https://doi.org/10.3324/haematol.2017.183970

Heumos, L., Schaar, A. C., Lance, C., Litinetskaya, A., Drost, F., Zappia, L., Lücken, M. D., Strobl, D. C., Henao, J., Curion, F., Aliee, H., Ansari, M., Badia-i-Mompel, P., Büttner, M., Dann, E., Dimitrov, D., Dony, L., Frishberg, A., He, D., … Theis, F. J. (2023). Best practices for single-cell analysis across modalities. *Nature Reviews Genetics*, *24*(8), 550–572. https://doi.org/10.1038/s41576-023-00586-w

Hindley, A., Catherwood, M. A., McMullin, M. F., & Mills, K. I. (2021). Significance of npm1 gene mutations in aml. *International Journal of Molecular Sciences*, *22*(18). https://doi.org/10.3390/ijms221810040

Holton, T. A., & Graham, M. W. (1991). A simple and efficient method for direct cloning of PCR products using ddT-tailed vectors. *Nucleic Acids Research*, *19*(5), 1156–1156. https://doi.org/https://doi.org/10.1093/nar/19.5.1156

Hsu, M. C., Luo, W. J., Guo, B. C., Chen, C. H., Hu, P. A., Tsai, Y. H., Su, K. Y., & Lee, T. S. (2022). Genetic Deletion of HLJ1 Does Not Affect Blood Coagulation in Mice. *International Journal of Molecular Sciences*, *23*(4). https://doi.org/10.3390/ijms23042064

Idres, N., Benoıˆt, G. B., Flexor, M. A., Lanotte, M., & Chabot, G. G. (2001). Granulocytic Differentiation of Human NB4 Promyelocytic Leukemia Cells Induced by All-trans Retinoic Acid Metabolites 1. *Cancer Research*, *61*(2), 700–705. http://aacrjournals.org/cancerres/article-pdf/61/2/700/3251499/ch020100700p.pdf

Indra, A. K., Warot, X., Brocard, J., Bornert, J.-M., Xiao, J.-H., Chambon, P., & Metzger, D. (1999). Temporally-controlled site-specific mutagenesis in the basal layer of the epidermis: comparison of the recombinase activity of the tamoxifen-inducible Cre-ER T and Cre-ER T2 recombinases. In *Nucleic Acids Research* (Vol. 27, Issue 22).

Issa, G. C., & DiNardo, C. D. (2021). Acute myeloid leukemia with IDH1 and IDH2 mutations: 2021 treatment algorithm. *Blood Cancer Journal*, *11*(6). https://doi.org/10.1038/s41408-021-00497-1

J. Sherr, C. (2004). Principles of Tumor Suppression. *Cell*, *116*(3), 235–246. https://doi.org/https://doi.org/10.1016/S0092-8674(03)01075-4

Jadayel, D. M., Osborne, L. R., Coignet, L. J. A., Zani, J., Tsui, L.-C., Scherer, S. W., & Dyer, M. J. S. (1998). The BCL7 gene family: deletion of BCL7B in Williams syndrome. *Gene*, *224*(1–2), 35–44. http://genome.wustl.edu/gsc/

Jassim, A., Rahrmann, E. P., Simons, B. D., & Gilbertson, R. J. (2023). Cancers make their own luck: theories of cancer origins. In *Nature Reviews Cancer*. Nature Research. https://doi.org/10.1038/s41568-023-00602-5

Jiang, D., Li, T., Guo, C., Tang, T. S., & Liu, H. (2023). Small molecule modulators of chromatin remodeling: from neurodevelopment to neurodegeneration. *Cell and Bioscience*, *13*(1). https://doi.org/10.1186/s13578-023-00953-4

Jinek, M., Chylinski, K., Fonfara, I., Hauer, M., Doudna, J. A., & Charpentier, E. (2012). A Programmable Dual-RNA-Guided DNA Endonuclease in Adaptive Bacterial Immunity. *Science*, *337*(6096), 816–821. https://www.science.org

Kadoch, C., Hargreaves, D. C., Hodges, C., Elias, L., Ho, L., Ranish, J., & Crabtree, G. R. (2013). Proteomic and bioinformatic analysis of mammalian SWI/SNF complexes identifies extensive roles in human malignancy. *Nature Genetics*, *45*(6), 592–601. https://doi.org/10.1038/ng.2628

Kadoch, C., Williams, R. T., Calarco, J. P., Miller, E. L., Weber, C. M., Braun, S. M. G., Pulice, J. L., Chory, E. J., & Crabtree, G. R. (2017). Dynamics of BAF-Polycomb complex opposition on heterochromatin in normal and oncogenic states. *Nature Genetics*, *49*(2), 213–222. https://doi.org/10.1038/ng.3734

Kantarjian, H., Kadia, T., DiNardo, C., Daver, N., Borthakur, G., Jabbour, E., Garcia-Manero, G., Konopleva, M., & Ravandi, F. (2021). Acute myeloid leukemia: current progress and future directions. *Blood Cancer Journal*, *11*. https://doi.org/10.1038/s41408-021-00425-3

Karagianni, P., Giannouli, S., & Voulgarelis, M. (2021). From the (Epi)genome to metabolism and vice versa; examples from hematologic malignancy. *International Journal of Molecular Sciences*, *22*(12). https://doi.org/10.3390/ijms22126321

Kavianpour, M., Ahmadzadeh, A., Shahrabi, S., & Saki, N. (2016). Significance of oncogenes and tumor suppressor genes in AML prognosis. *Tumor Biology*, *37*, 10041–10052. https://doi.org/10.1007/s13277-016-5067-1

Khanna-Gupta, A., Kolibaba, K., Zibello, T. A., & Berliner, N. (1994). NB4 Cells Show Bilineage Potential and an Aberrant Pattern of Neutrophil Secondary Granule Protein Gene Expression. *Blood*, *84*(1), 294–302.

Khoury, J. D., Solary, E., Abla, O., Akkari, Y., Alaggio, R., Apperley, J. F., Bejar, R., Berti, E., Busque, L., Chan, J. K. C., Chen, W., Chen, X., Chng, W. J., Choi, J. K., Colmenero, I., Coupland, S. E., Cross, N. C. P., De Jong, D., Elghetany, M. T., … Hochhaus, A. (2022). The 5th edition of the World Health Organization Classification of Haematolymphoid Tumours: Myeloid and Histiocytic/Dendritic Neoplasms. In *Leukemia* (Vol. 36, Issue 7, pp. 1703–1719). Springer Nature. https://doi.org/10.1038/s41375-022-01613-1

Klein, U., Tu, Y., Stolovitzky, G. A., Keller, J. L., Haddad, J., Miljkovic, V., Cattoretti, G., Califano, A., & Dalla-Favera, R. (2003). Transcriptional analysis of the B cell germinal center reaction. *Proc Natl Acad Sci U S A*, *100*(5), 2639–2644. www.pnas.orgcgidoi10.1073pnas.0437996100

Knudson, A. G. (1971). *Mutation and Cancer: Statistical Study of Retinoblastoma*. *68*(4), 820–823. https://www.pnas.org

Kongkiatkamon Sunisa, Gu Xiaorong, Peng Ng Kwok, Pagliuca Simona, Adema Vera, Walter Wencke, Nagata Yasunobu, Kerr Cassandra M, Kerr Cassandra M, Meggendorfer Manja, Awada Hassan, Hutter Stephan, Gurnari Carmelo, Haferlach Claudia, Jha Babal K., Visconte Valeria, Haferlach Torsten, Maciejewski Jaroslaw P., & Sauntharajah Yogenthiran. (2021). Epigenetic Enzyme Mutations in Myeloid Malignancies Are Selected By Chromatin-Remodeling Requirements That Vary By Lineage- and Maturation-Stage. In *Blood* (Vol. 138, Issue S1, pp. 1148–1148). American Society of Hematology. https://doi.org/10.1182/blood.v128.22.1467.1467

Kontomanolis, E. N., Koutras, A., Syllaios, A., Schizas, D., Mastoraki, A., Garmpis, N., Diakosavvas, M., Angelou, K., Tsatsaris, G., Pagkalos, A., Ntounis, T., & Fasoulakis, Z. (2020). Role of oncogenes and tumor-suppressor genes in carcinogenesis: A review. In *Anticancer Research* (Vol. 40, Issue 11, pp. 6009–6015). International Institute of Anticancer Research. https://doi.org/10.21873/anticanres.14622

Kumar, S., Warrell, J., Li, S., McGillivray, P. D., Meyerson, W., Salichos, L., Harmanci, A., Martinez-Fundichely, A., Chan, C. W. Y., Nielsen, M. M., Lochovsky, L., Zhang, Y., Li, X., Lou, S., Pedersen, J. S., Herrmann, C., Getz, G., Khurana, E., & Gerstein, M. B. (2020). Passenger Mutations in More Than 2,500 Cancer Genomes: Overall Molecular Functional Impact and Consequences. *Cell*, *180*(5), 915-927.e16. https://doi.org/10.1016/j.cell.2020.01.032

Lai, W. K. M., & Pugh, B. F. (2017). Understanding nucleosome dynamics and their links to gene expression and DNA replication. *Nature Reviews Molecular Cell Biology*, *18*(9), 548–562. https://doi.org/10.1038/nrm.2017.47

Lawrence, M., Daujat, S., & Schneider, R. (2016). Lateral Thinking: How Histone Modifications Regulate Gene Expression. *Trends in Genetics*, *32*(1), 42–56. https://doi.org/10.1016/j.tig.2015.10.007

Lawrence, M. S., Stojanov, P., Polak, P., Kryukov, G. V., Cibulskis, K., Sivachenko, A., Carter, S. L., Stewart, C., Mermel, C. H., Roberts, S. A., Kiezun, A., Hammerman, P. S., McKenna, A., Drier, Y., Zou, L., Ramos, A. H., Pugh, T. J., Stransky, N., Helman, E., … Getz, G. (2013). Mutational heterogeneity in cancer and the search for new cancer-associated genes. *Nature*, *499*(7457), 214–218. https://doi.org/10.1038/nature12213

Le, P., Romano, G., Nana-Sinkam, P., & Acunzo, M. (2021). Non-coding rnas in cancer diagnosis and therapy: Focus on lung cancer. *Cancers*, *13*(6). https://doi.org/10.3390/cancers13061372

Lee, T. I., & Young, R. A. (2013). Transcriptional regulation and its misregulation in disease. *Cell*, *152*(6), 1237–1251. https://doi.org/10.1016/j.cell.2013.02.014

Lessard, J., Wu, J. I., Ranish, J. A., Wan, M., Winslow, M. M., Staahl, B. T., Wu, H., Aebersold, R., Graef, I. A., & Crabtree, G. R. (2007). An Essential Switch in Subunit Composition of a Chromatin Remodeling Complex during Neural Development. *Neuron*, *55*(2), 201–215. https://doi.org/10.1016/j.neuron.2007.06.019

Li, T., Yang, Y., Qi, H., Cui, W., Zhang, L., Fu, X., He, X., Liu, M., Li, P. feng, & Yu, T. (2023). CRISPR/Cas9 therapeutics: progress and prospects. *Signal Transduction and Targeted Therapy*, *8*. https://doi.org/10.1038/s41392-023-01309-7

Li, Y., Gong, H., Wang, P., Zhu, Y., Peng, H., Cui, Y., Li, H., Liu, J., & Wang, Z. (2021). The emerging role of ISWI chromatin remodeling complexes in cancer. *Journal of Experimental and Clinical Cancer Research*, *40*. https://doi.org/10.1186/s13046-021-02151-x

Litvinov, I. V., Zhou, Y., Kupper, T. S., & Sasseville, D. (2013). Loss of BCL7A expression correlates with poor disease prognosis in patients with early-stage cutaneous T-cell lymphoma. *Leukemia and Lymphoma*, *54*(3), 653–654. https://doi.org/10.3109/10428194.2012.717695

Liu, Y. V, Bassal, M. A., Xiao, Q., Lin, X., Wu, C.-S., Kwon, J., Zhou, Q., Kee Tan, H., Ebralidze, A. K., Chai, L., Benoukraf, T., Ruscio, A. Di, & Tenen, D. G. (2020). Targeted intragenic demethylation initiates chromatin rewiring for gene activation. In *bioRxiv*. bioRxiv. https://doi.org/10.1101/2020.07.16.205922

Liu, W., Li, L., Jiang, J., Wu, M., & Lin, P. (2021). Applications and challenges of CRISPR-Cas gene-editing to disease treatment in clinics. *Precision Clinical Medicine*, *4*(3), 179–191. https://doi.org/10.1093/pcmedi/pbab014

Liu, Y.-C., Kwon, J., Fabiani, E., Xiao, Z., Liu, Y. V., Follo, M. Y., Liu, J., Huang, H., Gao, C., Liu, J., Falconi, G., Valentini, L., Gurnari, C., Finelli, C., Cocco, L., Liu, J.-H., Jones, A. I., Yang, J., Yang, H., … Chai, L. (2022). Demethylation and Up-Regulation of an Oncogene after Hypomethylating Therapy. *New England Journal of Medicine*, *386*(21), 1998–2010. https://doi.org/10.1056/nejmoa2119771

Lopez-Serra, P., & Esteller, M. (2012). DNA methylation-associated silencing of tumor-suppressor microRNAs in cancer. *Oncogene*, *31*, 1609–1622. https://doi.org/10.1038/onc.2011.354

Lu, P., & Roberts, C. W. M. (2013). The SWI/SNF tumor suppressor complex: Regulation of promoter nucleosomes and beyond. *Nucleus (United States)*, *4*(5), 374–378. https://doi.org/10.4161/nucl.26654

Luger, K., Dechassa, M. L., & Tremethick, D. J. (2012). New insights into nucleosome and chromatin structure: An ordered state or a disordered affair? *Nature Reviews Molecular Cell Biology*, *13*(7), 436–447. https://doi.org/10.1038/nrm3382

Luger, K., Mä Der, A. W., Richmond, R. K., Sargent, D. F., & Richmond, T. J. (1997). Crystal structure of the nucleosome core particle at 2.8 A ° resolution. *Nature*, *389*, 251–260.

Maclennan, I. C. M. (1994). Germinal Centers. *Annu. Rev. Immunol*, *12*, 117–139. www.annualreviews.org

Madan, V., Shyamsunder, P., Han, L., Mayakonda, A., Nagata, Y., Sundaresan, J., Kanojia, D., Yoshida, K., Ganesan, S., Hattori, N., Fulton, N., Tan, K. T., Alpermann, T., Kuo, M. C., Rostami, S., Matthews, J., Sanada, M., Liu, L. Z., Shiraishi, Y., … Koeffler, H. P. (2016). Comprehensive mutational analysis of primary and relapse acute promyelocytic leukemia. *Leukemia*, *30*(8), 1672–1681. https://doi.org/10.1038/leu.2016.69

Mahalingaiah, P. K., Palenski, T., & Van Vleet, T. R. (2018). An In Vitro Model of Hematotoxicity: Differentiation of Bone Marrow–Derived Stem/Progenitor Cells into Hematopoietic Lineages and Evaluation of Lineage-Specific Hematotoxicity. *Current Protocols in Toxicology*, *76*(1). https://doi.org/10.1002/cptx.45

Marchuk, D., Drumm, M., Saulino, A., & Collins, F. S. (1991). Construction of T-vectors, a rapid and general system for direct cloning of unmodified PCR products. *Nucleic Acids Research*, *19*(5), 1154–1154. https://doi.org/https://doi.org/10.1093/nar/19.5.1154

Mardinian, K., Adashek, J. J., Botta, G. P., Kato, S., & Kurzrock, R. (2021). SMARCA4: Implications of an altered chromatin-remodeling gene for cancer development and therapy. *Molecular Cancer Therapeutics*, *20*(12), 2341–2351. https://doi.org/10.1158/1535-7163.MCT-21-0433

Martin, L. J., Koegl, M., Bader, G., Cockcroft, X. L., Fedorov, O., Fiegen, D., Gerstberger, T., Hofmann, M. H., Hohmann, A. F., Kessler, D., Knapp, S., Knesl, P., Kornigg, S., Müller, S., Nar, H., Rogers, C., Rumpel, K., Schaaf, O., Steurer, S., … McConnell, D. (2016). Structure-Based Design of an in Vivo Active Selective BRD9 Inhibitor. *Journal of Medicinal Chemistry*, *59*(10), 4462–4475. https://doi.org/10.1021/acs.jmedchem.5b01865

Martinez-Delgado, B., Meléndez, B., Cuadros, M., Alvarez, J., Castrillo, J. M., Ruiz De La Parte, A., Mollejo, M., Bellas, C., Diaz, R., Lombardía, L., Al-Shahrour, F., Domínguez, O., Cascon, A., Robledo, M., Rivas, C., & Benitez, J. (2004). Expression Profiling of T-Cell Lymphomas Differentiates

Peripheral and Lymphoblastic Lymphomas and Defines Survival Related Genes. *Clinical Cancer Research*, *10*(15), 4971–4982. http://aacrjournals.org/clincancerres/article-pdf/10/15/4971/1952816/zdf01504004971.pdf

Mashtalir, N., D'Avino, A. R., Michel, B. C., Luo, J., Pan, J., Otto, J. E., Zullow, H. J., McKenzie, Z. M., Kubiak, R. L., St. Pierre, R., Valencia, A. M., Poynter, S. J., Cassel, S. H., Ranish, J. A., & Kadoch, C. (2018). Modular Organization and Assembly of SWI/SNF Family Chromatin Remodeling Complexes. *Cell*, *175*(5), 1272-1288.e20. https://doi.org/10.1016/j.cell.2018.09.032

Mashtalir, N., Suzuki, H., Farrell, D. P., Sankar, A., Luo, J., Filipovski, M., D'Avino, A. R., St. Pierre, R., Valencia, A. M., Onikubo, T., Roeder, R. G., Han, Y., He, Y., Ranish, J. A., DiMaio, F., Walz, T., & Kadoch, C. (2020). A Structural Model of the Endogenous Human BAF Complex Informs Disease Mechanisms. *Cell*, *183*(3), 802-817.e24. https://doi.org/10.1016/j.cell.2020.09.051

Massagué, J., & Obenauf, A. C. (2016). Metastatic colonization by circulating tumour cells. In *Nature* (Vol. 529, Issue 7586, pp. 298–306). Nature Publishing Group. https://doi.org/10.1038/nature17038

Mead, D. A., Pey, N. K., Herrnstadt1, C., Marcil\, R. A., & Smith, L. M. (1991). *A UNIVERSAL MRHOD FOR THE DIREO CLONING OF PCR AMPLIFIED NUCLEIC ACID*. http://www.nature.com/naturebiotechnology

Medina, P. P., Romero, O. A., Kohno, T., Montuenga, L. M., Pio, R., Yokota, J., & Sanchez-Cespedes, M. (2008). Frequent BRG1/SMARCA4-Inactivating mutations in human lung cancer cell lines. *Human Mutation*, *29*(5), 617–622. https://doi.org/10.1002/humu.20730

Menssen, A. J., & Walter, M. J. (2020). Genetics of progression from MDS to secondary leukemia. *Blood*, *136*(1), 50–60. http://ashpublications.org/blood/article-pdf/136/1/50/1747573/bloodbld2019000942c.pdf

Metzeler, K. H., Herold, T., Rothenberg-Thurley, M., Amler, S., Sauerland, M. C., Schneider, S., Konstandin, N. P., Dufour, A., BräundlBr, K., Ksienzyk, B., Zellmeier, E., Hartmann, L., Greif, P. A., Fiegl, M., Subklewe, M., Bohlander, S. K., Krug, U., Faldum, A., Berdel, W. E., … Spiekermann, K. (2016). Spectrum and prognostic relevance of driver gene mutations in acute myeloid leukemia. *Blood*, *128*(5), 686–698. https://doi.org/10.1182/blood-2016-01

Michel, B. C., D'Avino, A. R., Cassel, S. H., Mashtalir, N., McKenzie, Z. M., McBride, M. J., Valencia, A. M., Zhou, Q., Bocker, M., Soares, L. M. M., Pan, J., Remillard, D. I., Lareau, C. A., Zullow, H. J., Fortoul, N., Gray, N. S., Bradner, J. E., Chan, H. M., & Kadoch, C. (2018). A non-canonical SWI/SNF complex is a synthetic lethal target in cancers driven by BAF complex perturbation. *Nature Cell Biology*, *20*(12), 1410–1420. https://doi.org/10.1038/s41556-018-0221-1

Mittal, P., & Roberts, C. W. M. (2020). The SWI/SNF complex in cancer — biology, biomarkers and therapy. *Nature Reviews Clinical Oncology*, *17*(7), 435–448. https://doi.org/10.1038/s41571-020-0357-3

Miyamoto, T., Iwasaki, H., Reizis, B., Ye, M., Graf, T., Weissman, I. L., & Akashi, K. (2002). Myeloid or Lymphoid Promiscuity as a Critical Step in Hematopoietic Lineage Commitment. *Developmental Cell*, *3*(1), 137–147.

Mojica, F. J. M., Díez-Villaseñor, C., García-Martínez, J., & Soria, E. (2005). Intervening sequences of regularly spaced prokaryotic repeats derive from foreign genetic elements. *Journal of Molecular Evolution*, *60*(2), 174–182. https://doi.org/10.1007/s00239-004-0046-3

Moore, L. D., Le, T., & Fan, G. (2013). DNA methylation and its basic function. *Neuropsychopharmacology*, *38*, 23–38. https://doi.org/10.1038/npp.2012.112

Moran-Crusio, K., Reavie, L., Shih, A., Abdel-Wahab, O., Ndiaye-Lobry, D., Lobry, C., Figueroa, M. E., Vasanthakumar, A., Patel, J., Zhao, X., Perna, F., Pandey, S., Madzo, J., Song, C., Dai, Q., He, C., Ibrahim, S., Beran, M., Zavadil, J., … Levine, R. L. (2011). Tet2 Loss Leads to Increased Hematopoietic Stem Cell Self-Renewal and Myeloid Transformation. *Cancer Cell*, *20*(1), 11–24. https://doi.org/10.1016/j.ccr.2011.06.001

Morrison, S. J., & Kimble, J. (2006). Asymmetric and symmetric stem-cell divisions in development and cancer. *Nature*, *441*, 1068–1074. https://doi.org/10.1038/nature04956

Mrózek, K., Marcucci, G., Paschka, P., Whitman, S. P., & Bloomfield, C. D. (2007). Clinical relevance of mutations and gene-expression changes in adult acute myeloid leukemia with normal cytogenetics: Are we ready for a prognostically prioritized molecular classification? In *Blood* (Vol. 109, Issue 2, pp. 431–448). American Society of Hematology. https://doi.org/10.1182/blood-2006-06-001149

Naldini, L., Blomer, U., Gallay, P., Ory, D., Mulligan, R., Gage, F. H., Verma, I. M., & Trono, D. (1996). In Vivo Gene Delivery and Stable Transduction of Nondividing Cells by a Lentiviral Vector. *Science*, *272*(5259), 263–267. https://doi.org/10.1126/science.272.5259.263

Nat Sternberg, & Daniel Hamilton. (1981). Bacteriophage P1 site-specific recombination: I. Recombination between loxP sites. *Journal of Molecular Biology*, *150*(4), 467–486. https://doi.org/https://doi.org/10.1016/0022-2836(81)90375-2

Nishiyama, A., & Nakanishi, M. (2021). Navigating the DNA methylation landscape of cancer. *Trends in Genetics*, *37*(11), 1012–1027. https://doi.org/10.1016/j.tig.2021.05.002

Ogawa, H., Oka, Y., Tsuboi, A., Kim, E. H., Masuda, T., Fujioka, T., Murakami, M., Kawakami, M., Tamaki, H., Hosen, N., Minamiguchi, H., Kimura, T., Sonoda, Y., Sugiyama, H., Motomura, M., Kanato, K., Asada, M., Oji, Y., & Soma, T. (2002). Very low frequencies of human normal CD34+ haematopoietic progenitor cells express the Wilms' tumour gene WT1 at

levels similar to those in leukaemia cells. *British Journal of Haematology*, *116*(2), 409–420. https://doi.org/10.1046/j.1365-2141.2002.03261.x

Okada, T., Nakamura, M., Nishikawa, J., Sakai, K., Zhang, Y., Saito, M., Morishige, A., Oga, A., Sasaki, K., Suehiro, Y., Hinoda, Y., & Sakaida, I. (2013). Identification of genes specifically methylated in Epstein-Barr virus-associated gastric carcinomas. *Cancer Science*, *104*(10), 1309–1314. https://doi.org/10.1111/cas.12228

Ostroverkhova, D., Przytycka, T. M., & Panchenko, A. R. (2023). Cancer driver mutations: predictions and reality. *Trends in Molecular Medicine*, *29*(7), 554–566. https://doi.org/10.1016/j.molmed.2023.03.007

Otto, J. E., & Kadoch, C. (2017). A Two-Faced mSWI/SNF Subunit: Dual Roles for ARID1A in Tumor Suppression and Oncogenicity in the Liver. *Cancer Cell*, *32*(5), 542–543. https://doi.org/10.1016/j.ccell.2017.10.014

Panuzzo, C., Signorino, E., Calabrese, C., Ali, M. S., Petiti, J., Bracco, E., & Cilloni, D. (2020). Landscape of tumor suppressor mutations in acute myeloid leukemia. *Journal of Clinical Medicine*, *9*(3). https://doi.org/10.3390/jcm9030802

Park, D. J., Kwon, A., Cho, B. S., Kim, H. J., Hwang, K. A., Kim, M., & Kim, Y. (2020). Characteristics of DNMT3A mutations in acute myeloid leukemia. *Blood Research*, *55*(1), 17–26. https://doi.org/10.5045/br.2020.55.1.17

Patiño-Mercau, J. R., Baliñas-Gavira, C., Andrades, A., Benitez-Cantos, M. S., Rot, A. E., Rodriguez, M. I., Álvarez-Pérez, J. C., Cuadros, M., & Medina, P. P. (2023). BCL7A is silenced by hypermethylation to promote acute myeloid leukemia. *Biomarker Research*, *11*(1). https://doi.org/10.1186/s40364-023-00472-x

Piunti, A., & Shilatifard, A. (2021). The roles of Polycomb repressive complexes in mammalian development and cancer. *Nature Reviews Molecular Cell Biology*, *22*(5), 326–345. https://doi.org/10.1038/s41580-021-00341-1

Pope, S. D., & Medzhitov, R. (2018). Emerging Principles of Gene Expression Programs and Their Regulation. *Molecular Cell*, *71*(3), 389–397. https://doi.org/10.1016/j.molcel.2018.07.017

Prelich, G. (2012). Gene overexpression: Uses, mechanisms, and interpretation. *Genetics*, *190*(3), 841–854. https://doi.org/10.1534/genetics.111.136911

Radzisheuskaya, A., Peña-Rømer, I., Lorenzini, E., Koche, R., Zhan, Y., Shliaha, P. V, Cooper, A. J., Fan, Z., Shlyueva, D., Johansen, J. V, Hendrickson, R. C., & Helin, K. (2023). An alternative NURF complex sustains acute myeloid leukemia by regulating the accessibility of insulator regions. *The EMBO Journal*, *42*(24). https://doi.org/10.15252/embj.2023114221

Rago, F., Rodrigues, L. U., Bonney, M., Sprouffske, K., Kurth, E., Elliott, G. N., Ambrose, J., Aspesi, P., Oborski, J., Chen, J. T., McDonald, E. R., Mapa, F. A., Ruddy, D. A., Kauffmann, A., Abrams, T., Bhang, H. E. C., & Jagani, Z.

(2022). Exquisite Sensitivity to Dual BRG1/BRM ATPase Inhibitors Reveals Broad SWI/SNF Dependencies in Acute Myeloid Leukemia. *Molecular Cancer Research*, *20*(3), 361–372. https://doi.org/10.1158/1541-7786.MCR-21-0390

Ramos-Medina, R., Montes-Moreno, S., Maestre, L., Cañamero, M., Rodríguez-Pinilla, M., Martínez-Torrecuadrada, J., Piris, M. Á., Majid, A., Dyer, M. J. S., Pulford, K., & Roncador, G. (2013). BCL7A protein expression in normal and malignant lymphoid tissues. *British Journal of Haematology*, *160*(1), 106–109. https://doi.org/10.1111/bjh.12080

Rao, X., Huang, X., Zhou, Z., & Lin, X. (2013). An improvement of the 2ˆ(-delta delta CT) method for quantitative real-time polymerase chain reaction data analysis. *Biostat Bioinforma Biomath*, *3*(3), 71–85.

Rauluseviciute, I., Drabløs, F., & Rye, M. B. (2020). DNA hypermethylation associated with upregulated gene expression in prostate cancer demonstrates the diversity of epigenetic regulation. *BMC Medical Genomics*, *13*. https://doi.org/10.1186/s12920-020-0657-6

Reyes, A. A., Marcum, R. D., & He, Y. (2021). Structure and Function of Chromatin Remodelers. *Journal of Molecular Biology*, *433*(14). https://doi.org/10.1016/j.jmb.2021.166929

Rieger, M. A., & Schroeder, T. (2012). Hematopoiesis. *Cold Spring Harbor Perspectives in Biology*, *4*(12). https://doi.org/10.1101/cshperspect.a008250

Ryme, J., Asp, P., Böhm, S., Cavellán, E., & Farrants, A. K. Ö. (2009). Variations in the composition of mammalian SWI/SNF chromatin remodelling complexes. *Journal of Cellular Biochemistry*, *108*(3), 565–576. https://doi.org/10.1002/jcb.22288

Saeidnia, S., Manayi, A., & Abdollahi, M. (2016). From in vitro Experiments to in vivo and Clinical Studies; Pros and Cons. *Current Drug Discovery Technologies*, *12*(4), 218–224. https://doi.org/10.2174/1570163813666160114093140

Salomoni, P., & Pandolfi, P. P. (2002). The Role of PML in Tumor Suppression. *Cell*, *108*(2), 165–170. https://doi.org/https://doi.org/10.1016/S0092-8674(02)00626-8

Sandhöfer, N., Bauer, J., Reiter, K., Dufour, A., Rothenberg, M., Konstandin, N. P., Zellmeier, E., Tizazu, B., Greif, P. A., Metzeler, K. H., Hiddemann, W., Polzer, H., & Spiekermann, K. (2016). The new and recurrent FLT3 juxtamembrane deletion mutation shows a dominant negative effect on the wild-Type FLT3 receptor. *Scientific Reports*, *6*. https://doi.org/10.1038/srep28032

Santiago Schiaffino-Ortega, Carlos Balinas, Marta Cuadros, & Pedro P Medina. (2014). SWI/SNF proteins as targets in cancer therapy. *Journal of Hematology & Oncology*, *7*(81). https://doi.org/10.1186/s13045-014-0081-5

Sasaki, M., & Ogiwara, H. (2020). Synthetic lethal therapy based on targeting the vulnerability of SWI/SNF chromatin remodeling complex-deficient cancers. In *Cancer Science* (Vol. 111, Issue 3, pp. 774–782). Blackwell Publishing Ltd. https://doi.org/10.1111/cas.14311

Shen, L., Shi, Q., & Wang, W. (2018). Double agents: Genes with both oncogenic and tumor-suppressor functions. *Oncogenesis*, *12*. https://doi.org/10.1038/s41389-018-0034-x

Shi, J., Whyte, W. A., Zepeda-Mendoza, C. J., Milazzo, J. P., Shen, C., Roe, J. S., Minder, J. L., Mercan, F., Wang, E., Eckersley-Maslin, M. A., Campbell, A. E., Kawaoka, S., Shareef, S., Zhu, Z., Kendall, J., Muhar, M., Haslinger, C., Yu, M., Roeder, R. G., … Vakoc, C. R. (2013). Role of SWI/SNF in acute leukemia maintenance and enhancer-mediated Myc regulation. *Genes and Development*, *27*(24), 2648–2662. https://doi.org/10.1101/gad.232710.113

Soh, J., Okumura, N., Lockwood, W. W., Yamamoto, H., Shigematsu, H., Zhang, W., Chari, R., Shames, D. S., Tang, X., MacAulay, C., Varella-Garcia, M., Vooder, T., Wistuba, I. I., Lam, S., Brekken, R., Toyooka, S., Minna, J. D., Lam, W. L., & Gazdar, A. F. (2009). Oncogene mutations, copy number gains and mutant allele specific imbalance (MASI) frequently occur together in tumor cells. *PLoS ONE*, *4*(10). https://doi.org/10.1371/journal.pone.0007464

Somarelli, J. A., Gardner, H., Cannataro, V. L., Gunady, E. F., Boddy, A. M., Johnson, N. A., Fisk, J. N., Gaffney, S. G., Chuang, J. H., Li, S., Ciccarelli, F. D., Panchenko, A. R., Megquier, K., Kumar, S., Dornburg, A., Degregori, J., & Townsend, J. P. (2020). Molecular Biology and Evolution of Cancer: From Discovery to Action. *Molecular Biology and Evolution*, *37*(2), 320–326. https://doi.org/10.1093/molbev/msz242

Sperling, A. S., Gibson, C. J., & Ebert, B. L. (2017). The genetics of myelodysplastic syndrome: From clonal haematopoiesis to secondary leukaemia. *Nature Reviews Cancer*, *17*, 5–19. https://doi.org/10.1038/nrc.2016.112

Stomper, J., Rotondo, J. C., Greve, G., & Lübbert, M. (2021). Hypomethylating agents (HMA) for the treatment of acute myeloid leukemia and myelodysplastic syndromes: mechanisms of resistance and novel HMA-based therapies. *Leukemia*, *35*, 1873–1889. https://doi.org/10.1038/s41375-021-01218-0

Stubbins, R. J., Francis, A., Kuchenbauer, F., & Sanford, D. (2022). Management of Acute Myeloid Leukemia: A Review for General Practitioners in Oncology. In *Current Oncology* (Vol. 29, Issue 9, pp. 6245–6259). MDPI. https://doi.org/10.3390/curroncol29090491

Sudarsanam Priya, & Winston Fred. (2000). The Swi/Snf family: nucleosome-remodeling complexes and transcriptional control. *Trends in Genetics*, *16*(8), 345–351.

Sun, X., Wang, S. C., Wei, Y., Luo, X., Jia, Y., Li, L., Gopal, P., Zhu, M., Nassour, I., Chuang, J. C., Maples, T., Celen, C., Nguyen, L. H., Wu, L., Fu, S., Li, W.,

Hui, L., Tian, F., Ji, Y., … Zhu, H. (2017). Arid1a Has Context-Dependent Oncogenic and Tumor Suppressor Functions in Liver Cancer. *Cancer Cell*, *32*(5), 574-589.e6. https://doi.org/10.1016/j.ccell.2017.10.007

Sun, Y., Chen, B. R., & Deshpande, A. (2018). Epigenetic regulators in the development, maintenance, and therapeutic targeting of acute myeloid leukemia. *Frontiers in Oncology*, *8*. https://doi.org/10.3389/fonc.2018.00041

Sung, H., Ferlay, J., Siegel, R. L., Laversanne, M., Soerjomataram, I., Jemal, A., & Bray, F. (2021). Global Cancer Statistics 2020: GLOBOCAN Estimates of Incidence and Mortality Worldwide for 36 Cancers in 185 Countries. *CA: A Cancer Journal for Clinicians*, *71*(3), 209–249. https://doi.org/10.3322/caac.21660

Tang, L., Nogales, E., & Ciferri, C. (2010). Structure and function of SWI/SNF chromatin remodeling complexes and mechanistic implications for transcription. *Progress in Biophysics and Molecular Biology*, *102*(2–3), 122–128. https://doi.org/10.1016/j.pbiomolbio.2010.05.001

Tejedor, J. R., Peñarroya, A., Gancedo-Verdejo, J., Santamarina-Ojeda, P., Pérez, R. F., López-Tamargo, S., Díez-Borge, A., Alba-Linares, J. J., González-del-Rey, N., Urdinguio, R. G., Mangas, C., Roberti, A., López, V., Morales-Ruiz, T., Ariza, R. R., Roldán-Arjona, T., Meijón, M., Valledor, L., Cañal, M. J., … Fraga, M. F. (2023). CRISPR/dCAS9-mediated DNA demethylation screen identifies functional epigenetic determinants of colorectal cancer. *Clinical Epigenetics*, *15*. https://doi.org/10.1186/s13148-023-01546-1

The Cancer Genome Atlas Research Network. (2013). Genomic and Epigenomic Landscapes of Adult De Novo Acute Myeloid Leukemia. *New England Journal of Medicine*, *368*(22), 2059–2074. https://doi.org/10.1056/NEJMoa1301689

Tolstorukov, M. Y., Sansam, C. G., Lu, P., Koellhoffer, E. C., Helming, K. C., Alver, B. H., Tillman, E. J., Evans, J. A., Wilson, B. G., Park, P. J., & Roberts, C. W. M. (2013). Swi/Snf chromatin remodeling/tumor suppressor complex establishes nucleosome occupancy at target promoters. *Proceedings of the National Academy of Sciences of the United States of America*, *110*(25), 10165–10170. https://doi.org/10.1073/pnas.1302209110

Torry, D. S., & Cooper, G. M. (1991). Proto-oncogenes in development and cancer. *American Journal of Reproductive Immunology*, *25*(3), 129–132. https://doi.org/10.1111/j.1600-0897.1991.tb01080.x

Tracey, L., Villuendas, R., Dotor, A. M., Spiteri, I., Ortiz, P., García, J. F., Rodríguez Peralto, J. L., Lawler, M., & Piris, M. A. (2003). Mycosis fungoides shows concurrent deregulation of multiple genes involved in the TNF signaling pathway: An expression profile study. *Blood*, *102*(3), 1042–1050. https://doi.org/10.1182/blood-2002-11-3574

Tyagi, M., Imam, N., Verma, K., & Patel, A. K. (2016). Chromatin remodelers: We are the drivers!! *Nucleus*, *7*(4), 388–404. https://doi.org/10.1080/19491034.2016.1211217

Van Doorn, R., Zoutman, W. H., Dijkman, R., De Menezes, R. X., Commandeur, S., Mulder, A. A., Van Der Velden, P. A., Vermeer, M. H., Willemze, R., Yan, P. S., Huang, T. H., & Tensen, C. P. (2005). Epigenetic profiling of cutaneous T-cell lymphoma: Promoter hypermethylation of multiple tumor suppressor genes including BCL7a, PTPRG, and p73. *Journal of Clinical Oncology*, *23*(17), 3886–3896. https://doi.org/10.1200/JCO.2005.11.353

Waddington, C. H. (1942). Canalization of development and the inheritance of acquired characters. *Nature*, *150*, 563–565. https://doi.org/https://doi.org/10.1038/150563a0

Wallwitz, J., Aigner, P., & Stoiber, D. (2021). Tumor suppressors in acute myeloid leukemia. *Leukemia and Lymphoma*, *62*(10), 2320–2330. https://doi.org/10.1080/10428194.2021.1907372

Wang, H. Y., Gong, S., Li, G. H., Yao, Y. Z., Zheng, Y. S., Lu, X. H., Wei, S. H., Qin, W. W., Liu, H. B., Wang, M. C., Xi, J. Y., Chen, L. M., Zhang, M., Zhang, X. X., Zhang, H. Y., Zhang, C. S., Wald, D. N., Zhu, H. H., Liu, L., & He, P. C. (2022). An effective and chemotherapy-free strategy of all-trans retinoic acid and arsenic trioxide for acute promyelocytic leukemia in all risk groups (APL15 trial). *Blood Cancer Journal*, *12*. https://doi.org/10.1038/s41408-022-00753-y

Wang, H., Zhang, D., Cui, X., Dai, Y., Wang, C., Feng, W., Lv, X., Li, Y., Wang, L., Ru, Y., Zhang, Y., Ren, Q., & Zheng, G. (2022). Loss of IRF7 accelerates acute myeloid leukemia progression and induces VCAM1-VLA-4 mediated intracerebral invasion. *Oncogene*, *41*(16), 2303–2314. https://doi.org/10.1038/s41388-022-02233-w

Wang, L. H., Wu, C. F., Rajasekaran, N., & Shin, Y. K. (2019). Loss of tumor suppressor gene function in human cancer: An overview. In *Cellular Physiology and Biochemistry* (Vol. 51, Issue 6, pp. 2647–2693). S. Karger AG. https://doi.org/10.1159/000495956

Wang, Z.-Y., & Chen, Z. (2008). Acute promyelocytic leukemia: from highly fatal to highly curable A historical view of acute promyelocytic leukemia (APL). *Blood*, *111*(5), 2505–2515. https://doi.org/10.1182/blood-2007

Wheat, J. C., & Steidl, U. (2021). Gene expression at a single-molecule level: implications for myelodysplastic syndromes and acute myeloid leukemia. *Blood*, *138*(8), 625–636.

Wieczorek, S., Combes, F., Lazar, C., Gianetto, Q. G., Gatto, L., Dorffer, A., Hesse, A. M., Couté, Y., Ferro, M., Bruley, C., & Burger, T. (2017). DAPAR & ProStaR: Software to perform statistical analyses in quantitative discovery proteomics. *Bioinformatics*, *33*(1), 135–136. https://doi.org/10.1093/bioinformatics/btw580

Winston Fred, & Carlson Marian. (1992). Yeast SNF/SWI transcriptional activators and the SPT/SIN chromatin connection. *Trends in Genetics*, *8*(11), 387–391.

Wischhof, L., Maida, S., Piazzesi, A., Gioran, A., Barragan Sanz, K., Irsen, S., Beyer, M., Schultze, J. L., Dyer, M. J., Salomoni, P., Ehninger, D., Nicotera, P., & Bano, D. (2017). The SWI/SNF subunit Bcl7a contributes to motor coordination and Purkinje cell function. *Scientific Reports*, *7*(1). https://doi.org/10.1038/s41598-017-17284-3

Wiśniewski, J. R., Zougman, A., Nagaraj, N., & Mann, M. (2009). Universal sample preparation method for proteome analysis. *Nature Methods*, *6*(5), 359–362. https://doi.org/10.1038/nmeth.1322

Workman, J. L., & Kingston, R. E. (1998). Alteration of nucleosome structure as a mechanism of transcriptional regulation. *Annu. Rev. Biochem*, *67*, 545–579. www.annualreviews.org

Wu, J. N., & Roberts, C. W. M. (2013). ARID1A mutations in cancer: Another epigenetic tumor suppressor? *Cancer Discovery*, *3*(1), 35–43. https://doi.org/10.1158/2159-8290.CD-12-0361

Wu, Y. L., Lin, Z. J., Li, C. C., Lin, X., Shan, S. K., Guo, B., Zheng, M. H., Li, F., Yuan, L. Q., & Li, Z. hong. (2023). Epigenetic regulation in metabolic diseases: mechanisms and advances in clinical study. *Signal Transduction and Targeted Therapy*, *8*. https://doi.org/10.1038/s41392-023-01333-7

Xiong, Z., & Laird, P. W. (1997). COBRA: a sensitive and quantitative DNA methylation assay. *Nucleic Acids Research*, *25*(12), 2532–2534. https://academic.oup.com/nar/article/25/12/2532/2901842

Xu, X., Tao, Y., Gao, X., Zhang, L., Li, X., Zou, W., Ruan, K., Wang, F., Xu, G. L., & Hu, R. (2016). A CRISPR-based approach for targeted DNA demethylation. *Cell Discovery*, *2*. https://doi.org/10.1038/celldisc.2016.9

Yao, H., Huo, L., Ping, N., Liu, H., Li, H., Ding, Z., Shen, H., Xie, J., Qiu, Q., Ma, L., Jiang, A., Wang, Q., Wu, D., Yang, X., Song, Y., & Chen, S. (2022). Recurrent mutations in multiple components of the SWI/SNF complex in myelodysplastic syndromes and acute myeloid leukaemia. In *British Journal of Haematology* (Vol. 196, Issue 2, pp. 441–444). John Wiley and Sons Inc. https://doi.org/10.1111/bjh.17795

Yu, N., Shin, S., Choi, J. R., Kim, Y., & Lee, K. A. (2017). Concomitant aid expression and bcl7a loss associates with accelerated phase progression and imatinib resistance in chronic myeloid leukemia. *Annals of Laboratory Medicine*, *37*(2), 177–179. https://doi.org/10.3343/alm.2017.37.2.177

Zani, V. J., Asou, N., Jadayel, D., Heward, J. M., Shipley, J., Nacheva, E., Takasuki, K., Catovsky, D., & Dyer, M. J. S. (1996). Molecular Cloning of Complex Chromosomal Translocation t(8; 14; 12)(q24.1; q32.3; q24.1) in a Burkitt Lymphoma Cell Line Defines a New Gene (BCL7A) With Homology to Caldesmon. *Blood*, *87*(8), 3124–3134.

Zarka, J., Short, N. J., Kanagal-Shamanna, R., & Issa, G. C. (2020). Nucleophosmin 1 mutations in acute myeloid leukemia. *Genes*, *11*(6). https://doi.org/10.3390/genes11060649

Zhang, F. L., & Li, D. Q. (2022). Targeting Chromatin-Remodeling Factors in Cancer Cells: Promising Molecules in Cancer Therapy. In *International Journal of Molecular Sciences* (Vol. 23, Issue 21). MDPI. https://doi.org/10.3390/ijms232112815

Zhang, N., Wu, J., Wang, Q., Liang, Y., Li, X., Chen, G., Ma, L., Liu, X., & Zhou, F. (2023). Global burden of hematologic malignancies and evolution patterns over the past 30 years. *Blood Cancer Journal*, *13*. https://doi.org/10.1038/s41408-023-00853-3

Zhao, J. C., Agarwal, S., Ahmad, H., Amin, K., Bewersdorf, J. P., & Zeidan, A. M. (2022). A review of FLT3 inhibitors in acute myeloid leukemia. *Blood Reviews*, *52*. https://doi.org/10.1016/j.blre.2021.100905

Zhao, S., Xu, Y., Wu, W., Wang, P., Wang, Y., Jiang, H., & Zhu, J. (2021). ARID1A Variations in Cholangiocarcinoma: Clinical Significances and Molecular Mechanisms. *Frontiers in Oncology*, *11*. https://doi.org/10.3389/fonc.2021.693295

Zhao, Z., & Shilatifard, A. (2019). Epigenetic modifications of histones in cancer. *Genome Biology*, *20*. https://doi.org/10.1186/s13059-019-1870-5

Zhou, C., Li, J., Du, J., Jiang, X., Xu, X., Liu, Y., He, Q., Liang, H., Fang, P., Zhan, H., & Zeng, H. (2021). HMGCS1 drives drug-resistance in acute myeloid leukemia through endoplasmic reticulum-UPR-mitochondria axis. *Biomedicine and Pharmacotherapy*, *137*. https://doi.org/10.1016/j.biopha.2021.111378

Zhou, M., Yuan, J., Deng, Y., Fan, X., & Shen, J. (2021). Emerging role of SWI/SNF complex deficiency as a target of immune checkpoint blockade in human cancers. *Oncogenesis*, *10*(1). https://doi.org/10.1038/s41389-020-00296-6

Zhou, M.-Y., & Gomez-Sanchez, C. E. (2000). Universal TA Cloning. *Issues Mol. Biol*, *2*(1), 1–7. https://doi.org/https://doi.org/10.21775/cimb.002.001

Zhou, Y., Zhou, B., Pache, L., Chang, M., Khodabakhshi, A. H., Tanaseichuk, O., Benner, C., & Chanda, S. K. (2019). Metascape provides a biologist-oriented resource for the analysis of systems-level datasets. *Nature Communications*, *10*(1). https://doi.org/10.1038/s41467-019-09234-6

Zhu, K., Liu, Q., Zhou, Y., Tao, C., Zhao, Z., Sun, J., & Xu, H. (2015). Oncogenes and tumor suppressor genes: Comparative genomics and network perspectives. *BMC Genomics*, *16*(7). https://doi.org/10.1186/1471-2164-16-S7-S8

Annex

Annex

Thesis article

Patiño-Mercau *et al. Biomarker Research* (2023) 11:32
https://doi.org/10.1186/s40364-023-00472-x

Biomarker Research

RESEARCH Open Access

BCL7A is silenced by hypermethylation to promote acute myeloid leukemia

Juan Rodrigo Patiño-Mercau[1,2†], Carlos Baliñas-Gavira[1,3†], Alvaro Andrades[1,2,4], Maria S. Benitez-Cantos[1,4,5], Ana Ercegovič Rot[1,6,7], Maria Isabel Rodriguez[1,4,5], Juan Carlos Álvarez-Pérez[1,2,4], Marta Cuadros[1,4,5] and Pedro P. Medina[1,2,4*]

Abstract

Background Recent massive sequencing studies have revealed that SWI/SNF complexes are among the most frequently altered functional entities in solid tumors. However, the role of SWI/SNF in acute myeloid leukemia is poorly understood. To date, SWI/SNF complexes are thought to be oncogenic in AML or, at least, necessary to support leukemogenesis. However, mutation patterns in SWI/SNF genes in AML are consistent with a tumor suppressor role. Here, we study the SWI/SNF subunit BCL7A, which has been found to be recurrently mutated in lymphomas, but whose role in acute myeloid malignancies is currently unknown.

Methods Data mining and bioinformatic approaches were used to study the mutational status of *BCL7A* and the correlation between BCL7A expression and promoter hypermethylation. Methylation-specific PCR, bisulfite sequencing, and 5-aza-2′-deoxycytidine treatment assays were used to determine if BCL7A expression was silenced due to promoter hypermethylation. Cell competition assays after BCL7A expression restoration were used to assess the role of BCL7A in AML cell line models. Differential expression analysis was performed to determine pathways and genes altered after BCL7A expression restoration. To establish the role of BCL7A in tumor development in vivo, tumor growth was compared between BCL7A-expressing and non-expressing mouse xenografts using in vivo fluorescence imaging.

Results BCL7A expression was inversely correlated with promoter methylation in three external cohorts: TCGA-LAML ($N = 160$), TARGET-AML ($N = 188$), and Glass et al. (2017) ($N = 111$). The AML-derived cell line NB4 silenced the BCL7A expression via promoter hypermethylation. Ectopic BCL7A expression in AML cells decreased their competitive ability compared to control cells. Additionally, restoration of BCL7A expression reduced tumor growth in an NB4 mouse xenograft model. Also, differential expression analysis found that *BCL7A* restoration altered cell cycle pathways and modified significantly the expression of genes like *HMGCS1*, *H1-0*, and *IRF7* which can help to explain its tumor suppressor role in AML.

Conclusions BCL7A expression is silenced in AML by promoter methylation. In addition, restoration of BCL7A expression exerts tumor suppressor activity in AML cell lines and xenograft models.

Keywords SWI/SNF complex, AML, Tumor suppressor, DNA hypermethylation

†Juan Rodrigo Patiño-Mercau and CarlosBaliñas-Gavira contributed equally to this work.

*Correspondence:
Pedro P. Medina
pedromedina@ugr.es
Full list of author information is available at the end of the article

Additional publications during the PhD

Andrades A, Álvarez-Pérez JC, **Patiño-Mercau JR**, Cuadros M, Baliñas-Gavira C, Medina PP. Recurrent splice site mutations affect key diffuse large B-cell lymphoma genes. Blood. **2022 Apr 14**;139(15):2406-2410.

doi: 10.1182/blood.2021011708. PMID: 34986231.

Peinado P, Andrades A, Cuadros M, Rodriguez MI, Coira IF, Garcia DJ, Álvarez-Perez JC, Baliñas-Gavira C, Arenas AM, **Patiño-Mercau JR**, Sanjuan-Hidalgo J, Romero OA, Montuenga LM, Carretero J, Sanchez-Cespedes M, Medina PP. Comprehensive Analysis of SWI/SNF Inactivation in Lung Adenocarcinoma Cell Models. Cancers (Basel). **2020 Dec 10**;12(12):3712.

doi: 10.3390/cancers12123712. PMID: 33321963; PMCID: PMC7763689.

Book chapters

Arenas AM*, Andrades A*, **Patiño-Mercau JR**, Sanjuán-Hidalgo J, Cuadros M, García DJ, Peinado P, Rodríguez MI, Baliñas-Gavira C, Álvarez-Pérez C, Medina PP. Opportunities of miRNAs in cancer therapeutics. In "MicroRNA in Human Malignancies, 1st Edition"; Negrini M, Calin G, Croce C (Eds); Elsevier, Feb 17, 2022; pp. 153-164. ISBN: 9780128222874

*Shared first-authorship is denoted by **

Intellectual property permissions

Gmail

Juan Rodrigo Patiño <juanrodrigopatino@gmail.com>

Permissions re Intellectual property query for my PhD dissertation.

Bhakta, Jyoti (BIDMC - Technology Ventures Office) <jbhakta@bidmc.harvard.edu> 10 de enero de 2024, 16:46

Para: Juan Rodrigo Patiño <juanrodrigopatino@gmail.com>
Cc: "Diruscio, Annalisa (BIDMC - Medicine)" <adirusci@bidmc.harvard.edu>

Hi Juan,

I am writing in regard to your request for inclusion in your Ph.D. dissertation the results generated from your work done at BIDMC at Dr. Annalisa Di Ruscio's lab.

The Crispr-Dir Platform that was used is co-owned with another academic institution (National University of Singapore, NUS) and after their independent evaluations they have conveyed that they permit inclusion of the results in your Ph.D. dissertation.

Thus, I formally write to inform that you may include the results "as-is" as provided to our office in the attached*. For clarity, this email serves as a formal grant of permissions from BIDMC and NUS.

Thank you and, in advance, best wishes for your thesis submission and the defense.

Jyoti

Jyoti Bhakta, Ph.D.

Hear my name https://www.name-coach.com/jyoti-bhakta

Senior Technology Licensing Associate

Technology Ventures Office (TVO)

E:jbhakta@bidmc.harvard.edu

Ph: (617) 667-4197

Note: Email is the best way to reach me. Please email to schedule a call

Beth Israel Lahey Health
Beth Israel Deaconess Medical Center

330 Brookline Avenue, Boston, MA 02215

Search Technologies for Licensing & Projects for Sponsored Research

CRISPR-DiR Juan Ro PhD dissertation Dec 27 2023.docx
546K

Agradecimientos

Agradecimientos

Un día de septiembre de 2014 "el Juan Ro de 18 años" estaba empezando el Grado en Biotecnología en la Universidad de Granada. Nueve años después sigo en la misma ciudad terminando un doctorado con la sensación de que hubiesen pasado 2 o 3 años nada más… Millones de historias, aprendizajes, pero principalmente personas:

Gracias a Pedro por aquel email en 3º de carrera ofreciéndonos pedir la beca de iniciación a la investigación de la AECC, la cual fue mi punto de partida como joven investigador y que ha resultado en mi crecimiento hasta llegar a ser PhD. Gracias por abrirme las puertas de tu lab en aquel momento!

Estoy superhappy de haber compartido todos esos años con los PMVs (que nunca fueron pocos), ya que tenemos un envidiable ambiente de trabajo: gracias a tod@s!!

Empezando por los "old school" :

Carlos Baliñas (¡qué pasa tronco!), enorme siendo mi mentor en todo lo de BCL7A (aunque a veces "se acabaron las preguntas! -.- "). No sé cuánto me habré podido reír con tu manera de hablar de las cosas con tanto carácter: gracias por esos momentos!

Carlos gallego ("Have you CHECK?"), mi codirector desde el TFG hasta el PhD ("ostia el esameeen!!"), poca broma! Mil gracias por haberme aguantado tanto tiempo y estar siempre para ayudarme recibiendo todas mis consultas científicas.

Alvaro ("are you doing a Postdoc randomly??"). Muchas gracias por haberme enseñado de ciencia y haberme ayudado tanto con muchísimos análisis! AKA: el Leo Messi de R, te mira y te plotea.

Paola (fan de tu "the Good the Bad and the Ugly of ARID1A") y Alberto ("no te problemes, que yo ya tenía tu hielo seco guardado para tu RNA-seq"): gracias por ser mis guías para

muchas "minidudas" que luego son las que, nada menos, hacen que los experimentos salgan. Gracias a Alberto por la intervention, la verdad que me supuso un cierto cambio a mejor personaje.

Juan San (mi revés fav y culpable de la creación de Juan Ro y Juan San, men men!), Dani (C.E.O. de FedEx… y a parte… experto en la gestión de paquetes) y Félix (no sabía que te había echado tanto de menos en U.S., porque cero fogueo lo que me rio contigo, eso no se paga con dinero): gracias por mantenerme siempre a full de mango con el pádel y por innumerables risas que NO TE LAS PODÉS CREER MEN!!

Marisol (la única que me entiende about Prog en to Graná, PMVn't de oro): mil gracias por enseñarme nueva música de la que solo a unos pocos nos mola y por ser always un enorme apoyo en lo científico!!

M. Cuadros ("cucha, chiqui!"), gracias por tu energía positiva en el lab! Y gracias a Maribel por las muchas horas que habremos pasado juntos pipeteando (incluido aquel domingo que pedimos que Genyo abriese de 10 a 22…)

Seguimos con los "new school":

Entre l@s chiquit@s agradecer muchos buenos momentos (laborales y de ocio) a Pablo MarLop (C.E.O. de Amazon heredero de BCL7A), Ana Utri (LA chiquita oficial), Patri Conch (supermegatop lab manager, plz don't hate me por todo lo sufrido con FedEx, tq mucho), Josema R. (ATAC-lover… la que nos dio NB4), Fernando (la que nos espera con los recent seqs…), Caye, Valentina, Miguel Ángel, Ana Rous… Sois un superteam que tira mucho palante!!

Thanks Bea TFM (tendremos 40 años y seguirás siendo "Bea TFM"), por sufrir mi mentorización para tu TFM e iniciar una amistad que dura más que ese TFM.

Entre los no tan chiquitos, agradecer la llegada de Ana Matia (sabia consejera de trayectorias científicas que soporta nuestras tonterias) y Sergio (new postdoc sumado al barco de BCL7A + envidia de tu happiness perpetua) que me ayudaron mucho en toma de decisiones científicas importantes en mis últimos meses de PhD.

En terreno PMVn't, agradezco mucho la ayuda prestada por toda la blue floor: Amador y María A. con sus masterclases de ChIP-seq y al resto del Landeira's lab (Meci, Andrea, , a la gente del lab22 (Ana Sori, Mati, Ángel, Inma, Virginia...) por la supercentrífuga, lab 16 (de antes), aguantando mis minichapas en los paseos a por el EtOH 100% (Carmen, Vivi, Elena, Ana P., Patri P., Vero, Sergio).

Agradezco mucho a todos los de Genyo presentes en los viernes de tapas, fiestas de la primavera, comidas de navidad, defensas de tesis, etc. Poco se habla el tremendo ocio que manejamos… Muchas gracias geny@s por todas las risas y momentazos!!

Aknowledgments to My Boston people!

Ad Annalisa, sarò sempre enormemente grata per aver accettato di accogliermi nel suo laboratorio e per avermi insegnato tanto, essendo questo l'inizio di un'esperienza che per me è stata incredibile dall'inizio alla fine.

To Lucrezia e Giulia, per avermi sempre aiutato in tutto ciò di cui avevo bisogno in laboratorio e per i bei momenti che abbiamo trascorso.

A mi "supermini" Boston Crew: Mireya, Sergio, Mikel, Ainhoa A. , Itsasne (bat, bi hiru, lau, Boston, saludos jaja), Ainhoa G (nunca olvidaré el tour por el Media Lab), Enya (la peque que tan solo hace neurosciences en HMS), Irene (con medio año me conoces mucho mejor que much@s), Goretti (no se si has recibido ya el premio por aguantarme un finde en NY y por ser mi peluquera oficial en MA) y Javi (menos mal que me dijiste que sí

a quedar aquel día nevado de enero, ya que fue el principio de todo y encima terminamos grabando un album que está en Spoty… muy loco esto). Aprendí mucho con tod@s vosotr@s!

Fuera de Genyo, tengo que agradecer:

A Abel, con el que vengo a la par desde que entramos en la carrera y resi hasta ahora, cero fogueo con estos 9 años. Oficialmente: mi máximo bro de Granada.

A Lucia Valencia C.F., pedazo de frikaza: te sabes mi vida en verso mejor que nadie de todas las chapas que te has llevado de mi parte… Oficialmente mi sis máxima de Granada.

Al resto de los Keo: JaviJa (o Javi mates, el funcionario de éxito del team), Segu (otra frikaza pero odontóloga de éxito) y Crimi (el almeriense que con un meñique te parte la camisa [y no es broma], pd: a dónde vamos? → a tu p… casa); grupazo de gente de bien, pero que cuando se junta el calabozo siempre es una posibilidad…

A los de siempre y que siempre están cuando paso por Aguadulce: Casto (ingeniero de moda y exitoso TT owner), Dani Melilla (elfamoso.Dan + mi personal trainer) y Fran (las bromas con Fran… terminan en el hospi). Y a Mis chicas de Aguadulce de siempre y para siempre too: Leti, Blanca, Marimar y Mary (sentados al lado desde la primaria, me tuviste que aguantar poco…).

A mis Biotecs: Pablo (siempre enterado de todo, 10/10 en bromas de padre), Carmen (tuu.. yasta bien de salir en esta sección no?), Ana, M Carmen, Cris, Sergio y Java. Grupo también conocido como "el imserso que mola", que tuvo su punto de inflexión al pasar por República Dominicana y no veas el ocio que hemos estado pilotando a posteriorii.

A Alba Biotec (ella me llama "wan", directamente), que, aunque estés haciéndote doctora en otro país hemos seguido siempre in touch!

A los ratones & company: nunca dio para tantísimo un curso de formación científica: Javi PhD, Mabel, Patri, Ali, Ana S.M. (poca broma la gracia e ilusión que te hacían mis denominados "miniocios"), Irene y Sergio (no hicisteis el curso, pero quiénes me llevaron a navegar a Matalascañas un octubre travieso eh?!), Ana G. (poca broma con la científica de renombre, experta en hacerme reflexionar) y Cris (imagínate en 30 sec en cámara rápida todos los planazos, viajes, miniocios y padels que nos marcamos… creo que en 30 sec no te da, pero no te problemes porque a buena entendedora → no le mires los dientes!).

A todas las personas con las que he compartido esa adicción al pádel, por sacarme a jugar partidos semanalmente durante estos años. En especial a mi actual capi de SNP: Victor C.

A Tania C., por darme la enorme oportunidad de hacer una breve estancia en un lab de University of Cambridge y enseñarme tanto en tan poco tiempo.

A muchas otras personas con las que he compartido planes y momentos durante los 4 años que ha durado esta tesis.

A mis profesores del pasado que me motivaron para iniciar una carrera en ciencias de la vida: Estrella e Isidro.

A Dream Theater y el resto de artistas de música Prog y no tan Prog. Seguro que han estado ambientandome más horas que nadie durante estos 4 años.

Por último, paso a mencionar a los closest, con los que por lo que sea comparto apellidos. Agradezco mucho:

A mi familia internacional, que está prácticamente toda al otro lado del Atlántico. Muy copado que pude ir DOS veces durante el doctorado a Argentina.

A los Mercaus: Magui, Agus, Belu, Pili, Marcos, Azu y Male por mil planazos around Buenos Aires! (mates + facturas, paseos, asados, timbas…) A los Mercau "Mex": Lu, Leo y Santi (tenemos que vernos máss). A Javi Pat., estuvo muy bueno ese finde durante mi estancia que aproveché para ir a GA, U.S. a verte again después de 9 años. Como nos cagamos de la risa con 460 CVs.

A mi abu Norma: que buenos las salidas a comer afuera, los scrables y todas las memorias que me contás de cuando yo era chiquito.

A mi abuela Alicia, me hubiera encantado que me vieras terminar la tesis, pero estoy muy feliz porque sí me viste empezarla y por todos los findes que bajaba a Aguadulce y nos veíamos.

A mis padres todos poderosos creadores! Siempre estáis, para todo, donde sea (ya vinisteis a U.K. en 2019, ahora recientemente también a U.S.; a donde el research me fue llevando). Necesito otro documento de la misma extensión que este para agradeceros todo y rememorar todas las historias + risas que hubo durante estos 4 años. Me apoyáis siempre con todo, es increíble, no es "lo normal": thus, soy muy afortunado.